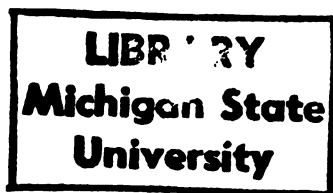


23931472



This is to certify that the

dissertation entitled

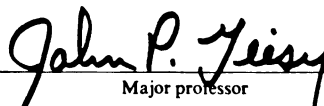
The effects of ultraviolet radiation
and the polycyclic aromatic hydrocarbon,
anthracene, on algae

presented by

William Robert Gala

has been accepted towards fulfillment
of the requirements for

Ph.D. degree in Fisheries and Wildlife
and Environmental Toxicology


Major professor

Date September 29, 1989

**PLACE IN RETURN BOX to remove this checkout from your record.
TO AVOID FINES return on or before date due.**

DATE DUE	DATE DUE	DATE DUE
_____	_____	_____
_____	_____	_____
_____	_____	_____
_____	_____	_____
_____	_____	_____
_____	_____	_____
_____	_____	_____

MSU Is An Affirmative Action/Equal Opportunity Institution

THE EFFECTS OF ULTRAVIOLET RADIATION AND THE POLYCYCLIC
AROMATIC HYDROCARBON, ANTHRACENE, ON ALGAE

By

William Robert Gala

A DISSERTATION

Submitted to
Michigan State University
in partial fulfillment of the requirements
for the degree of

DOCTOR OF PHILOSOPHY

Department of Fisheries and Wildlife and
Center for Environmental Toxicology

1989

6030804

ABSTRACT

THE EFFECTS OF ULTRAVIOLET RADIATION AND THE POLYCYCLIC AROMATIC HYDROCARBON, ANTHRACENE, ON ALGAE

By

William Robert Gala

The direct effects of ultraviolet (UV) radiation and the photo-induced toxicity of polycyclic aromatic hydrocarbons (PAH) to algae have been assessed. The penetration of solar UV radiation into offshore Lake Michigan was characterized. The direct effects of solar UV radiation to the primary production of natural phytoplankton assemblages in Lake Michigan was determined utilizing in situ incubations in chambers which selectively removed portions of the solar UV spectrum. A predictive hazard assessment model to estimate the impact of current and potential UV intensities on total lake productivity was developed.

The photo-induced toxicity of the linear 3-ring PAH, anthracene, to the green alga, Selenastrum capricornutum, was characterized. The dose-response relationships among anthracene concentration, UV radiation intensity, and algal growth rate, ¹⁴C-bicarbonate incorporation, and flow cytometric endpoints were determined. The potential environmental hazard of PAH contamination to algal communities was assessed.

Flux

util

acti

cell

inter

commu

indir

strato

solar

neglig

assemb

Fluridone, a carotenoid biosynthesis inhibiting herbicide, was utilized to investigate possible sites and modes of toxic action and the protection provided by carotenoids in algal cells to the photo-induced toxicity of anthracene.

It was concluded that solar UV radiation at current UV intensities can have considerable impact on natural algal communities through the direct effects of UV radiation and indirectly due to the photo-induced toxicity of PAH. However, stratospheric ozone depletion and the concomitant increase in solar UV radiation which is currently predicted will have negligible effects on primary production of phytoplankton assemblages in the Great Lakes.

profe

guida

my gr

and a

friend

gradua

and D

discus

thank

Sheneh

Research

dissert

I

and my f

you to k

And fina

friends

support

friendsh

ACKNOWLEDGEMENTS

I would like to express my appreciation to my major professor, Dr. John P. Giesy, for all of his assistance, guidance, patience, and knowledge he has imparted to me during my graduate training at MSU. My development as a scientist and a person has been greatly enhanced by his guidance and friendship. I would like to thank the other members of my graduate committee, Dr. Darrell King, Dr. Kenneth L. Poff, and Dr. Matthew J. Zabik, for all of their thoughtful discussions and help along the way. I would also like to thank the scientists and personnel of GLERL/NOAA, R/V Shenehon, MSU Flow Cytometry Facility, and the Pesticide Research Center for their assistance to my research and dissertation.

I can only begin to express my gratitude to my parents and my family for all of their love and encouragement. I want you to know that you were always there when I needed you most. And finally, to Ed, Jay, Don, Robin and Bob, five special friends who have truly enriched my life. Thanks guys for the support and assistance, but mostly, thanks for your friendship.

LIST C

LIST C

INTROD

CHAPT

P

P

X

M

CHAPT

TABLE OF CONTENTS

	<u>Page</u>
LIST OF TABLES	viii
LIST OF FIGURES	xi
INTRODUCTION	1
CHAPTER 1. PENETRATION OF ULTRAVIOLET RADIATION INTO LAKE MICHIGAN AND THE EFFECTS ON THE PRIMARY PRODUCTION OF NATURAL PHYTOPLANKTON ASSEMBLAGES .	14
INTRODUCTION	14
MATERIALS AND METHODS	17
Study site	17
Solar radiation measurements	18
¹⁴ C-bicarbonate assimilation	20
Other data	25
Statistical analysis	25
RESULTS	27
Penetration of ultraviolet radiation into Lake Michigan	27
Inhibition of primary production by UV radiation	35
DISCUSSION	43
Hazard assessment model	49
Conclusions	64
CHAPTER 2. THE PHOTO-INDUCED TOXICITY OF ANTHRACENE TO THE GREEN ALGA, <u>Selenastrum capricornutum</u>	66
INTRODUCTION	66
MATERIALS AND METHODS	69
Test organism	69
Toxicant	71
Experimental design	71
Lighting apparatus	72

CHAPTER

I

I

C

I

M

RE

CO

SUMMARY

REFEREN

Experimental schedule	74
Toxicity endpoints	81
Specific growth rate	82
¹⁴ C-bicarbonate incorporation	82
Flow cytometry	83
Controls	92
Statistical analysis	94
RESULTS	95
Controls	95
Anthracene photo-induced toxicity	98
Specific growth rate	98
¹⁴ C-bicarbonate incorporation	103
Cell size	113
Cellular chlorophyll concentration	122
Cell viability index	126
% Non-viable cells	136
DISCUSSION	143
Ecological consequences	151
Conclusions	154
CHAPTER 3. THE EFFECT OF THE CAROTENOID BIOSYNTHESIS INHIBITING HERBICIDE, FLURIDONE, ON THE PHOTO- INDUCED TOXICITY OF ANTHRACENE TO <u>Selenastrum</u> <u>capricornutum</u>	156
INTRODUCTION	156
MATERIALS AND METHODS	158
RESULTS AND DISCUSSION	162
CONCLUSIONS	168
SUMMARY	170
REFERENCES	175

LIST OF TABLES

<u>Table</u>	<u>Page</u>
1 Monthly averages of PAR, UV-A and UV-B maximum surface intensity and penetration into Lake Michigan from 1983, 1985 and 1986 cruises	29
2 Broad-band UV-B (310 +/- 34 nm) diffuse attenuation coefficients along a transect due west from Grand Haven, Michigan into Lake Michigan on 5-23-83	34
3 Incubation conditions, cumulative PAR and UV incident dose on the incubation chambers, dominant algal genera of the phytoplankton assemblages and inhibition of primary production in the UV-transparent chambers, relative to the UV-opaque chambers, measured during the <u>in situ</u> incubations at the 19 km station in Lake Michigan during 1986	36
4 Mean UV-B inhibition efficiencies for inhibition of primary production of different Lake Michigan phytoplankton assemblages	41
5 UV-B dose-response relationship for different Lake Michigan phytoplankton assemblages	43
6 Inhibition of areal primary production (mg C/m ³ -day) of offshore Lake Michigan at current and predicted future (21% UV-B increase) solar UV radiation intensities	57
7 Modified (2X) EPA algal assay medium (pH = 7.5)	69
8 Test conditions for the photo-induced toxicity of anthracene experiments	72
9 The effects of anthracene (ANTH) and UV-A radiation on the specific growth rate (0-22 h) of <u>Selenastrum capricornutum</u>	98

Table

10

11

12

13

14

15

16

17

18

19

<u>Table</u>		<u>Page</u>
10	EC ₅₀ and EC ₁₀ for the specific growth rate (0-22 h) of <u>Selenastrum capricornutum</u> exposed to anthracene and UV-A radiation	101
11	The effects of anthracene (ANTH) and UV-A radiation on the incorporation of ¹⁴ C-bicarbonate in <u>Selenastrum capricornutum</u> after 4 h exposure	104
12	The effects of anthracene (ANTH) and UV-A radiation on the incorporation of ¹⁴ C-bicarbonate in <u>Selenastrum capricornutum</u> after 24 h exposure	106
13	EC ₅₀ and EC ₁₀ for ¹⁴ C-bicarbonate incorporation of <u>Selenastrum capricornutum</u> after 24 h UV-A exposure	108
14	The effects of anthracene (ANTH) and UV-A radiation on forward blue scatter (cell size) of <u>Selenastrum capricornutum</u> , as measured by flow cytometric techniques	113
15	The effects of anthracene (ANTH) and UV-A radiation on red fluorescence (cellular chlorophyll concentration), normalized for cell size, of <u>Selenastrum capricornutum</u> , as measured by flow cytometric techniques	118
16	The effects of anthracene (ANTH) and UV-A radiation on the cell viability index (CVI) of <u>Selenastrum capricornutum</u> , as measured by flow cytometric techniques	122
17	EC ₅₀ and EC ₁₀ for the cell viability index (CVI) of <u>Selenastrum capricornutum</u> after 4 and 28 h UV-A exposure	126
18	The effects of anthracene (ANTH) and UV-A radiation on cell viability (% non-viable cells) of <u>Selenastrum capricornutum</u> , as measured by flow cytometric techniques	131
19	EC ₅₀ and EC ₁₀ for the cell viability (% non-viable cells) of <u>Selenastrum capricornutum</u> after 28 h UV-A exposure	137

Table

Page

20	The effect of the concentration of colored carotenoid pigments in <u>S. capricornutum</u> cells on the percent inhibition of ¹⁴ C-bicarbonate incorporation due to the photo-induced toxicity of 35 µg/L anthracene in the presence of 375 µW/cm ² UV-A radiation	156
----	---	-----

Figure

1

2

3

4

5

6

7

8

9

S
I
A
a
e
O
C

LIST OF FIGURES

<u>Figure</u>	<u>Page</u>
1 Transmittance characteristics of Plexiglass II-UVT (UV-transparent chamber) and Plexiglass II-UVA (UV-opaque chamber) to ultraviolet and visible radiation (280-700 nm)	21
2 Monthly average depth (in meters) at which PAR (400-700 nm), UV-A (365 +/- 36 nm) and UV-B (310 +/- 34 nm) was reduced to 1% of their surface intensities at the 19 km station in Lake Michigan	32
3 Monthly average UV-B inhibition efficiencies, micro-phytoplankton density (cells/ml) and composition of the phytoplankton assemblages of the <u>in situ</u> incubations performed at the 19 km station in Lake Michigan in 1986	39
4 Primary production depth profiles for offshore Lake Michigan during the spring	53
5 Primary production depth profiles for offshore Lake Michigan during the summer	55
6 Primary production depth profiles for offshore Lake Michigan during May and August for current and future (+21% UV-B) UV-B intensities	61
7 Spectral characteristics of General Electric F40 BLB blacklight fluorescent lamps	74
8 Anthracene concentration in test medium during a photo-induced toxicity of anthracene experiment at 218 $\mu\text{W}/\text{cm}^2$ UV-A	78
9 Optical configuration of the Ortho Instruments Cytofluorograf 50-H	83

Figure

10

11

12

13

14

15

16

17

18

19

<u>Figure</u>		<u>Page</u>
10	Flow cytometric analysis cytogram of fluorescein (green) fluorescence and chlorophyll (red) fluorescence of <u>Selenastrum capricornutum</u> cells stained with FDA	88
11	The effects of anthracene and UV-A radiation on the specific growth rate (0-22 h) of <u>Selenastrum capricornutum</u>	99
12	Effects isopleths for the specific growth rate (0 - 22 h) of <u>Selenastrum capricornutum</u> exposed to anthracene and UV-A radiation . . .	102
13	The effects of anthracene and UV-A radiation on the ¹⁴ C-bicarbonate incorporation on a per cell basis of <u>Selenastrum capricornutum</u> after 24 h UV-A exposure	107
14	Effects isopleths for the primary production (¹⁴ C-bicarbonate incorporation in DPM/ml) of <u>Selenastrum capricornutum</u> after 24 h UV-A exposure	110
15	The effects of anthracene and UV-A radiation on cell size (forward blue scatter) of <u>Selenastrum capricornutum</u> after 4 and 28 h UV-A exposure	115
16	The effects of anthracene and UV-A radiation on cellular chlorophyll concentration (red fluorescence), normalized to cell size, of <u>Selenastrum capricornutum</u> after 4 and 28 h UV-A exposure	119
17	The effects of anthracene and UV-A radiation on the cell viability index (CVI) of <u>Selenastrum capricornutum</u> after 4 and 28 h UV-A exposure	124
18	Effects isopleths for the cell viability index (CVI) of <u>Selenastrum capricornutum</u> after 4 and 28 h UV-A exposure	127
19	The effects of anthracene and UV-A radiation on the percentage of non-viable <u>Selenastrum capricornutum</u> cells after 28 h UV-A exposure	133

Figure

20

21

<u>Figure</u>		<u>Page</u>
20	Effects isopleths for the percentage of non-viable <u>Selenastrum capricornutum</u> cells after 28 h UV-A exposure	134
21	The effect of the concentration of colored carotenoid pigments (ng carotenoids/ 10^6 cells) on the percent inhibition of ^{14}C -bicarbonate incorporation (DPM/ 10^4 cells) after an 8 h exposure to 35 $\mu\text{g/L}$ anthracene and 375 $\mu\text{W/cm}^2$ UV-A radiation	159

respo
biolo
energ
chlor
and o
Light
photob
and vi
benign
presen
photoch
inhibit
radiati
molecul
acids a
1982; N
photo-in
whereby
compound
(Foote, 1

INTRODUCTION

The absorption of light by chemical molecules is responsible for important photochemical processes in biological systems. Photosynthetic organisms utilize the energy generated from the absorption of solar radiation by chlorophyll and accessory pigments to produce organic carbon and oxygen, which form the basis for life on this planet. Light is also utilized by organisms for other important photobiological processes, such as phototaxis, photoperiodism, and vision. However, not all light absorptive processes are benign to biological organisms. Ultraviolet (UV) radiation present in solar irradiance can cause detrimental photochemical alterations in biological systems, leading to inhibition or death (Giese, 1964). Direct absorption of UV radiation by macromolecules can result in breakage of molecular bonds and inactivation of cellular proteins, nucleic acids and other macromolecules (Giese, 1964; Peak and Peak, 1982; Noorudeen and Kulandaivelu, 1982). Alternatively, the photo-induced toxicity can proceed via an indirect pathway, whereby absorption of UV radiation by a photosensitizer compound produces toxic free radicals and oxygen species (Foote, 1976; Peak et al., 1981). Concern about depletion of

the stratospheric ozone layer and the concomitant increase in UV radiation reaching the earth's surface has provided the impetus for determining the effects of UV radiation on aquatic organisms (Calkins, 1982a), especially phytoplankton which form the base of aquatic food chains.

Environmental matrices, such as the atmosphere and natural waters, and their associated components have differential absorptive capacities for the ultraviolet portion of the electromagnetic spectrum. Ozone in the stratosphere effectively removes all solar radiation with wavelengths shorter than approximately 290 nm. Therefore, the UV portion of the solar spectrum is from 290-400 nm. Originally, solar UV radiation (SUVR) was thought to be greatly attenuated by natural waters so that it does not penetrate to significant depths in surface waters. However, Jerlov (1950) determined that oceanic waters were fairly transparent to SUVR. Later studies (Smith and Baker, 1981; Calkins, 1982b) conclusively demonstrated that SUVR penetrates to ecologically significant depths in marine and freshwater systems.

Both components of SUVR, UV-B (290-320 nm) and UV-A (320-400 nm) radiation, have been observed to be inhibitory to phytoplankton (Calkins and Thordardottir, 1980; Worrest, 1983; Jokiel and York, 1984). However, most phytoplankton species are not affected by UV-A radiation, even at full sunlight intensities (Jokiel and York, 1984). Therefore, the shorter and more biologically injurious UV-B wavelengths are

thought to be mainly responsible for the inhibitory effects of solar radiation on phytoplankton assemblages in natural waters (Lorenzen, 1979; Smith et al., 1980; Worrest, 1983). UV-B radiation has been demonstrated to inhibit many important processes in phytoplankton. Inhibition of photosynthesis and primary production by UV-B radiation has been observed in marine and freshwater phytoplankton assemblages (Lorenzen, 1979; Smith et al., 1980; Hobson and Hartley, 1983; Paerl et al., 1985). UV-B radiation inhibits photosynthesis by direct inactivation of the photosystem II reaction center (Brandle et al., 1977; Noorudeen and Kulandaivelu, 1982). Cell division was inhibited in freshwater and marine phytoplankton species by environmentally relevant UV-B intensities (Calkins and Thordardottir, 1980; Jokiel and York, 1984; Dohler, 1985). Protein biosynthesis and photosynthetic pigment concentrations decreased in diatoms and blue-green algae which were exposed to UV-B radiation (Dohler, 1985; Dohler et al., 1986). It was suggested that the decreased protein biosynthesis and accumulation of free amino acids in algae exposed to UV-B radiation resulted from inhibition of glutamine synthetase and glutamate synthase (GOGAT) by UV-B radiation (Dohler, 1985).

Besides the inhibitory effects of UV-B radiation on primary production and other functional processes of phytoplankton communities, UV-B radiation can alter phytoplankton community structure due to species-specific differences in sensitivity to UV-B radiation. Marine diatoms

are g

green

algae

leopo

produ

diator

microc

Chaetc

(Worre

intrag

been ol

SUVR a

possibl

hydros

algae,

diatoms

photosy

As

radiati

systems

effects

penetra

effects

charact

Baker, .

suggest

are generally more sensitive to UV-B radiation than freshwater green algae (Calkins and Thordardottir, 1980). Blue-green algae, such as Anabaena cylindrica and Synechococcus leopoliensis, are more resistant to inhibition of primary production and growth by UV-B radiation, relative to marine diatoms (Dohler, 1985; Dohler et al., 1986). In estuarine microcosms exposed to simulated solar UV-B radiation, Chaetoceros spp. was more tolerant than other diatom species (Worrest et al., 1981). Although large intraphyla and intragenera differences in sensitivity to UV-B radiation have been observed, the relative sensitivities of phytoplankton to SUVR appears to be diatom > green > blue-green. It is possible that the great intensities of SUVR penetrating the hydrosphere in the summer may favor production of blue-green algae, which are more resistant to UV radiation, relative to diatoms which are more sensitive to inhibition of photosynthesis and growth by UV-B radiation.

Assessment of the environmental consequences of solar UV radiation on the primary production of marine and freshwater systems requires characterization of both the exposure and the effects of SUVR on natural phytoplankton assemblages. The penetration of UV-B radiation into oceanic waters and its effects on marine primary production has been well characterized (Worrest, 1983; Smith and Baker, 1981; Smith and Baker, 1982). Results from in situ phytoplankton incubations suggest that current intensities of SUVR are inhibiting

primary

coastal

1983).

product

1980).

of SUV

SUVR on

et al.

available

predict

freshwa

UV

sensiti

When

electro

singlet

triplet

(or pho

sensiti

from ba

reactio

interac

electro

(Grossw

can als

dismuta

primary production in the top third of the euphotic zone in coastal marine waters (Lorenzen, 1979; Hobson and Hartley, 1983). In oligotrophic oceanic waters, SUVR inhibited primary production in the top 40% of the euphotic zone (Smith et al., 1980). However, few studies have investigated the penetration of SUVR in fresh waters (Calkins, 1982b) or the effects of SUVR on natural freshwater phytoplankton assemblages (Paerl et al., 1985). Insufficient information is currently available to accurately estimate the effects of current and predicted future UV intensities on primary production in freshwater systems.

UV radiation can also induce toxicity indirectly via sensitizer-mediated phototoxic reactions (Foote, 1968; 1976). When a photosensitizer absorbs UV radiation, it is electronically excited to its singlet state. The excited singlet photosensitizer quickly converts to its longer-lived triplet state. With very few exceptions, sensitizer-mediated (or photo-induced) toxic reactions proceed via the triplet sensitizer (Foote, 1976). Photo-induced toxicity can result from basically two types of sensitizer-mediated phototoxic reactions. In type I reactions, a triplet photosensitizer interacts with a substrate directly via hydrogen atom, electron, or energy transfer, thereby generating free radicals (Grossweiner and Zwicker, 1961). The reduced photosensitizer can also react with oxygen producing superoxide, which can dismutate to hydrogen peroxide (Freeman and Crapo, 1982).

Free radicals, superoxide and hydrogen peroxide have all been implicated in lipid peroxidation which can lead to membrane destabilization and subsequent toxicity (Freeman and Crapo, 1982; Foote, 1976). Type II reactions involve the transfer of excitation energy from the triplet photosensitizer to molecular oxygen thereby generating singlet oxygen (Foote, 1968). Singlet oxygen can oxidize enzymes, RNA and other subcellular structures and macromolecules resulting in photo-induced toxicity (Foote, 1976).

The dominance of type I or II mechanisms depends on the photosensitizer involved in the reaction. Sensitizers that are readily oxidized, such as phenols and amines, or reduced, such as quinones, will react via type I reactions, especially at small concentrations of oxygen (Grossweiner and Zwicker, 1961; Foote, 1976). Compounds not so easily reduced or oxidized, including thiophene compounds (Arnason et al., 1981; Kagan et al., 1984), photosensitizing dyes (Jahnke and Frenkel, 1978; Foote et al., 1970), psoralens (Joshi and Pathak, 1983), and polycyclic aromatic hydrocarbons (Foote, 1976; Sinha and Chignell, 1983), favor type II reactions. Indirect evidence, consisting of chemical trapping, kinetic and quenching studies (Jahnke and Frenkel, 1978; Foote et al., 1970; Pooler and Valenzano, 1979; Sinha and Chignell, 1983), overwhelmingly supports the intermediacy of singlet oxygen in most photosensitized reactions.

Polycyclic aromatic hydrocarbons (PAH) are the most important photosensitizing contaminants in the environment. PAH constitute a class of organic compounds consisting of two or more fused benzene rings. They are ubiquitous pollutants and are found in all environmental matrices: Atmosphere (Andren and Strand, 1981; Neff, 1979); marine and freshwater systems (Bates et al., 1987; Eadie et al., 1983); sediments and soil (Barrick and Prah1, 1987; Hites et al., 1980; Means et al., 1980); and the biota (Baumann et al., 1987; Eadie et al., 1983; McCain et al., 1988). The major environmental sources of PAH include both man-made inputs, such as fossil fuel combustion, coking and steel operations, petroleum refining and oil spills, and natural inputs, such as forest and prairie fires (Neff, 1979; Eisler, 1987). Nearly 230,000 metric tons of PAH are estimated to enter the world's surface waters every year (Neff, 1979). PAH reach the aquatic environments in domestic and industrial sewage effluents, in urban surface runoff, from deposition of airborne particulates, and especially from spillage of petroleum and petroleum products into water bodies (Hoffman et al., 1984; Barrick and Prah1, 1987; Readman et al., 1987; Eisenreich et al., 1981). In heavily contaminated aquatic systems, PAH concentrations in aquatic sediments are in the mg/kg range and in surface waters due to their limited solubility reach concentrations of 2 $\mu\text{g/L}$ (Neff, 1979; Eisler, 1987). The continued reliance on fossil fuels for transportation and

power generation and the resulting PAH contamination of aquatic environments necessitates an accurate assessment of the hazard of the photo-induced toxicity of PAH to aquatic organisms.

Photo-induced toxicity, where the toxicity of PAH is greatly enhanced by simultaneous UV radiation exposure, has been demonstrated with a wide variety of PAH and aquatic organisms. The photo-induced toxicity of PAH to Paramecium was observed more than 50 years ago (Mottram et al., 1938). The photo-induced toxicity of anthracene, a linear three-ring PAH, has been well characterized for fishes (Kagan et al., 1985; Oris and Giesy, 1985; 1986), aquatic insects (Oris et al., 1984; Kagan et al., 1985), zooplankton (Morgan and Warshawsky, 1977; Allred and Giesy, 1985; Kagan et al., 1985; Newsted and Giesy, 1987; Holst, 1987) and amphibians (Kagan et al., 1984). Other PAH which have exhibited photo-induced toxicity due to simultaneous UV radiation exposure include: fluoranthene, pyrene, benzo[a]pyrene, benzo[a]anthracene, acridine, and benzo[a]fluorene (Oris and Giesy, 1987; Newsted and Giesy, 1987; Kagan et al., 1985). Quantitative structure-activity models for the photo-induced toxicity of PAH to fishes (Oris and Giesy, 1987) and daphnids (Newsted and Giesy, 1987) have determined that PAH triplet (phosphorescence) lifetime is the best predictor of the potential photo-induced toxicity of a PAH. Hazard assessments of the photo-induced toxicity of PAH (Oris and Giesy, 1986; Holst, 1987) suggest

that aquatic systems heavily contaminated with PAH may be experiencing increased mortality and reduced reproductive success of aquatic organisms.

Although the photo-induced toxicity of PAH has been well characterized for aquatic animals, few studies have investigated the effects of the photo-induced toxicity of PAH to algae. PAHs (anthracene, benzo[a]pyrene, and benzo[a]anthracene), which have demonstrated great photo-induced toxicity to aquatic animals, had been observed to have no effects on algal photosynthesis (Oris et al., 1984) or growth (Cody et al., 1984) at PAH concentrations less than their aqueous solubility. It was suggested that the resistance of algae to the photo-induced toxicity of PAH results from the great concentrations of singlet-oxygen quenching carotenoids present in algal cells (Landrum et al., 1986). However, both algal studies were limited in scope and their experimental designs were inadequate to accurately assess the photo-induced toxicity of PAH to algae. The importance of algae in aquatic food chains requires that an accurate characterization of the photo-induced toxicity of PAH to algae be performed such that phytoplankton can be included in hazard assessments of the photo-induced toxicity of PAH to aquatic ecosystems.

The purpose of the present study was to (1) characterize the direct effects of solar UV radiation to the primary production of natural freshwater phytoplankton assemblages,

and (2) investigate UV radiation indirect toxicity, via the photo-induced toxicity of PAH, to algae, in general. Several studies have already assessed the hazard of current and predicted future UV intensities to marine primary production, but insufficient information was available to complete such an assessment for primary production in freshwater systems. The absence of conclusive evidence of the photo-induced toxicity of PAH to algae at environmentally relevant PAH concentrations necessitated examining the photo-induced toxicity of PAH to algae in the laboratory under well-defined conditions of lighting and water quality. Anthracene was the chosen PAH to be investigated because it is non-carcinogenic, it is a commonly occurring PAH in the environment (Neff, 1979), and it demonstrates intermediate water solubility and photo-induced toxicity potency (Newsted and Giesy, 1987; Oris and Giesy, 1987). The green alga, Selenastrum capricornutum, was utilized as the test organism.

Objectives

The overall objectives of the present study were two-fold:

I. To characterize the penetration of solar UV radiation (SUVR) into an oligotrophic freshwater system, specifically offshore Lake Michigan, and to determine the effect of SUVR on the primary production of natural phytoplankton assemblages in Lake Michigan in an effort to estimate the potential hazard

current and predicted future UV intensities may pose to primary production in freshwater systems.

The specific objectives were to:

1. Measure the penetration of UV-A and UV-B radiation into Lake Michigan, as well as to monitor for seasonal changes in SUVR penetration;

2. Investigate the inhibition of primary production of natural phytoplankton assemblages in Lake Michigan by SUVR, as determined by in situ incubations in chambers which selectively removed portions of the solar UV spectrum;

3. Use the information from 1) and 2) to determine the dose-response relationships between UV dose and inhibition of primary production;

4. Determine if seasonal phytoplankton assemblages are differentially sensitive to inhibition of primary production by SUVR;

5. Construct a predictive hazard assessment model utilizing the above information to determine the effect of current and predicted future UV intensities on total lake productivity.

II. To investigate in detail the toxicity of anthracene to algae under simulated SUVR to ascertain the hazard the photo-induced toxicity of PAH may pose to algae in the aquatic environment.

The specific objectives were to:

1. Determine the dose-response relationships among anthracene concentrations, UV radiation intensity, and algal growth rate, ^{14}C incorporation, and flow cytometric endpoints;
2. Use the information gained in 1) to assess the potential hazard of PAH contamination and photo-induced toxicity to algae in aquatic systems under natural conditions;
3. Determine site(s) and mode(s) of toxic action by examining the differential sensitivity of the various toxicity endpoints investigated in 1);
4. Investigate the protection provided by carotenoids in algal cells to the photo-induced toxicity of anthracene, as well as to determine if the photo-induced toxicity of anthracene proceeds via a type II (singlet oxygen) mechanism, in vivo.

Organization of dissertation

This dissertation is organized into three chapters. The first chapter is concerned with studies investigating the penetration of solar UV radiation into Lake Michigan and its effects on natural phytoplankton assemblages. The last portion of Chapter 1 describes the predictive hazard assessment model constructed to estimate the effects of current and predicted future UV intensities on freshwater primary production. The second chapter describes experiments conducted to investigate the photo-induced toxicity of

anthracene to algae. The third chapter describes an experiment, specifically addressing Objective II.4 above, where the effects of a carotenoid biosynthesis inhibiting herbicide on the photo-induced toxicity of anthracene were investigated. The dissertation concludes with a brief summary of the major conclusions of these studies.

CHAPTER 1

PENETRATION OF ULTRAVIOLET RADIATION INTO LAKE MICHIGAN AND THE EFFECTS ON THE PRIMARY PRODUCTION OF NATURAL PHYTOPLANKTON ASSEMBLAGES.

INTRODUCTION

Concern about the depletion of ozone in the atmosphere resulting from man-made trace gases and the resultant increase in UV radiation reaching the earth's surface (NRC 1979; 1982) has caused increased interest in the effects of UV radiation on natural phytoplankton assemblages. Little work had been conducted in this area because solar UV radiation (SUVR) was thought to be greatly attenuated by surface waters, and thus, not penetrate to significant depths in oceans and lakes. However, Jerlov (1950) determined that oceanic waters are fairly transparent to SUVR. UV-B radiation (290-320 nm) was known to inhibit primary production in the upper surface waters of the ocean (Steemann Nielsen, 1964; Jitts et al., 1976; Lorenzen 1979; Smith et al., 1980; Worrest et al., 1981; Hobson and Hartley, 1983), but little information was available on the penetration of SUVR into fresh waters (Calkins, 1982b) or the effects of SUVR on freshwater

phytoplankton (Calkins and Thordardottir, 1980; Paerl et al., 1985). The inhibition of photosynthesis and other biological processes in natural phytoplankton assemblages by UV radiation has also received little attention relative to photoinhibition caused by visible light because special incubation chambers, lighting and light sensors are required to quantify the UV portion of solar radiation and its effects on phytoplankton populations.

The inhibition of primary production of marine phytoplankton assemblages by SUVR has been well characterized (Smith and Baker, 1982). Incubations of phytoplankton in chambers completely transparent to solar radiation (quartz bottles or Vycor tubing) in situ in oceanic and coastal marine waters resulted in reduced primary production relative to phytoplankton incubated in mylar-covered or pyrex glass chambers, which are nearly opaque to UV-B radiation (Smith et al., 1980; Lorenzen, 1979; Hobson and Hartley, 1983). In coastal waters, inhibition of primary production by SUVR was observed to a maximum depth of 1.5 m, corresponding to UV-B intensities of less than 0.1% of UV-B intensities at the surface (Lorenzen, 1979). This suggests that primary production in the top third of the euphotic zone is less than would be predicted from incubations of phytoplankton in UV-B opaque containers. Inhibition of the primary production of phytoplankton was observed to a depth of 3 m in a productive fjord (chlorophyll-a concentrations ranged from 5-30 $\mu\text{g/l}$) in

British Columbia (Hobson and Hartley 1983). This also corresponded to approximately the top third of the euphotic zone. In oligotrophic oceanic waters, SUVR inhibits primary production in the top 40 % of the euphotic zone (Smith et al., 1980). Thus, it appears that solar UV radiation is a heretofore often neglected, but important, environmental parameter in the upper portion of the euphotic zone in all marine waters.

Although much is known about inhibition of phytoplankton primary production by SUVR in marine waters, I am aware of only one other in situ experiment, performed in a freshwater system. In that experiment, Paerl et al. (1985) observed inhibition of primary production of natural freshwater assemblages and laboratory cultures in quartz incubation chambers relative to UV-B opaque pyrex chambers. No measurements of the SUVR associated with the observed inhibition were recorded, though. Therefore, the specific objectives of this research were to: (1) Measure the penetration of both the UV-A and UV-B portions of SUVR into Lake Michigan; (2) Investigate the inhibition of primary production of natural freshwater phytoplankton assemblages by SUVR, as determined by in situ incubations in chambers which selectively removed portions of the solar UV spectrum; (3) Measure the incident dose of UV-A and UV-B radiation received by each chamber during the in situ incubations to determine the dose-response relationship of the inhibition of primary

production by SUVR; (4) Monitor the seasonal changes in the penetration of SUVR; (5) Determine if different phytoplankton assemblages are differentially sensitive to inhibition by SUVR; and (6) Develop a predictive hazard assessment model for the effect of current and predicted future UV intensities on total lake productivity. These results will enable limnologists to correct estimates of primary production measured under inappropriate conditions, such as utilizing UV-B opaque incubation chambers or artificial lighting which does not contain UV-B radiation, for the inhibitory effects of SUVR expected in the natural environment. This will increase the accuracy of Lake Michigan primary production and carrying capacity estimates.

MATERIALS AND METHODS

Study site

Measurements of solar radiation and in situ determinations of primary production were made in Lake Michigan (43°28.76 N, 86°28.76 W); 19 km off Grand Haven, Michigan, from April to October 1986, during daily cruises of the R/V Shenelon (GLERL/NOAA). Measurements of solar radiation also were conducted in the spring and summer of 1983 and 1985 at the same location and in 1983 along a transect from Grand Haven to the station 19 km offshore. The water at this station is 85 m deep and is typical of the oligotrophic

waters found in offshore Lake Michigan. Epilimnetic chlorophyll-a concentrations in offshore Lake Michigan range from 1-3 $\mu\text{g/l}$ and the euphotic zone, defined here as the depth to which 1% of the surface PAR intensity penetrates, is usually 20-30 meters in the summer (Scavia et al., 1986).

Solar radiation measurements

Solar UV radiation and visible light were measured by different broad-band spectroradiometers. Broad-band UV-A (365 \pm 36 nm) and UV-B (310 \pm 34 nm) radiation were quantified by a Macam Photometrics Ltd. Model UV-103 radiometer with Model SD103 cosine-corrected Ge-As photodiodes modified for underwater use (fitted with water-tight, wavelength selective filters) and reported in units of microWatt/cm² ($\mu\text{W}/\text{cm}^2$). Photosynthetically active radiation (PAR, 400 - 700 nm) was quantified by a Li-Cor LI-510 Integrator with a LI-192s Underwater Quantum Sensor, which was cosine-corrected and calibrated for underwater use, by using the conversion tables in the LI-150 Integrator manual and reported in units of microMoles/meter²-second ($\mu\text{M}/\text{m}^2\text{-sec}$).

UV-A, UV-B and PAR were measured at one meter intervals from one meter to five meters, to determine the broad-band attenuation coefficients in Lake Michigan. The depths at which the penetration of solar radiation into Lake Michigan was measured were rarely greater than five optical depths, which is the depth in meters equal to five divided by

attenuation coefficient (m^{-1}). Therefore, both shifts in the shape of the waveband being measured and the systematic error associated with measuring broad-band attenuation coefficients due to differential penetration of different wavelengths of light should be small (less than 10%) (Smith and Calkins, 1976). Solar radiation intensity decreases with depth according to equation 1,

$$\ln(I_z) = \ln(I_0) - K * Z \quad [1]$$

where Z = depth in meters, I_z = intensity at depth Z , I_0 = intensity just below the water surface and K = broad-band diffuse attenuation coefficient. The broad-band diffuse attenuation coefficient (K) was estimated as the negative slope of the linear regression of the natural log of intensity as a function of depth in meters.

The cumulative incident dose, the amount of solar radiation incident on each chamber during the incubation, was determined for each of the three wavebands. The intensity of solar radiation at the lake surface was monitored by measuring UV-A and UV-B hourly and continuously recording PAR on-deck during in situ phytoplankton incubations. The cumulative incident dose was calculated by converting surface intensity values to the estimated cumulative dose, in units of kJ/m^2 for the UV wavebands and M/m^2 for PAR, at the incubation depth for each of the three bandwidths using the measured attenuation

coefficient on that day. The surface measurements were first corrected for loss at the air/water interface before using the attenuation coefficient to estimate the dose at each incubation depth. When the PAR attenuation coefficient was not measured it was estimated by assuming $K_{\text{PAR}} = 1.7/Z_{\text{SD}}$, where Z_{SD} is the Secchi disk depth (in meters) on that day. The constant 1.7 represented the mean of the relationship of PAR attenuation coefficient measurements and Secchi disk depth observed during 1983, 1985 and 1986 cruises.

¹⁴C-bicarbonate assimilation

A total of twenty-nine in situ incubations at depths ranging from 1 m to 7 m, were performed from April to October in 1986 at the 19 km station in Lake Michigan. Lake water was collected just after dawn from the depths at which the incubation chambers were to be incubated in situ using 4- or 10-liter Niskin bottles. Water samples were incubated in two types of chambers. One type was constructed from UV-opaque plexiglass (Plexiglass II-UVA, Rohm and Haas Co.), and transmitted less than 1% of solar radiation at wavelengths < 370 nm. The second type was constructed of UV-transparent plexiglass (Plexiglass II-UVT, Rohm and Haas Co.), and transmitted less than 1% of solar radiation at wavelengths < 292 nm (Figure 1). The transmittance of both chambers in the visible portion of the solar spectrum was identical. A chamber of each type was incubated at each of two depths

Figure 1. Transmittance characteristics of Plexiglass II-UVT (UV-transparent chamber) and Plexiglass II-UVA (UV-opaque chamber) to ultraviolet and visible radiation (280-700 nm) as measured by a Gilford 2600 UV/Vis Spectrophotometer (referenced to air). Relative spectral response of Macam SD103 UV-B and UV-A photodiodes (dashed lines) is superimposed over Plexiglass transmittance characteristics.

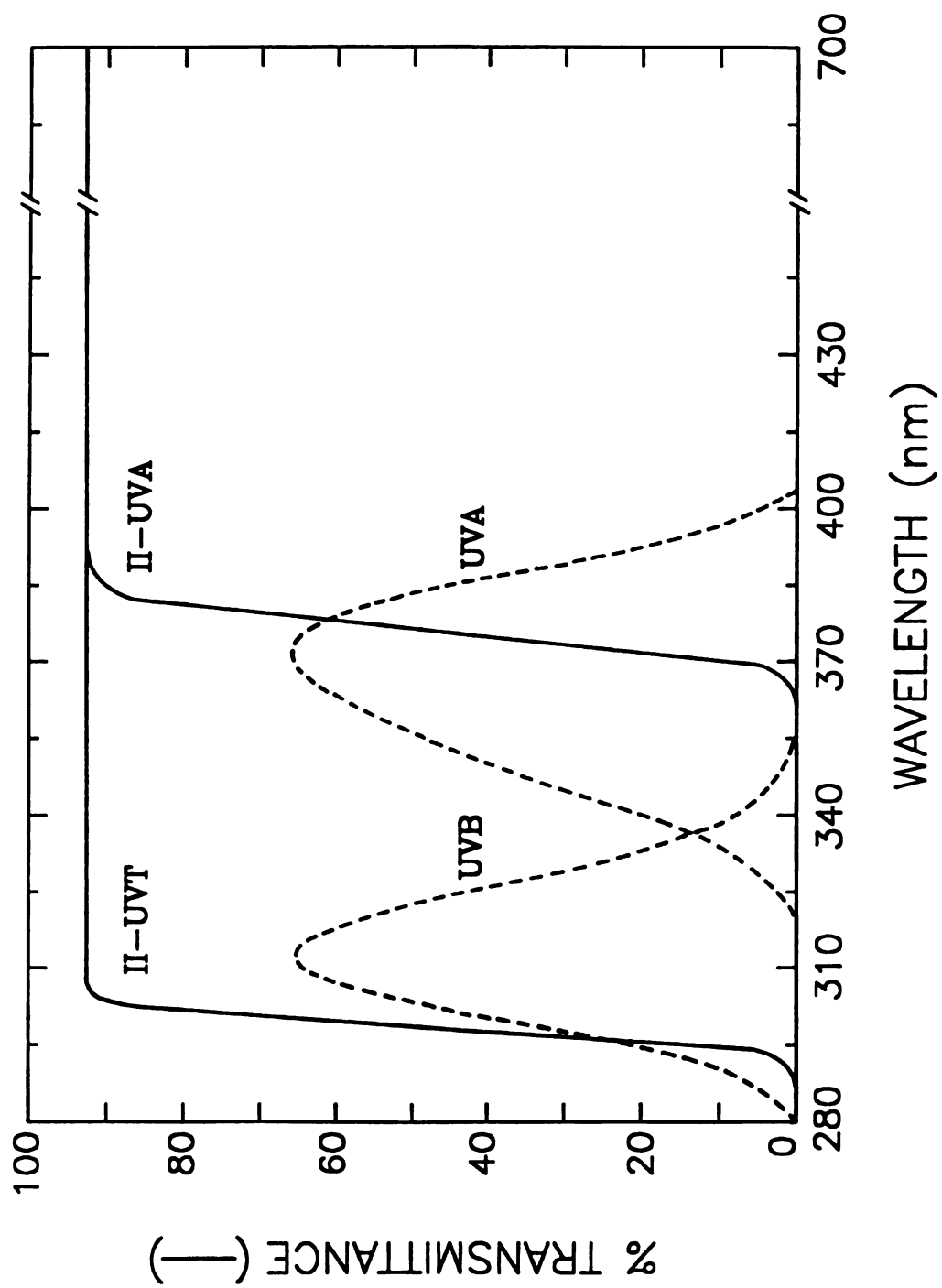


Figure 1.

during each daily cruise. Each chamber contained six discrete 178 ml compartments, therefore, six replications of each treatment were performed at each depth. The chambers were incubated in situ on station for approximately eight hours, centered around solar noon, to obtain an accurate estimate of the effects of UV radiation on daily phytoplankton production. All possible precautions were taken to prevent the chambers from being exposed to full sunlight prior to in situ incubations.

Primary production of the natural phytoplankton assemblages was assessed by the traditional ^{14}C technique (Vollenweider, 1969). Each compartment was spiked with 10 μCi of ^{14}C -sodium bicarbonate (Research Products International). The algae were collected by filtering through GF/C glass fiber filters (1.2 μm apparent porosity) at less than 3 p.s.i. (75 mm Hg). All chambers were kept in darkness until they were processed. Filtering was performed on-board ship in a dimly-lit laboratory within one hour of the termination of the incubation. The filters were placed in individual scintillation vials. The vials were dried in a desiccator, exposed to HCl fumes for two hours, and placed back in the desiccator and dried overnight. Ten ml of Safety Solve scintillation cocktail (Research Products International) was added to each vial. After waiting 24 hours to allow the filters to clear, the vials were counted by a BetaTrac 6895 liquid scintillation counter.

The ^{14}C incorporated was converted to primary production estimates using the method described in Vollenweider (1969) and reported as $\text{mg C/m}^3/\text{hr}$. The percent inhibition of primary production due to UV radiation was calculated as $1 - (\text{PP}_\text{T}/\text{PP}_0)$, where PP_T and PP_0 equal the mean primary production of the UV-transparent and UV-opaque chambers, respectively.

Each phytoplankton assemblage incubated was characterized by the dominant microplankton species and % diatom, blue-green, chrysophyte and green algae. A 1 L sample of phytoplankton from the same Niskin bottle used to fill the chamber pair was preserved in Lugol's solution. The sample was filtered through a $0.45\ \mu\text{m}$ membrane filter. The filter was cleared using immersion oil and enumeration and identification of microplankton ($5 - 100\ \mu\text{m}$) were performed using a 400x phase-contrast objective. Because of the experimental design, ultraplankton were not counted or fully included in the ^{14}C assimilation measurements.

In contrast to laboratory studies where identical irradiation conditions allow easy interpretation of the differential algal sensitivity to UV radiation, field incubations under differing UV irradiation conditions require that the response, inhibition of primary production, be normalized to the incident dose. The spectral region causing the inhibition of primary production was considered to contain UV-B radiation because UV-B radiation is known to inhibit

primary production (Worrest et al., 1980; Lorenzen, 1979) and the measured UV-B waveband (276-344 nm) represented most of the SUVR to which the UV-transparent chamber was transparent, but which was blocked in the UV-opaque chamber. To normalize the inhibition observed to the UV-B dose, the inhibition efficiency of the UV-B radiation was calculated by dividing the % inhibition observed by the cumulative incident UV-B dose. UV-B inhibition efficiency is expressed in units of % inhibition per kJ/m^2 of UV-B radiation.

Other data

Surface temperature, Secchi disk depth, pH, dissolved oxygen concentration, total alkalinity and hardness were all measured using standard methods during each incubation at the 19 km station. A bathythermograph measurement of temperature and water transparency profiles was made during most of the incubations.

Statistical analysis

The mean primary production of phytoplankton in the UV-opaque chamber was compared to the primary production in the UV-transparent chamber for each incubation using a t-test (SAS Institute, 1985).

Non-parametric statistical analysis was utilized to compare the UV-B inhibition efficiencies of different phytoplankton assemblages because heterogeneous variances were typically observed. The small number of samples of each

phytoplankton assemblage did not allow normality to be assumed or tested. Because basic assumptions of the parametric t-test were not valid, comparisons of sensitivity to UV radiation between different assemblages were tested using the randomization test (Green, 1977). The randomization test is a non-parametric test that only assumes that the observations are randomly sampled. Even when assumptions of normality and homogeneous variance are valid, the randomization test is as powerful as its parametric counterpart, the t-test (Romesburg, 1985). For the analyses, the two incubations where ^{14}C incorporation was greater in the UV-transparent chamber were assigned a UV-B inhibition efficiency of zero, signifying a complete resistance to inhibition of primary production by UV radiation. Incubations photoinhibited by PAR were excluded from the analyses. An incubation was considered to be significantly photoinhibited by PAR if the average incident PAR was greater than $1000 \mu\text{M}/\text{m}^2\text{-sec}$ and the primary production measured in the UV-opaque chamber was considerably reduced compared to other incubations with similar assemblage composition and cell density. Because of the small number of samples and the large variability associated with field studies, a type I error (α) of 0.10 was used for all UV-B inhibition efficiency comparisons with the randomization test. For all comparisons, the use of the parametric t-test would have resulted in the same conclusions.

Typically, the relative sensitivity of different species to a toxicant, in this case UV radiation, are compared via the effective dose to cause a 50% decrease in the measured endpoint (ED_{50}). The ED_{50} was estimated by probit analysis (Finney, 1971), in which the percent inhibition values were transformed to their probit values and regressed against the \log_{10} of the cumulative UV-B dose. Incubations photoinhibited by PAR were not used in the probit analyses of the different phytoplankton assemblages. Also, the two incubations in which stimulation of primary production was observed in the UV-transparent chamber were not used in the probit regressions because there are no valid probit values for responses less than or equal to zero (Finney, 1971). The ED_{10} and ED_{25} , the effective incident UV-B dose to cause a 10% or 25% inhibition in primary production, respectively, were also calculated from the probit regression. The 90% confidence limits for the ED_{xx} values were calculated using equations given by Neter et al. (1985).

RESULTS

Penetration of ultraviolet radiation into Lake Michigan

A portion of the solar radiation reaching the surface of a lake will be reflected or scattered at the air/water interface and will not penetrate into the lake. The portion reflected/scattered at the surface must be known to enable

accurate modelling of the penetration of PAR and UV radiation. The portion reflected/scattered at the surface was considered to be the difference between the predicted surface intensity from the diffuse attenuation coefficient regression and the surface value measured at the same time. This value includes the error associated with the measurement of the diffuse attenuation coefficient, however, the regressions were all of great statistical significance and the error was thus small. The portion reflected/scattered at the surface was assumed to be 10% for PAR, and empirically calculated to be 36% for UV-A and 43% for UV-B. These values are characteristic of calm seas, only. In rough seas (3-5 foot waves), inaccuracies in measuring light penetration at specified depths increased the difference between the predicted surface intensity from the diffuse attenuation coefficient regression and the measured surface value by 50-60% compared to values for calm seas.

The other component required to calculate the cumulative incident dose at a specific depth is the diffuse attenuation coefficient for that waveband. Attenuation coefficients for UV-A and UV-B radiation were inversely related to the seasonal trend in Secchi disk depth, which is a measure of water transparency to the visible light waveband. The Secchi disk depth was greatest in August, and PAR, UV-A and UV-B attenuation coefficients were all at a minimum in August (Table 1).

Table 1. Monthly averages of PAR, UV-A and UV-B maximum surface intensity and penetration into Lake Michigan from 1983, 1985 and 1986 cruises.

	MONTH									
	APRIL	MAY	JUNE	JULY	AUGUST	SEPT.	OCT.			
PAR (n=)	2	5	5	4	7	2	1			
$K_{PAR} (m^{-1})^1$	0.340	0.321	0.233	0.233	0.165	0.261	0.283			
$Z_{SD} (m)^2$	5.0	5.3	7.3	7.3	10.3	6.5	6.0			
Max. Surface intensity ($\mu M/m^2\text{-sec}$)	1530	2000	2000	2000	2000	1900	1500			
$Z_{1\%} (m)^3$	13.2	14.0	19.3	19.3	27.3	17.2	15.9			
UV-A (n=)	1	4	4	5	3	4	1			
$K_{UV-A} (m^{-1})$	0.334	0.534	0.404	0.342	0.263	0.424	0.726			
Max. Surface intensity ($\mu W/cm^2$)	5840	6200	6800	6400	6000	5000	3500			
$Z_{1\%} (m)$	12.4	7.8	10.3	12.1	15.8	9.8	5.7			
$\% PAR E.Z.^4$	94.2	55.5	53.3	62.9	57.8	56.9	36.0			

Table 1. Cont.

	MONTH						
	APRIL	MAY	JUNE	JULY	AUGUST	SEPT.	OCT.
UV-B (n=)	1	5	7	5	4	4	1
K_{W-8} (m^{-1})	1.023	0.749	0.623	0.559	0.465	0.693	0.908
Max. Surface intensity ($\mu W/cm^2$)	490	680	750	770	710	600	450
$Z_{1\%}$ (m)	4.0	5.4	6.5	7.2	8.7	5.8	4.5
% PAR E.Z.	30.0	38.6	33.7	37.6	31.9	34.0	28.1

30

¹ K = Diffuse attenuation coefficient

Note: K_{PAR} values were estimated from Secchi depth using the relationship, $K_{PAR}=1.7/Z_{SD}$. K_{W-A} and K_{W-8} were measured directly.

² Z_{SD} = Secchi disk depth

³ $Z_{1\%}$ = Depth at which solar radiation is reduced to 1% of the surface intensity. Loss at the air/water interface was assumed to be 10% for PAR, and was empirically derived to be 36% for UV-A, and 43% for UV-B.

⁴ % PAR E.Z. = the percentage of PAR euphotic zone ($Z_{1\%}$) that 1% of the surface UV radiation penetrates.

The depth at which each waveband was reduced to 1% of its surface intensity, $Z_{1\%}$, can be calculated from the monthly average of each waveband's attenuation coefficient (Table 1). The $Z_{1\%}$ for PAR is considered to be the lower limit of the euphotic zone. The $Z_{1\%}$ for each waveband was at a maximum in August (Figure 2). The $Z_{1\%}$ for UV-A and UV-B was a relatively constant proportion of the euphotic zone from April to October. One percent of the surface UV-A and UV-B radiation penetrated to depths corresponding to 58% and 35% of the euphotic zone, respectively, averaged across the months studied. The abnormally deep $Z_{1\%}$ in April and shallow $Z_{1\%}$ in October for UV-A (Figure 2) were both based on only one attenuation coefficient determination and may not be characteristic of typical April and October values.

In 1983, a transect perpendicular to the coast of Lake Michigan at Grand Haven, Michigan was performed to measure the penetration of UV-B radiation into Lake Michigan at different distances from shore (Table 2). Both the portion of UV-B radiation lost (reflected/scattered) at the air/water interface and UV-B attenuation coefficients decreased with increasing distance from the shoreline. Once outside of the plume of the Grand River, only a 30% decrease in UV-B attenuation coefficients was observed from 3 to 19 km offshore.

Figure 2. Monthly average depth (in meters) at which PAR (400-700 nm), UV-A (365 +/- 36 nm) and UV-B (310 +/- 34 nm) was reduced to 1% of their surface intensities at the 19 km station in Lake Michigan.

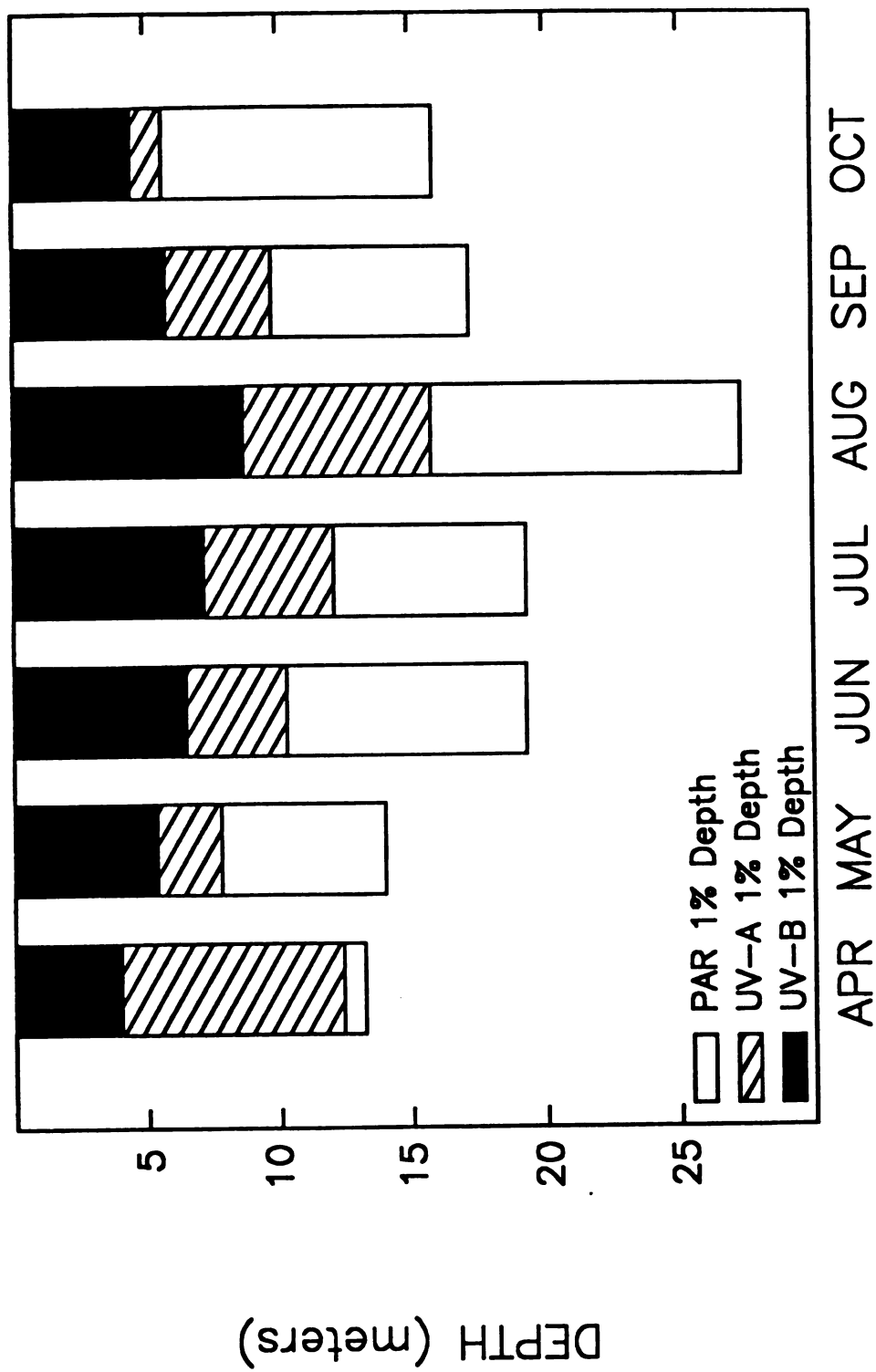


Figure 2.

Table 2. Broad-band UV-B (310 +/- 34 nm) diffuse attenuation coefficients along a transect due west from Grand Haven, Michigan into Lake Michigan on 5-23-83.

Kilometer Offshore	Loss at Air/Water Interface (%)	Attenuation Coefficient(m^{-1})	$Z_{1\%}(m)$ ¹
1 ²	92	2.005	1.0
3	73	0.964	3.4
6	69	0.875	3.9
10	27	0.822	5.2
13	36	0.825	5.0
16	40	0.731	5.6
19	39	0.684	6.0

¹ $Z_{1\%}$ = the depth at which UV-B radiation is reduced to 1% of surface intensities.

² Attenuation coefficient measured while in the plume of the Grand River.

Inhibition of primary production by UV radiation

Because of the spectral characteristics of the plexiglass chambers utilized during the in situ incubations, only inhibition of primary production by UV-B and the short wavelength portion of UV-A (320-360 nm) was investigated. Transparency to longer wavelength UV-A (370-400 nm) and visible light was identical in the two chamber types (Figure 1). Therefore, any effects of light wavelengths > 370 nm were identical in the two chamber types. However, large PAR intensities (i.e., great enough to cause photoinhibition), did cause problems in this experiment. Photoinhibition by visible light reduced ^{14}C uptake in both types of incubation chambers sufficiently to obscure the effect of inhibition by SUVR observed in some instances.

Inhibition of primary production which could be attributable to SUVR was observed during each month and for all types of phytoplankton assemblages, irrespective of dominant taxa (Table 3). Inhibition of phytoplankton production by SUVR in Lake Michigan was greatest in the spring and smallest in midsummer (Table 3). The smallest cumulative dose of UV-B radiation to significantly inhibit primary production was 1.0 kJ/m^2 , which was observed on May 15, 1986. The greatest depth at which a statistically significant inhibition was observed was 6 m (Table 3).

The algal succession pattern observed in Lake Michigan permitted the investigation of the differential sensitivity

Table 3. Incubation conditions, cumulative PAR and UV incident dose on the incubation chambers, dominant algal genera of the phytoplankton assemblages and inhibition of primary production in the UV-transparent chambers, relative to the UV-opaque chambers, measured during the in situ incubations at the 19 km station in Lake Michigan during 1986.

Date	Incub. time(h)	Depth (m)	Cumulative Dose ¹		Dominant genera	% Inhibition
			UV-A	UV-B	PAR	
4/03	8.00	1	114.5	15.2	7.7	<u>Melosira/Fragilaria</u> 55.0 **
4/03	7.72	1	111.6	14.8	7.4	<u>Melosira/Fragilaria</u> 55.1 **
4/04	7.77	1	476.5	29.9	16.1	<u>Melosira</u> 72.0 **
5/14	7.87	1	423.8	17.9	11.2	<u>Melosira</u> 54.9 **
5/14	7.98	2	243.8	8.2	7.7	<u>Melosira</u> 3.8 ns
5/15	7.78	3	54.1	2.5	5.3	<u>Melosira</u> 5.4 ns
5/15	7.63	4	30.5	1.0	3.7	<u>Melosira</u> 9.0 **
5/22	8.05	1	252.3	13.5	14.5	<u>Melosira/Dinobryon</u> 33.6 **
5/22	7.92	2	156.5	7.0	11.3 ²	<u>Mixed</u> 68.3 **
6/04	7.98	1	842.0	37.4	31.0 ³	<u>Dinobryon</u> 20.0 **
6/04	7.93	3	392.3	8.0	19.7	<u>Dinobryon</u> 24.4 **
6/05	7.93	1	273.8	13.7	14.7	<u>Dinobryon/Microcystis</u> +7.3 ⁴ *
6/05	7.93	2	179.1	6.3	11.5	<u>Dinobryon</u> 21.4 **
7/08	7.00	1	565.3	42.2	27.3	<u>Anabaena</u> 0.0 ns
7/08	6.95	3	288.4	13.1	17.3	<u>Anabaena</u> 15.0 ns
7/17	8.00	2	430.9	27.9	13.4	<u>Anabaena</u> 12.4 **
7/17	8.02	6	80.6	2.2	5.8	<u>Microcystis/Anabaena</u> 7.4 **
7/29	8.52	3	265.3	9.6	19.4	<u>Microcystis</u> +6.6 ns
7/29	8.28	7	75.8	1.0	7.2	<u>Microcystis</u> 3.3 ns
8/06	7.33	5	49.6	2.4	1.9	<u>Microcystis</u> 2.0 ns
8/07	7.88	1	531.0	43.3	26.3 ³	<u>Microcystis</u> 3.9 ns
8/07	7.87	2	410.2	29.2	22.0	<u>Microcystis</u> 46.8 **
8/28	7.47	2	222.6	15.7	16.2	<u>Microcystis</u> 23.1 **

Table 3. Cont.

Date	Incub. time(h)	Depth (m)	Cumulative Dose ¹		Dominant genera	% Inhibition
			UV-A	UV-B PAR		
9/23	7.75	1	311.5	23.3	15.9	<u>Microcystis</u> 34.8 **
9/23	7.78	2	212.4	11.5	12.2	<u>Microcystis</u> 40.5 **
9/24	8.10	3	160.5	7.9	10.1	<u>Microcystis</u> 12.9 *
9/24	8.10	4	107.5	3.8	7.8	<u>Microcystis</u> 15.7 ns
10/17	7.20	2	43.7	4.6	7.7	<u>Microcystis</u> 24.7 **
10/17	7.17	3	21.1	1.8	5.8	<u>Microcystis</u> 2.5 ns

ns = not significant

* = $p < 0.05$ ** = $p < 0.01$

¹ Cumulative PAR (400 -700 nm) incident dose in M/m^2 at the incubation depth. Cumulative UV-A (365 +/- 36 nm) and UV-B (310 +/- 34 nm) incident dose in kJ/m^2 at the incubation depth.

² Mixed assemblage included Anabaena, Asteronella, and Dinobryon.

³ Photoinhibited by PAR.

⁴ Plus sign signifies stimulation in the UV-transparent chamber compared to the UV-opaque chamber.

of the seasonal phytoplankton assemblages to inhibition of primary production by SUVR. Diatoms were the dominant micro-phytoplankton in the spring from April through May (Figure 3). Melosira islandica was the most abundant species in the spring diatom assemblages, with Cyclotella spp., Tabellaria fenestrata and Fragilaria crotonensis also being important. Because of the small numbers of cells observed in the spring (< 250 cells/ml), the peak of the spring diatom bloom was probably not sampled. The diatom-dominated assemblages were replaced in late May by chrysophytes of the genus Dinobryon, mostly D. sociale, which remained the most abundant micro-phytoplankton species into June. Blue-green algae were present in late May to early June and dominated all assemblages from July to October. Anabaena spp. were dominant in the early summer but were replaced by Microcystis aeruginosa as the summer progressed. M. aeruginosa remained dominant through October.

A seasonal difference in the sensitivity to UV-B radiation of Lake Michigan phytoplankton assemblages was observed (Table 4). Spring assemblages (April - June), in which microplankton were typically dominated by diatoms and chrysophytes, were significantly more sensitive to inhibition of primary production by UV-B radiation than summer assemblages (July - August), which were dominated by blue-green algae ($p = 0.05$). Fall assemblages (September - October), also dominated by blue-greens, were of intermediate

Figure 3. Monthly average UV-B inhibition efficiencies, micro-phytoplankton density (cells/ml) and composition of the phytoplankton assemblages of the in situ incubations performed at the 19 km station in Lake Michigan in 1986. UV-B inhibition efficiency is the % inhibition observed divided by the cumulative incident UV-B dose. Algal types abbreviations: blue-green algae (BG), diatoms (DT), chrysophytes (CH), green algae (G) and other algae, including unidentified (O).

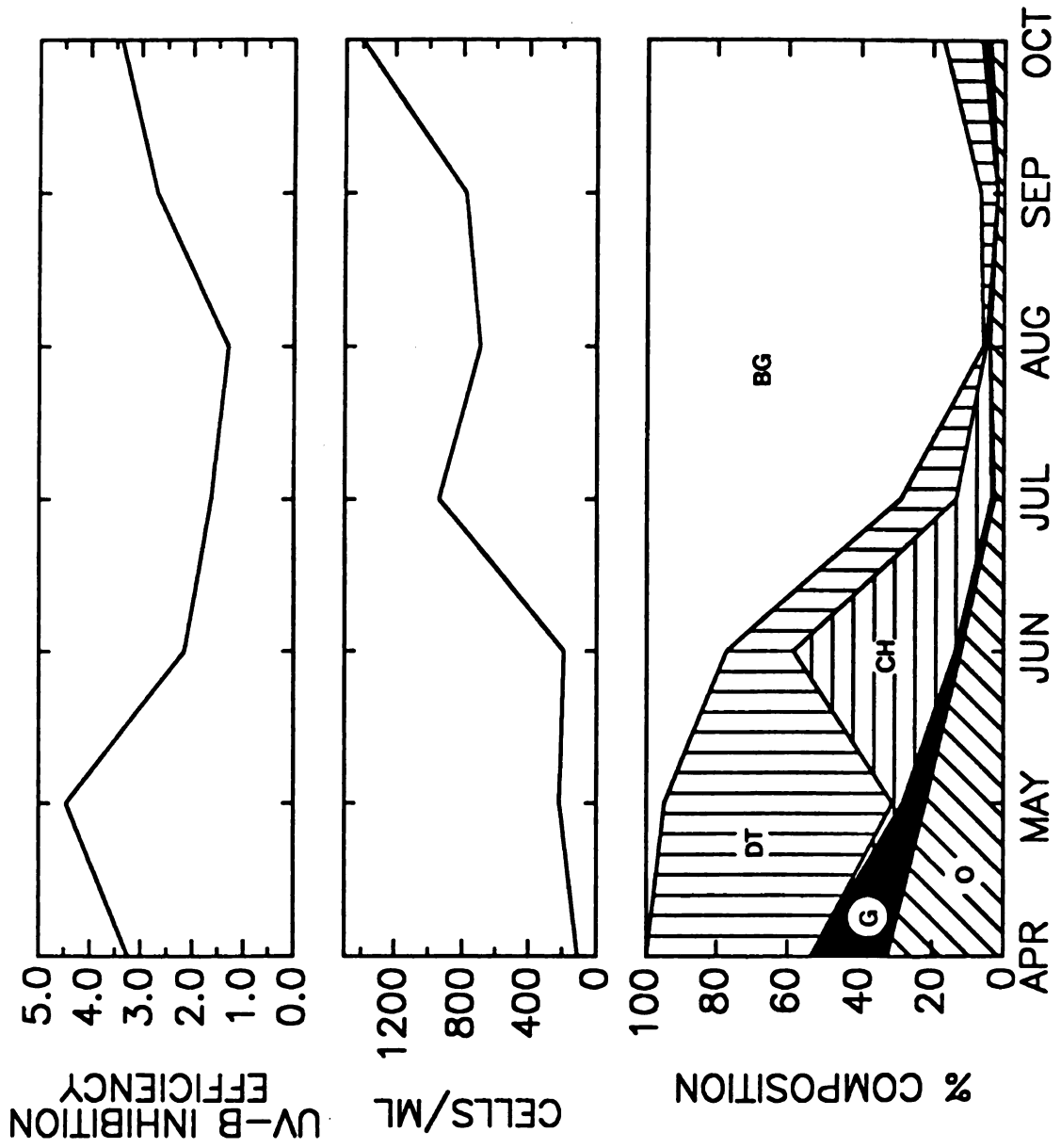


Figure 3.

U
U
U
U

P

(A

(J

(S

1

2

Table 4. Mean UV-B inhibition efficiencies for inhibition of primary production of different Lake Michigan phytoplankton assemblages. UV-B inhibition efficiency is equal to the percent inhibition of primary production in the UV-transparent chamber divided by the cumulative incident UV-B dose.

Phytoplankton assemblages	n ¹	Mean UV-B inhibition efficiency ²	90% confidence limits
Spring (April-June)	12	3.6	2.1 - 5.1
Summer (July-August)	8	1.5	0.7 - 2.3
Fall (Sept.-Oct.)	6	2.9	1.5 - 4.3

¹ n = number of incubations

² UV-B inhibition efficiency has units of % inhibition/(kJ/m² UV-B).

sensitivity and were not significantly different from spring assemblages, but were significantly more sensitive to inhibition of primary production by SUVR than summer assemblages ($p = 0.09$). The spring assemblages exhibited an ED_{50} of $17.6 \text{ kJ/m}^2 \text{ UV-B}$. Fall assemblages exhibited an ED_{50} of $30.5 \text{ kJ/m}^2 \text{ UV-B}$. In the summer when the assemblages were the least sensitive, the ED_{50} was $131.6 \text{ kJ/m}^2 \text{ UV-B}$. ED_{25} and ED_{10} , the cumulative UV-B dose required to inhibit primary production by 25% and 10%, respectively, were also calculated for the different assemblages discussed above (Table 5).

DISCUSSION

The calculation of the incident UV radiation dose at a specific depth requires that the SUVR intensity at the water's surface, the total loss at the air/water interface and the diffuse attenuation coefficient be known. The broad-band UV-A and UV-B surface intensities reported in this study are applicable to other aquatic systems near 43°N latitude. If the surface UV intensity is required for different latitudes or narrower wavebands are desired, a model (Baker et al., 1980) is available to calculate the spectral intensity incident on the earth's surface as a function of wavelength, solar zenith angle, ozone thickness, aerosol thickness and surface albedo.

Table 5. UV-B dose-response relationship for different Lake Michigan phytoplankton assemblages. ED_{xx} is the effective cumulative incident dose of UV-B radiation (in units of kJ/m^2) to cause a xx% inhibition of primary production in the UV-transparent incubation chamber, compared to the UV-opaque chamber. The 90% confidence limits are given in parentheses.

Phytoplankton assemblage	n^1	ED_{50}	ED_{25}	ED_{10}
Spring (April-June)	11	17.6 (10.2-30.4)	6.0 (3.5-10.4)	2.3 (1.3-3.9)
Summer (July-August)	7	131.6 (59.0-293.1)	25.5 (11.8-55.1)	5.7 (2.7-12.3)
Fall (Sept.-Oct.)	6	30.5 (16.8-55.4)	9.5 (5.3-17.2)	3.3 (1.8-6.0)

¹ n = number of incubations used in the probit regression.

Probit regression equations:

Spring: $\text{PROBIT} = -1.100 + 1.437 \cdot \text{Log}_{10}(\text{UV-B dose}); r^2 = 0.509$

Summer: $\text{PROBIT} = 0.182 + 0.941 \cdot \text{Log}_{10}(\text{UV-B dose}); r^2 = 0.690$

Fall: $\text{PROBIT} = -0.950 + 1.327 \cdot \text{Log}_{10}(\text{UV-B dose}); r_2 = 0.686$

Attenuation coefficients for broad-band UV radiation in Lake Michigan generally followed changes in water transparency, as measured by Secchi disk depth. Minimum attenuation coefficients for UV-A and UV-B radiation occurred in August in Lake Michigan and were six and four times greater, respectively, than attenuation coefficients for transparent oceanic waters measured at 360 nm (UV-A) and 310 nm (UV-B) (Smith and Baker, 1981). The only other attenuation coefficients for UV-B radiation in the Great Lakes were measured using the Robertson-Berger meter (Calkins, 1982b), which is heavily weighted to shorter wavelengths, and can not be directly compared to UV-B attenuation coefficient values reported here.

Inhibition of primary production of natural phytoplankton assemblages in Lake Michigan by SUVR was similar to the inhibition observed during in situ incubations in marine waters (Smith et al., 1980, Lorenzen, 1979; Hobson and Hartley, 1983). In Lake Michigan, significant inhibition by SUVR was measured to a depth of six meters and at 1% of surface UV-B intensities. Although inhibition of phytoplankton primary production by SUVR was limited to the top 1.5 m in marine coastal waters, it did occur at intensities of UV-B radiation less than 0.1% of surface UV-B intensities (Lorenzen, 1979). In productive marine waters, the top third of the euphotic zone is presently being affected by SUVR (Lorenzen, 1979; Hobson and Hartley, 1983). In

a
a
a
a
H
p
b
d
a
M
(K
o
UV
me
ty
ot
re
19
th
li
ca

offshore Lake Michigan, inhibition of phytoplankton primary production by SUVR was also restricted to the top third of the euphotic zone. Although, this is slightly less than values observed in oligotrophic oceanic waters (Smith et al., 1980), it does not appear that freshwater phytoplankton assemblages are less sensitive to inhibition by SUVR than marine assemblages.

Differential sensitivity of freshwater phytoplankton assemblages to inhibition by SUVR was observed in this study. Hobson and Hartley (1983) also observed that summer phytoplankton assemblages were less sensitive to inhibition by SUVR than spring phytoplankton assemblages dominated by diatoms. The relative sensitivity of phytoplankton assemblages to inhibition by SUVR which was observed in Lake Michigan was spring (diatoms and chrysophytes) > summer (blue-greens). This relative sensitivity to the inhibition of primary production of natural phytoplankton assemblages by UV radiation is similar to sensitivities of unialgal cultures measured under laboratory and in situ conditions. Diatoms are typically more sensitive to inhibition by UV radiation than other types of algae, while blue-green algae are relatively resistant (Worrest et al., 1981; Dohler, 1985; Dohler et al., 1986; Paerl et al., 1985). Blue-green algae can increase their content of carotenoid pigments when exposed to greater light intensities (Paerl et al., 1983), and this increased carotenoid content may confer protection against UV radiation.

u
U
d
m
I
c
a
g
o
re
a
in

by
M.
On
pr
de
in
in
kj
ob

Carotenoids are known to inhibit free radical reactions, quench singlet oxygen and photosensitized macromolecules and protect cellular systems from photooxidations induced by visible and ultraviolet radiation (Krinsky, 1979). It is unclear if other algae types can also adapt to high PAR and UV intensities by increasing carotenoid biosynthesis. The differential sensitivity of algal groups to inhibition by SUVR may be important in structuring phytoplankton communities. Inhibition of phytoplankton production by SUVR may be a contributing factor in the typical dominance of blue-green algae and the absence of diatoms in summer assemblages. The great UV dose received by phytoplankton in the epilimnion of oligotrophic systems may be favoring species which are resistant to inhibition by UV radiation, such as blue-green algae, over species, such as diatoms, which are sensitive to inhibition by UV radiation.

The depth at which 50% inhibition of primary production by SUVR would be expected to occur on a sunny day in Lake Michigan can be calculated for each seasonal algal assemblage. One would never expect to observe a 50% inhibition of primary production of summer and fall assemblages (micro-phytoplankton dominated by blue-green algae) due to environmentally relevant intensities of UV-B radiation. In the summer, the predicted incident UV-B dose required to cause a 50% inhibition is 131.6 kJ/m² UV-B. The ED₅₀ dose is much greater than would ever be observed in the Lake Michigan water column. In the fall, the

ED₅₀ dose would occur in the top meter and on a sunny day these cells would probably be photoinhibited by PAR to the extent that inhibition by SUVR would not be observed. For spring assemblages dominated by chrysophytes or diatoms, the depth of the ED₅₀ dose would be approximately 3 m on a sunny day in June. Therefore, drastic inhibition (> 50% inhibition) of primary production would be expected in Lake Michigan only during the spring.

The maximum depth at which SUVR would be expected to cause a statistically significant inhibition of primary production (ED₁₀ value from Table 5) can also be estimated. For spring assemblages, typically dominated by diatoms or chrysophytes, primary production in the upper six meters would be significantly inhibited by SUVR. For blue-green algal assemblages during the summer, the depth to which significant inhibition would be expected is also the top six meters. In the fall, the depth would be 4.5 m. It appears that the depth at which UV-B is reduced to between 1-3% of its surface intensity is the lower limit of inhibition by SUVR in Lake Michigan throughout the year (Table 1). Therefore, on a sunny day at current UV intensities, SUVR in Lake Michigan is expected to inhibit daily primary production in the top third of the euphotic zone. The above estimates of the maximum depth at which a 10% inhibition of primary production is expected assumed no vertical mixing, similar to the constant

depth in situ incubations used to generate the probit regressions.

Hazard assessment model

While the previous discussions characterized the magnitude and limits of inhibition of primary production by SUVR in the upper surface waters of Lake Michigan, it is also important to consider the potential environmental consequences of SUVR on total lake productivity. In oligotrophic systems, such as Lake Michigan, a large fraction of primary production occurs below the top third of the euphotic zone (Fahnenstiel and Scavia, 1987). Inhibition of primary production by SUVR appears to be limited to the top third of the euphotic zone in freshwater and marine systems (this study; Smith et al., 1980; Lorenzen, 1979; Hobson and Hartley, 1983). Therefore, to accurately assess the hazard of SUVR to total lake primary productivity, the magnitude of inhibition in the upper surface waters must be compared to the daily areal primary production, which is the primary production of the total water column. Assessing the effects of SUVR on areal primary production will be a more accurate predictor or potential hazard of SUVR to the lake's carrying capacity than isolated measures of the magnitude of the inhibition of primary production by specific UV intensities.

A hazard assessment model is composed of both exposure and inhibition. The results of this study provided accurate

characterization of both components for the assessment of current and predicted future intensities of SUVR on areal primary production of offshore Lake Michigan. This study represents the first accurate determination of the penetration of SUVR into Lake Michigan, which was necessary for the exposure component of the model. The study also addressed the inhibition component because the relationship between the SUVR dose and inhibition of primary production was quantified for natural phytoplankton assemblages in Lake Michigan. Seasonal differences in surface UV intensities, penetration of SUVR into Lake Michigan, phytoplankton sensitivity to SUVR, and depth profiles of primary production observed in this and other studies would have to be accounted for in the hazard assessment model. It was determined that these seasonal differences in the model's input parameters would be adequately characterized by utilizing monthly time steps for the model.

The UV exposure component of the model is composed of three parameters: surface UV intensity, loss at the air/water interface and UV attenuation in the water column. Only the penetration of broad-band UV-B radiation was modelled because UV-B is considered the inhibitory component of SUVR (this study, Lorenzen, 1979), and the dose-response relationships to be utilized in the toxicity component of the model were in units of % inhibition per kJ/m^2 UV-B. The daily surface UV-B dose for a cloudless day was adequately characterized by a

no
day
nor
the
the
(Tab
curv
kJ/m

was c
UV-B
first
air/w
measu
Michi

dose-
UV-B
produ
UV-B
UV-B
perce
the
radia
perce
of p

normal curve centered on the solar noon, with the length of day equal to 5.4 standard deviations. For each month, a normal curve with the above parameter was generated, utilizing the daylength of the 15th day of that month for the width and the maximum surface UV-B intensity measured in this study (Table 1) for the height. Integration of the area under the curve provided the average monthly surface UV-B dose (in kJ/m^2), for a cloudless day.

The penetration of the daily UV-B dose into Lake Michigan was calculated in one meter intervals by utilizing the mean UV-B attenuation coefficient for each month (Table 1), after first correcting the surface UV-B dose for losses at the air/water interface. It was assumed attenuation coefficients measured at the 19 km station were typical of offshore Lake Michigan.

The inhibitory component, as characterized by the UV-B dose-response relationship, was utilized to convert the daily UV-B dose at each depth to the percent inhibition of primary production expected at that depth. For each month, the daily UV-B dose (in kJ/m^2) at each depth was multiplied by the mean UV-B inhibition efficiency (Figure 3), which was in units of percent inhibition per kJ/m^2 , to obtain the depth profile of the percent inhibition of primary production by UV-B radiation. The final step was the utilization of the monthly percent inhibition depth profiles to correct depth profiles of primary production measured in the absence of UV-B

radiation for the inhibition expected due to current UV-B intensities.

Depth profiles of primary production were not measured during this study. However, during the spring and summer of 1982, 1983 and 1984 in situ incubations in polycarbonate vessels were performed to generate depth profiles of primary production for offshore Lake Michigan (Fahnenstiel and Scavia, 1987). These depth profiles of primary production were measured at a station within 6 km of the 19 km station used to generate the exposure component of the model. The differences in the penetration of solar radiation at these two stations was expected to be minimal. Because polycarbonate is opaque to UV-B radiation (Dwyer, 1988), these depth profiles represent measurements of primary production in the absence of UV-B radiation. The depth profiles of primary production (Fahnenstiel and Scavia, 1987) were averaged for each month (May - August) and then were corrected by utilizing the percent inhibition depth profiles for the inhibition expected due to current UV-B intensities. The daily, areal, primary production was estimated for each depth profile by integrating the area under the curve. Daily areal production was multiplied by the number of days in each month to obtain estimates of the monthly areal primary production expected at current UV-B intensities and in the absence of UV-B radiation. The percent inhibition of areal primary production by UV-B radiation was the areal productivity expected at current UV-B

intensities divided by the areal productivity measured in the absence of UV-B radiation.

Large inhibitions of areal primary production are evident for offshore Lake Michigan at current UV-B intensities. During the spring, when a large fraction of primary production is near the surface and sensitive phytoplankton dominate the assemblages, a large inhibition in areal primary production is evident (Figure 4). This inhibition was maximal in May, when a decrease in total water column primary production of 19% is expected due to current UV-B intensities (Table 6). Even though UV-B exposure was greater during the summer, a much smaller inhibition of areal primary production is observed (Figure 5). The presence of a phytoplankton chlorophyll maxima below the epilimnion (Fahnenstiel and Scavia, 1987) and UV-B resistant phytoplankton assemblages are the most probable explanations for the much smaller inhibition of areal primary production by UV-B radiation observed during the summer, which is only 8% during the summer.

Current UV-B intensities are predicted to be reducing areal primary production of offshore Lake Michigan by 13% during the period of May to August (Table 6). For marine systems, current UV-B intensities are estimated to be decreasing areal primary production by 12% (Worrest, 1983). It appears that in both freshwater and marine waters, current UV-B intensities are causing a small, but real, decrease in areal primary production. This inhibition of areal primary

Figure 4. Primary production depth profiles for offshore Lake Michigan during the spring. The solid line represents primary production in the absence of UV-B radiation. The dashed line represents primary production at current UV-B intensities. The number in parentheses is the percent inhibition of areal primary production by UV-B radiation.

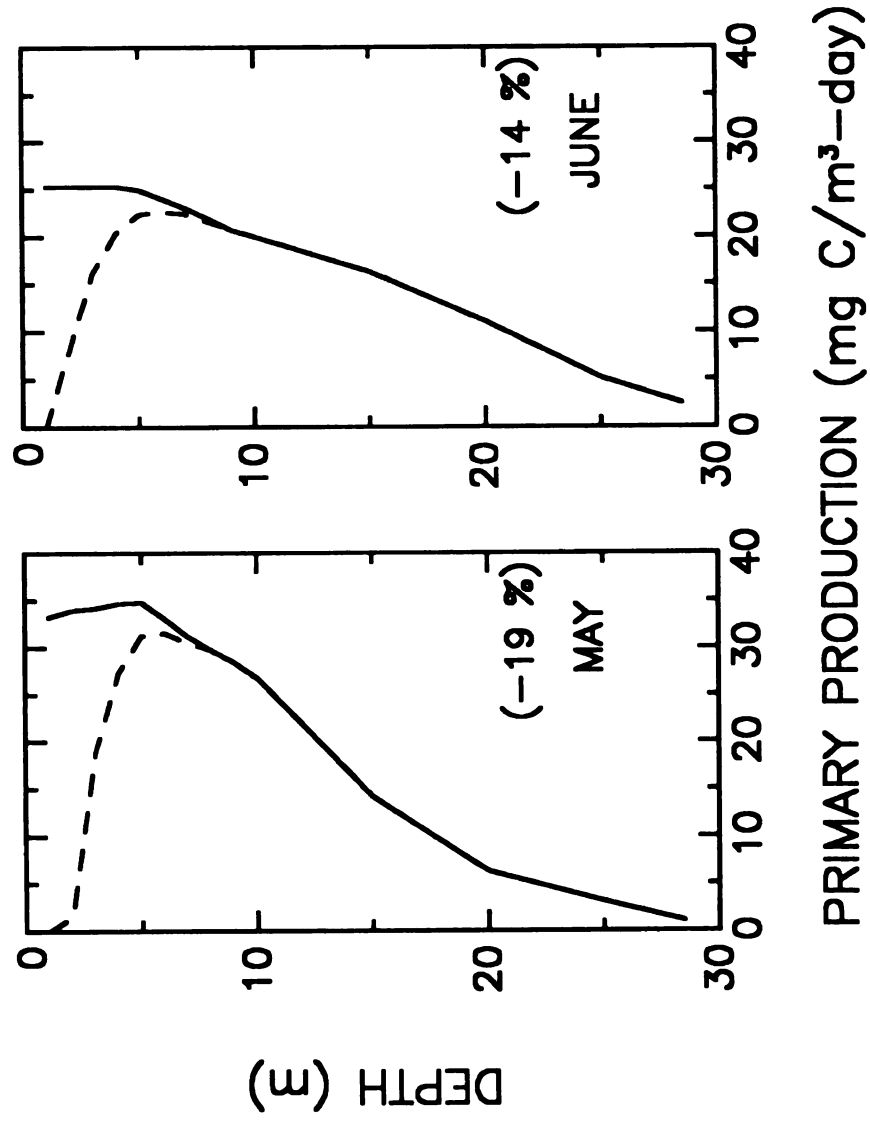


Figure 4.

Figure 5. Primary production depth profiles for offshore Lake Michigan during the summer. The solid line represents primary production in the absence of UV-B radiation. The dashed line represents primary production at current UV-B intensities. The number in parentheses is the percent inhibition of areal primary production by UV-B radiation.

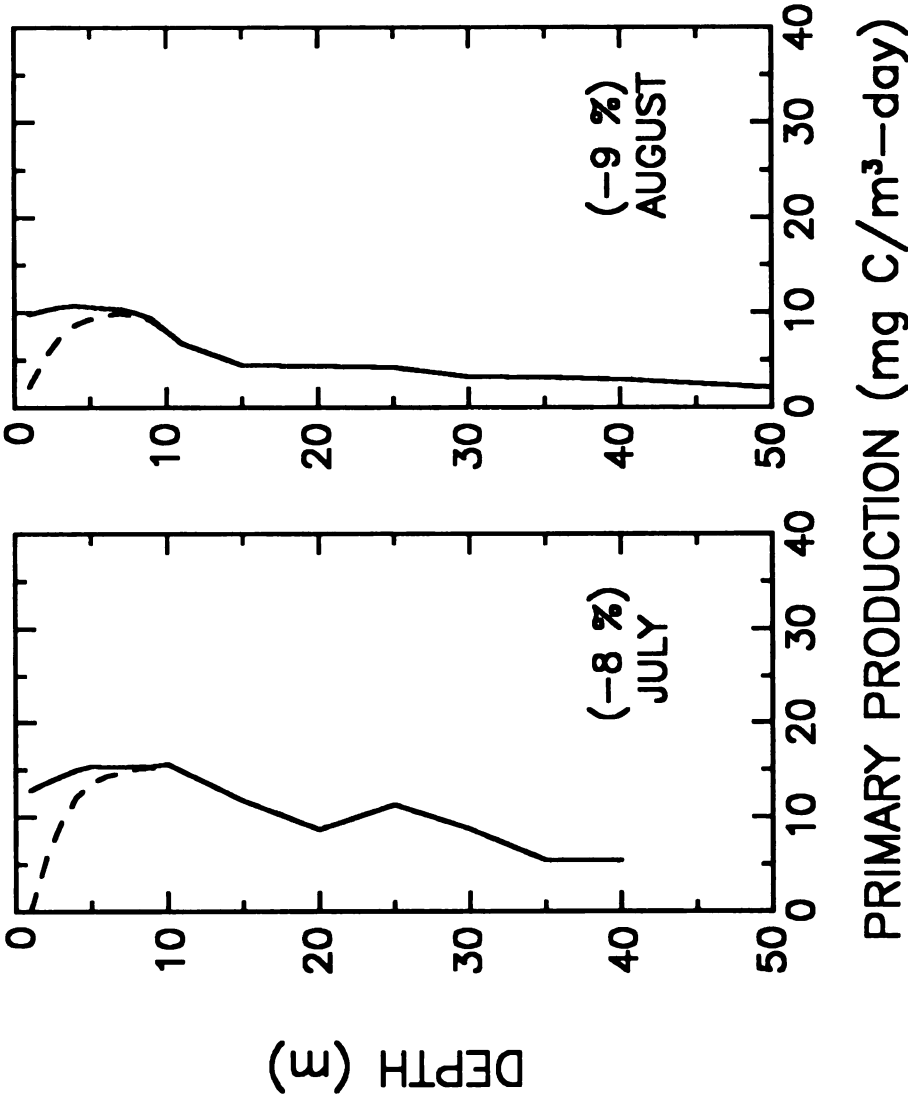


Figure 5.

Table 6. Inhibition of areal primary production ($\text{mg C/m}^3\text{-day}$) of offshore Lake Michigan at current and predicted future (21% UV-B increase) solar UV radiation intensities.

Month	Areal primary production ($\text{mg C/m}^3\text{-day}$)		
	No UV-B radiation	Current UV-B intensities	+21% UV-B radiation
May	486.6	389.1	387.1
June	439.4	378.4	370.8
July	426.7	395.0	391.6
August	<u>247.0</u>	<u>225.7</u>	<u>221.9</u>
Total PP ¹ (g C/m^3)	49.2	42.7	42.1
(% inhibition)		(-13.2%)	(-14.4%)

¹ Total PP = Total primary production (May - August).

production suggests that the carrying capacities of aquatic systems are overestimated because current and past methods for primary production determination completely neglect the importance of SUVR in aquatic systems. The error associated in the determination of areal primary production utilizing current methods has been estimated to be as great as 50% (Peterson, 1980). Not accounting for the effects of SUVR is a systematic error of current primary production methods, and therefore, would increase the error associated with primary production determinations.

Concern about depletion of the stratospheric ozone layer and the concomitant increase of SUVR provided the impetus for investigation of the effects of SUVR on natural phytoplankton assemblages. The hazard assessment model can be utilized to predict the additional hazard to areal primary production associated with potentially increased UV-B intensities in the future. Estimates of ozone depletion have been decreasing since the 1970s (NRC, 1979; 1982). Current estimates, assuming continued usage of chlorofluoro-carbons (CFC) at 1980 world rates, predict a 6-8% decrease in total column ozone for 43° N latitude by the year 2050 (Cicerone, 1987). The magnitude of the decrease in total column ozone depends on the season, being greatest in the winter. However, for the period of May to August, a 7% decrease is predicted for the latitude (43° N) of the 19 km offshore Lake Michigan station. Certainly, as photochemical and atmospheric models are

modified to incorporate new information from ozone depletion studies in the Antarctic (Cox and Hayman, 1988) and the older estimates of CFC emissions (Hammitt et al., 1987) are adjusted for the new Montreal Protocol emissions regulations, alterations in the predicted ozone depletion will be forthcoming. However, a 7% decrease in the total column ozone is the best estimate at the current time.

The relative increase in SUVR reaching the earth's surface due to a specific decrease in the ozone layer depends on the action spectrum of the response of interest. The amplification factors, which equal the percent increase in the UV dose for each 1% decrease of ozone, for the various action spectra describing the response of algae and plants to UV radiation have a greater than 10-fold range. The inhibition of short-term primary production (^{14}C -bicarbonate incorporation) by SUVR during in situ incubations of marine phytoplankton was consistent with an action spectrum for the photoinhibition of photosynthetic electron transport (Jones and Kok, 1966). However, inhibition of marine algal communities during chronic UV radiation exposures appeared to be described by a DNA action spectrum for UV-induced skin cancers (Setlow, 1974). The amplification factor for the photoinhibition action spectrum equals 0.2, which would represent an increase of 1.4% in the UV dose due to a 7% ozone reduction (Worrest, 1983). The DNA action spectrum (amplification factor = 3) is weighted more heavily at the

shorter UV wavelengths (Worrest, 1983), and, therefore, a 7% ozone reduction would cause a 21% increase in the UV dose reaching the earth's surface.

The hazard assessment model developed previously can be utilized to determine the effects of potentially increased UV dose to areal primary production. The model was recalibrated, altering the surface UV intensities to reflect possible increases in SUVR due to a 7% ozone reduction. Not surprisingly, a 1.4% increase of surface UV radiation, the increase expected if inhibition of primary production followed the photoinhibition action spectrum, would not be expected to cause a significant increase in inhibition of areal primary production relative to current UV-B intensities. Unexpectedly, even a 21% increase in surface UV intensities would cause little additional inhibition of areal primary production (Table 6). The negligible additional inhibition of primary production from a 21% increase in surface UV intensities was evident at all depths during the spring and summer (Figure 6). A 21% increase of surface UV intensities would be expected to decrease areal primary production by less than 2% for the period of May to August, relative to primary production expected at current UV intensities (Table 6). Models assessing the hazard of increased UV intensities on marine primary production also predicted similar minimal additional decreases in areal primary production relative to current UV intensities (NRC, 1982; Worrest, 1983; Smith and

Figure 6. Primary production depth profiles for offshore Lake Michigan during May and August for current and future (+21% UV-B) UV-B intensities. The solid line represents primary production in the absence of UV-B radiation. The dashed line represents primary production at current UV-B intensities. The dotted line represents the primary production expected at UV-B intensities increased by 21%, relative to current intensities.

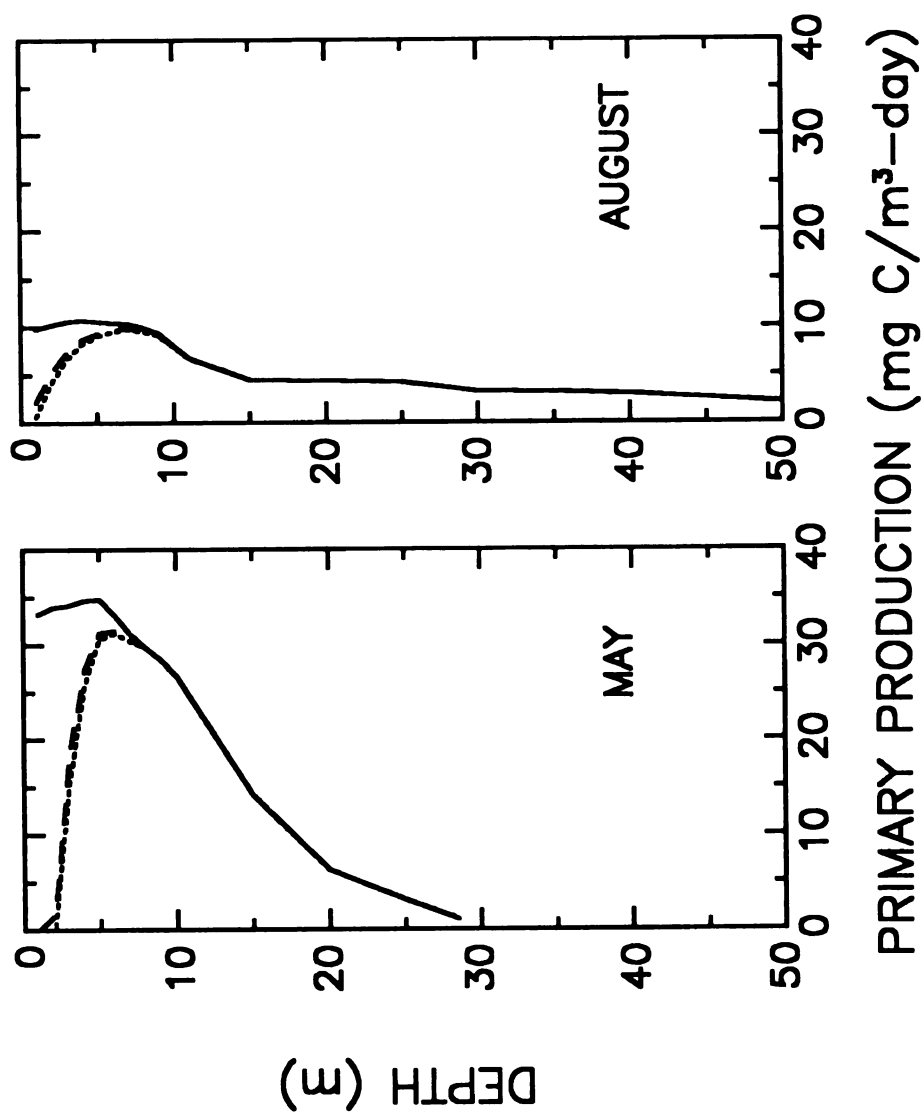


Figure 6.

Baker, 1982). It appears that in both marine and freshwater systems, an additional inhibition of areal primary production of approximately 1% is expected for every 10% increase in the surface UV-B intensity. Therefore, unless current ozone depletion estimates are greatly underestimated, concern about the effects of depletion of the ozone layer on primary production of aquatic systems is unwarranted.

Conclusions

Solar UV radiation (SUVR) penetrated to ecologically significant depths in offshore Lake Michigan. Significant inhibition of primary production of natural phytoplankton assemblages during in situ incubations in Lake Michigan by SUVR was restricted to the top third of the euphotic zone. Spring assemblages, dominated by diatoms and chrysophytes, were more sensitive to SUVR than summer assemblages, which were dominated by blue-greens. A hazard assessment model predicted a significant reduction (13%) in areal (total water column) primary production for offshore Lake Michigan due to current UV intensities. Concern about possible increased reduction of primary production due to depletion of the ozone layer appears to be unwarranted. Future research investigating the effects of SUVR on algal communities should focus on measuring the penetration of SUVR into eutrophic and riverine systems because of scarcity of quality data from such systems. The effects of SUVR on algal community

photosynthesis-irradiance (PI) parameters should be investigated because PI parameters demonstrate great generality between aquatic systems and, therefore, comparisons of phytoplankton assemblage's sensitivity to SUVR could be performed more easily.

CHAPTER 2

THE PHOTO-INDUCED TOXICITY OF ANTHRACENE TO THE GREEN ALGA, Selenastrum capricornutum.

INTRODUCTION

Polycyclic aromatic hydrocarbons (PAH) are a large class of environmental contaminants composed of two or more fused benzene rings. PAH are ubiquitous pollutants and are produced as a result of natural and man-made processes. Elevated concentrations of PAH in the aquatic environment are associated with point and non-point discharges, such as fossil fuel combustion, automobile emissions, steel and coking operations and petroleum refining (Neff, 1979; Eisler, 1987). Energy conservation and the switch to oil and natural gas as the primary fossil fuels, which emit less PAH upon combustion than coal, have limited increases of PAH environmental concentrations in recent years (Gschwend and Hites, 1981). However, exponential increases in PAH fluxes from 1960s to 1980s have occurred in some aquatic systems, especially ones heavily impacted by urban runoff and automobile emissions (Readman et al., 1987).

The photo-induced toxicity of PAH has been observed in a wide range of aquatic organisms at PAH concentrations well below their aqueous solubility (Bowling et al., 1983; Allred and Giesy, 1985). The photo-induced toxicity of PAH to organisms has been well recognized by the biomedical community for many decades (Mottram et al., 1938; Epstein et al., 1963; Morimura et al., 1964; Morgan and Warshawsky, 1977). However, it was not until recently that the photo-induced toxicity of PAH was demonstrated with standard aquatic bioassay organisms, such as fishes (Bowling et al., 1983; Oris and Giesy, 1985), daphnids (Allred and Giesy, 1985; Newsted and Giesy, 1987), and algae (Cody et al., 1984). It is evident that the environmental hazard of PAH has been severely underestimated because all of these studies observed greatly enhanced toxicity of PAH with simultaneous exposure to environmentally relevant UV radiation.

The photo-induced toxicity of PAH to algae, unlike the effects on aquatic animals, has been poorly characterized. The two studies (Cody et al., 1984; Oris et al., 1984) investigating photo-induced toxicity of PAH to algae were poorly designed and generated contradictory conclusions. The green alga, Chlorella pyrenoidosa, was not adversely affected by exposure to the three-ring PAH, anthracene, in the presence of UV radiation (Oris et al., 1984). However, inhibition of ^{14}C -bicarbonate incorporation in the anthracene/UV treatment was compared to an inappropriate control treatment. The

control treatment was designed to contain algae exposed to anthracene in the absence of UV radiation, but the control test vessel was constructed of plexiglass which was transparent to anthracene-excitating UV radiation. In the other study (Cody et al., 1984), three PAHs, anthracene, benzo[a]pyrene and benz[a]anthracene, demonstrated photo-induced toxicity to the green alga, Selenastrum capricornutum. Although, an appropriate control treatment was utilized and the light intensity was quantified, no measurement of the PAH concentration during the four to seven day exposures was performed. Therefore, the PAH concentration component of the photo-induced toxicity dose-response relationship is unknown. It was suggested that algae may be resistant to photo-induced toxicity of PAH because the nominal PAH concentrations utilized and the resulting EC_{50} were greater than the PAH aqueous solubilities. It has been hypothesized that carotenoid pigments may be protecting algae from photo-induced toxicity of PAH (Landrum et al., 1986).

The main objective of this study was to determine if algae are resistant to photo-induced toxicity of PAH and, if not, to fully characterize the photo-induced toxicity of anthracene, a linear three-ring PAH, to the green alga, Selenastrum capricornutum. Anthracene is considered a model PAH for laboratory fate and toxicity studies. The relationship of anthracene concentration and UV intensity to their inhibition of several algal growth, viability and

photosynthetic endpoints will be quantified. The anthracene concentration and UV intensity thresholds for the photo-induced toxicity of anthracene to algae will be compared to environmental PAH concentrations and UV intensities to assess the hazard of PAH contamination of aquatic systems to algae.

MATERIALS AND METHODS

Test organism

The test algae was the unicellular freshwater green alga, Selenastrum capricornutum Printz, which is the standard freshwater alga used in bioassays of the effects of both nutrients and toxicants (Miller et al., 1978; Anon, 1981). Unialgal stock cultures were maintained at 21°C (+/-1°C) under continuous illumination (PAR intensity of 40 $\mu\text{M}/\text{m}^2\text{-sec}$). The algal culture and test medium was double-strength EPA algal assay medium (Table 7, Miller et al., 1978). Double-strength EPA algal assay medium was utilized to increase the bicarbonate buffering capacity of the medium and to prevent algal cultures from becoming carbon or nutrient limited during the toxicant exposure. Stock cultures were restarted monthly from algal cells stored in liquid N₂ to keep culture senescence and bacterial contamination to a minimum. Stock cultures contaminated with bacteria, as determined by microscopic observation, were discarded.

Table 7. Modified (2X) EPA algal assay medium (pH = 7.5).

<u>Macronutrients</u>	<u>Concentration (mg/L)</u>
NaNO ₃	51.00
MgCl ₂ ·6H ₂ O	24.33
CaCl ₂ ·2H ₂ O	8.82
MgSO ₄ ·7H ₂ O	29.40
K ₂ HPO ₄	2.09
NaHCO ₃	30.00
 <u>Micronutrients</u>	 <u>Concentration (μg/L)</u>
H ₃ BO ₃	371.04
MnCl ₂ ·4H ₂ O	831.22
ZnCl ₂	6.54
CoCl ₂ ·6H ₂ O	2.86
CuCl ₂ ·2H ₂ O	0.024
Na ₂ MoO ₄ ·2H ₂ O	14.52
FeCl ₃ ·6H ₂ O	320.00
Na ₂ EDTA·2H ₂ O	600.00

Toxicant

Stock solutions of anthracene (Sigma grade III, lot 84F-34, 99.9% purity) were prepared in HPLC grade acetonitrile. A carrier solvent was necessary because a toxicant renewal system was chosen to maintain constant anthracene exposure concentrations. Acetonitrile is the recommended carrier solvent for photochemical studies in water (Mill et al., 1982) because it is completely miscible with water, is photochemically inert at the wavelengths utilized in this study, does not transfer triplet energy and does not absorb ultraviolet radiation present in the solar spectrum or in the artificial lighting used in this study. Anthracene stock solutions were prepared such that no more than 50 μ l of the toxicant renewal solution was added to the test flasks at any one renewal.

Experimental design

The experimental design and test conditions were identical for the five anthracene phototoxicity experiments, except that the UV-A intensity was systematically varied among experiments. Each experiment contained four treatments: an acetonitrile control treatment and three anthracene exposure concentrations. Each treatment contained three replicate flasks. Anthracene exposure concentrations were maintained by utilizing a toxicant renewal exposure system, in which small volumes of anthracene stock solutions were added to each

flask periodically to maintain the anthracene exposure concentration at a specific target concentration. The control treatment received an addition of acetonitrile equal to the maximum volume of anthracene (in acetonitrile) stock solution added to the three anthracene treatments during each toxicant renewal period. The target anthracene concentration for the three treatments was 35, 15, and 7 $\mu\text{g/L}$. During the exposure period, all four treatments were exposed to UV-A radiation. Standard algal toxicity test conditions were modified slightly for these experiments (Table 8).

Lighting apparatus

The lighting apparatus consisted of a PAR source illuminating the flasks from the top and a UV-A radiation source illuminating them from the below. The PAR source was six Chroma F40C50 (General Electric) white fluorescent bulbs covered by a sheet of Plexiglass UF-3 (Rohm and Haas), which eliminated all wavelengths less than 390 nm. UV-A radiation was supplied by four F40 BLB (General Electric) blacklight fluorescent bulbs. A sheet of 0.005 mm thick Mylar (Dupont) was used to eliminate wavelengths shorter than 315 nm because UV-B radiation (280-320 nm) is toxic to photosynthetic organisms (Brandle et al., 1977; Lorenzen, 1979). The transmittance characteristics of Plexiglass UF-3 and Mylar were measured by a Gilford 2600 UV/Vis Spectrophotometer (referenced to air). The F40 BLB bulbs were selected for the

Table 8. Test conditions for the photo-induced toxicity of anthracene experiments.

Test vessel: 250 ml erlenmeyer flask (PYREX)

100 ml (2x) EPA AA medium (pH = 7.5)

Test organism: Selenastrum capricornutum Printz

Starting algal density: 1×10^5 cells/ml

Pre-incubation (No UV-A exposure): 12 h

Test duration (UV-A exposure): 28 h

Temperature: 21°C (+/-1°C)

Continuous illumination

PAR intensity: 47-53 $\mu\text{M}/\text{m}^2\text{-sec}$

UV-A intensity: varied between experiments

(range = 125-765 $\mu\text{W}/\text{cm}^2$)

Target anthracene concentrations

35, 15, and 7 $\mu\text{g}/\text{L}$ anthracene

Toxicant renewal (anthracene in acetonitrile)

every 12 h during pre-incubation

every 8 h during UV-A exposure

UV-A source because the spectral characteristics of the F40 BLB bulbs (Figure 7) match the action spectrum for the photo-induced toxicity of anthracene, which is between 320 and 380 nm with peak activity around 360 nm (Allred and Giesy, 1985; Kaidbey and Nonaka, 1984). The test vessels were PYREX erlenmeyer flasks because PYREX glass is transparent to wavelengths greater than 310 nm, as measured by the Gilford 2600 UV/Vis Spectrophotometer (referenced to air). Therefore, Pyrex glass will not absorb anthracene-excitation wavelengths. Neutral density screening was used to reduce UV-A radiation to the desired intensities. UV-A radiation at the surface of the flasks was quantified using the UV-A (365 +/- 36 nm) probe of the Macam Photometrics Model UV-103 radiometer (Livingstone, Scotland). PAR (400-700 nm) at the flasks surface was quantified using the LI-192s quantum sensor coupled to a Li-Cor LI-150 integrator (Lincoln, NE).

Experimental schedule

Experiments were initiated with the addition of 100 ml of filter-sterilized (0.45 μ m membrane filter) 2x algal medium to autoclaved flasks. Prior to autoclaving, each flask was soaked overnight in NaOH and HCl baths and rinsed with de-ionized water. They were then rinsed with acetone and hexane to remove any organic residues from the glassware. One ml algal inoculum was added to each flask such that the starting algal density was 1×10^5 cells/ml. The algal

Figure 7. Spectral characteristics of General Electric F40 BLB blacklight fluorescent lamps (modified from General Electric).

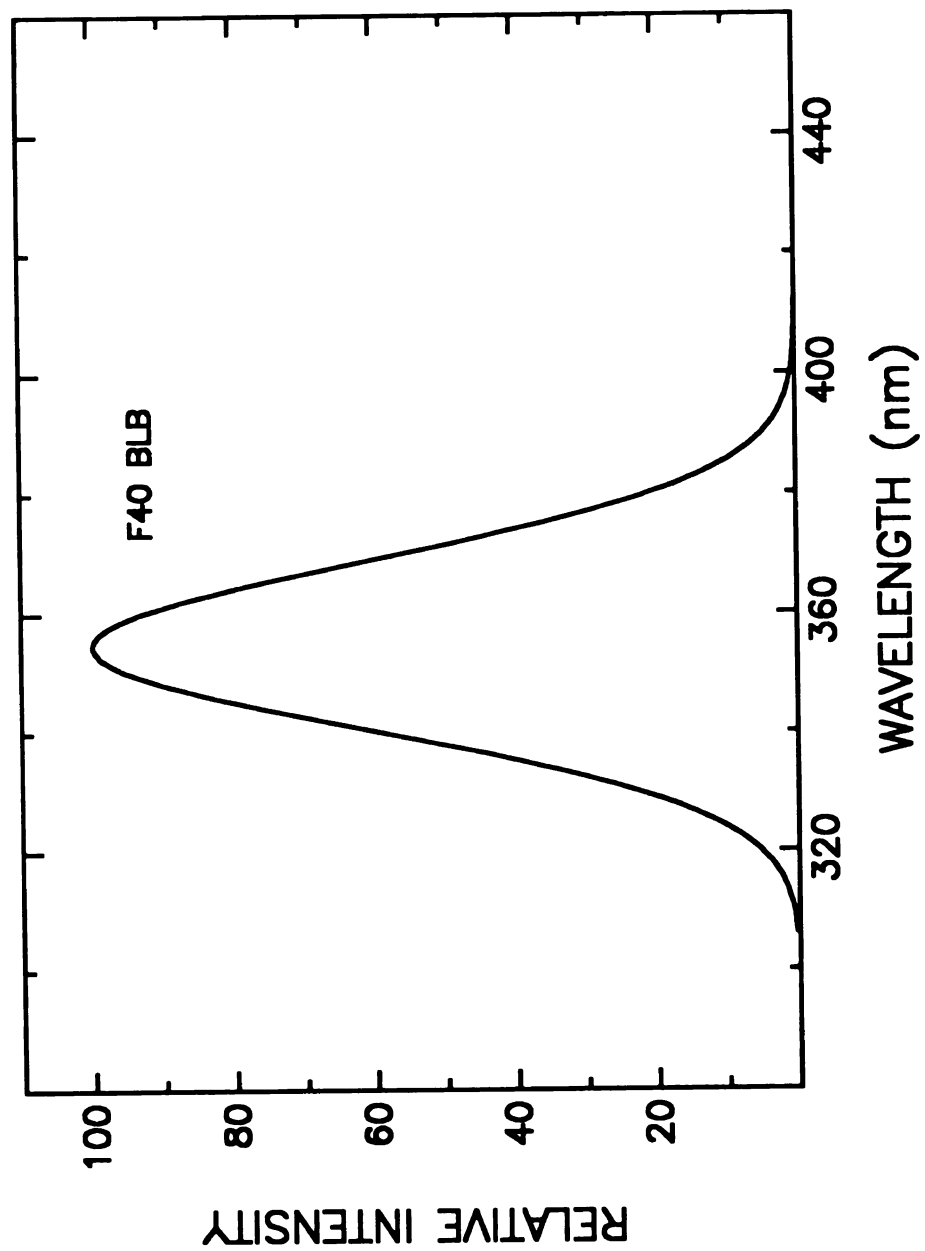


Figure 7.

inoculum consisted of cells in log-growth phase which were centrifuged (10 min x 2000 g) and washed with fresh 2x algal medium twice. Anthracene stock solution was added to bring the three replicate flasks for each anthracene treatment to their target anthracene concentration (Table 8). Acetonitrile, corresponding to the maximum volume of anthracene stock solution added to a treatment, was added to the control flasks. The flasks were placed under the PAR lighting, in the absence of UV-A radiation, for the 12 h pre-incubation period. The pre-incubation period enabled the algal cells to reach steady state with the anthracene in the algal medium prior to UV-A exposure (Giesy et al., 1978; Mailhot, 1987).

Anthracene concentrations in the test medium was measured at the beginning of the pre-incubation and before and after each toxicant renewal. A one ml aliquant was removed from each flask and centrifuged in solvent cleaned glass centrifuge tubes for 10 min x 2000g to remove algal cells. Anthracene concentrations in the test medium were determined directly by reverse phase HPLC (Oris and Giesy, 1985). The detection limit of anthracene in water was 0.1 $\mu\text{g/L}$. Anthracene concentrations in the control treatment flasks were always below the detection limit.

As mentioned in the experimental design, a toxicant renewal system was utilized to maintain constant anthracene exposure. Anthracene concentrations were renewed with an

addition of anthracene stock solution at the start of the UV-A exposure and every eight hours, thereafter. Prior to each renewal, the mean anthracene concentration for each treatment was determined. The volume of anthracene stock solution required to elevate the anthracene concentration back to the target anthracene concentration was added to each treatment's flasks. The maximum volume of acetonitrile added during any renewal never exceeded 50 μ l per flask.

After each renewal, a one ml aliquant was removed from each flask for anthracene determination. Typically, the anthracene concentration measured just after renewal was less than 70% of the target concentration. This inability to achieve the target concentration probably resulted from the rapid uptake of the added anthracene by algae and glass surfaces (Futoma et al., 1981). Anthracene concentrations typically decreased to half the initial measured values between renewals (Figure 8). The major routes of anthracene loss appeared to be volatilization and photolysis, depending on the UV-A intensity.

The anthracene exposure concentration was calculated assuming anthracene loss followed first-order kinetics between renewals. Preliminary experiments corroborated the assumption that anthracene loss followed first-order kinetics. A separate first-order rate constant was calculated for each treatment and renewal period (equation 2),

Figure 8. Anthracene concentration in test medium during a photo-induced toxicity of anthracene experiment at $218 \mu\text{W}/\text{cm}^2$ UV-A. The target concentrations for the three treatments were 35, 15, and 7 $\mu\text{g}/\text{L}$ anthracene.

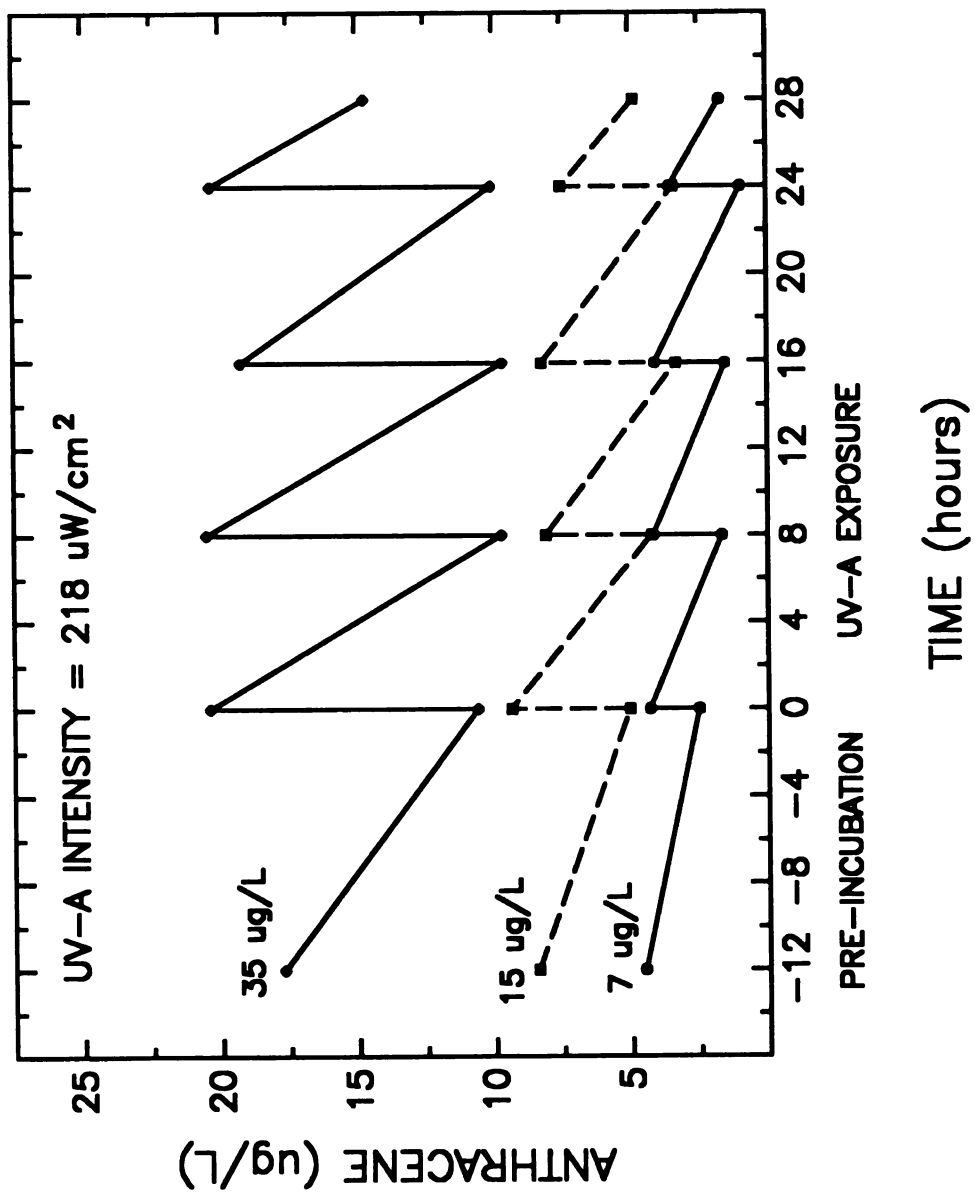


Figure 8.

$$k = -(\ln(C_e) - \ln(C_o))/t \quad [2]$$

where: k = rate constant (1/h), t = time between anthracene measurements (h), C_o = initial mean anthracene concentration after renewal ($\mu\text{g/L}$), and C_e = mean anthracene concentration at end of the renewal period ($\mu\text{g/L}$). The rate constant for the last renewal interval (24-28 h) was not calculated and was assumed to be equal to the prior renewal interval (16-24 h). The mean anthracene exposure concentration for any exposure duration was calculated utilizing the first-order rate equation (equation 3) and the treatment and renewal interval-specific rate constants (k) and the initial renewal concentrations (C_o),

$$C_t = C_o e^{-kt} \quad [3]$$

where: C_t = predicted concentration ($\mu\text{g/L}$) at time t . The predicted concentrations (0.1 h intervals) were summed and averaged for the desired exposure duration.

Toxicity endpoints

The effects of anthracene and UV-A radiation on specific growth rate, ^{14}C -bicarbonate incorporation, and several flow cytometric measures were determined. The time involved in anthracene determination and renewal, measuring toxicity endpoints and the availability of the flow cytometer prevented

measuring all toxicity endpoints after identical exposure duration. The specific sampling schedules and methodologies for the toxicity endpoints measured are described in detail in the following sections.

Specific growth rate -- Algal cell density was enumerated at approximately 0, 10 and 22 h UV-A exposure by microscopic visual observation using a hemocytometer. Because of the anthracene determination and renewal operation performed at the initiation of UV-A exposure, the 0 h cell counts were actually performed up to two hours prior to UV-A exposure. Because inherent variability of algal cell enumeration would prevent resolution of cell density changes for such a brief growth interval, the cell counts were assumed to represent initial exposure cell density (0 h). The specific growth rate (0 - 22 h) was calculated for each flask and the three replicates were combined to obtain a mean growth rate for each treatment.

^{14}C -bicarbonate incorporation -- A 5 ml aliquant was removed from each flask after 4 and 24 h UV-A exposure and placed into chemically cleaned, autoclaved test tubes (screw top, 16 x 125 mm). The tubes were spiked with 100 μl of ^{14}C -bicarbonate stock (^{14}C - NaHCO_3 , specific activity = 56.6 mCi/mM, Amersham) equivalent to 0.2-0.5 μCi , and were incubated for 2 h in PAR lighting (40-50 $\mu\text{M}/\text{m}^2\text{-sec}$) at 21°C ($\pm 2^\circ\text{C}$). The entire contents of each test tube were poured into a labelled scintillation vial, acidified and bubbled for

5 minutes to remove unfixed ^{14}C -bicarbonate (Schindler et al., 1972). Ten ml of Safety Solve (R.P.I.) was then added to each vial. Vials were stored in darkness at 4°C overnight prior to quantification by a liquid scintillation counter. Algal medium-only procedural blanks demonstrated bubbling removed greater than 99.5% of the unfixed ^{14}C -bicarbonate. The mean blank DPM was subtracted from each measurement to correct for background.

Incorporation of ^{14}C -bicarbonate was expressed on a per volume (ml of test medium) and a per cell basis. The total DPM incorporated per sample represented the volume-based ^{14}C incorporation endpoint. This corresponded to effects on primary production, which was a function of cell numbers (growth) and photosynthesis rate. To isolate the direct toxic effects on photosynthesis, ^{14}C incorporation was also expressed on a per cell basis. The cell density for each ^{14}C sample was estimated from each flask's growth curve. The three replicate ^{14}C incorporation values were combined to obtain a mean ^{14}C incorporation for each treatment after 4 and 24 h exposure.

Flow cytometry -- A one ml aliquant was removed from each flask after 4 and 28 h UV-A exposure for flow cytometric analyses. The flow cytometer was an Ortho Instrument Cytofluorograf 50-H (Figure 9). The algal cells were excited by the 488 nm light from an argon laser tuned to 400 mW. Forward blue scatter and red (>620 nm) and green (515-530 nm) fluorescence were measured simultaneously for both unstained

Figure 9. Optical configuration of the Ortho Instruments
Cytofluorograf 50-H.

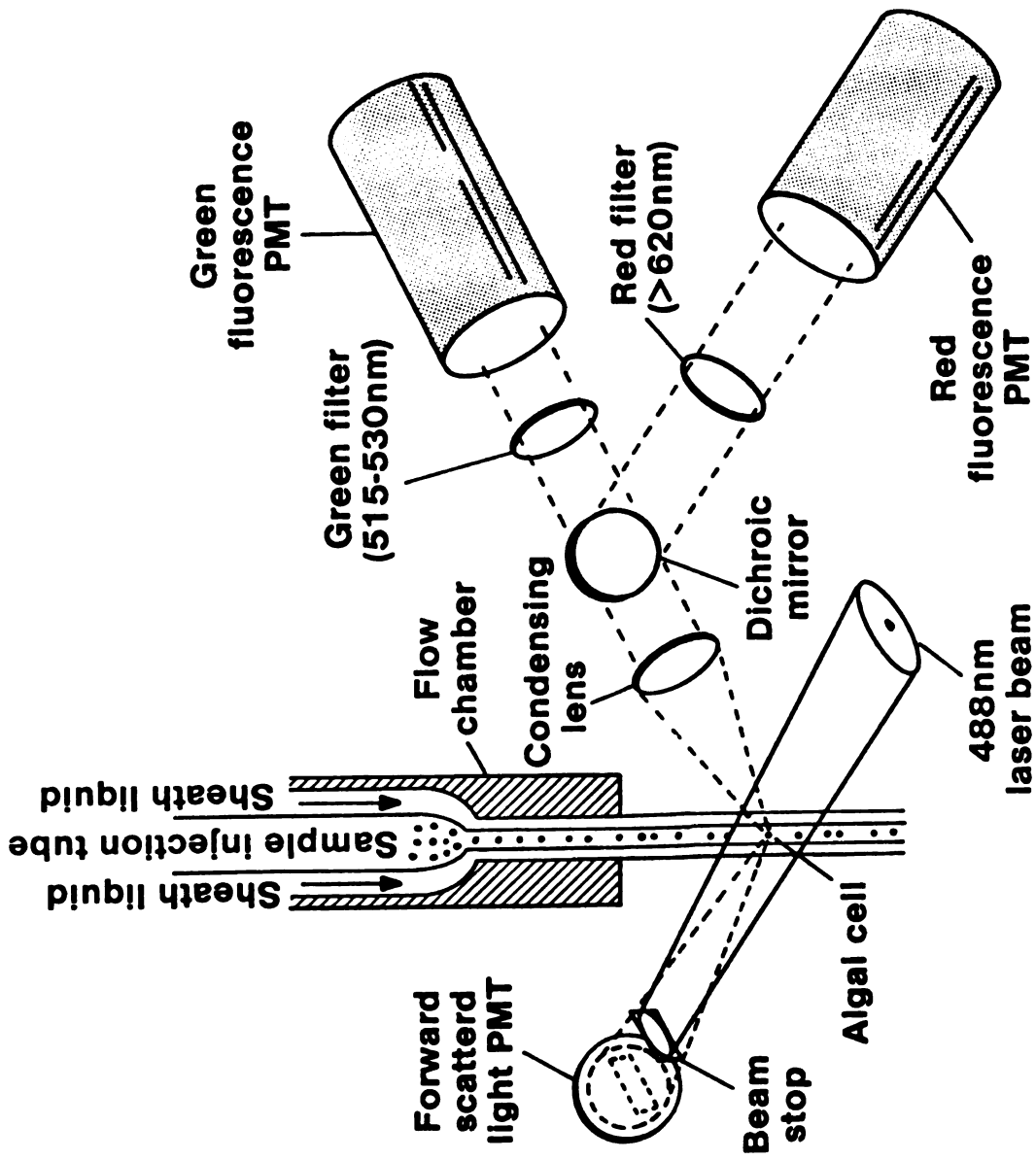


Figure 9.

and FDA-stained samples. Individual measurements of 5000 cells were recorded for each unstained and FDA-stained sample at flow rates of 200-600 cells/second. Flow cytometric analyses was completed within one hour of sample removal.

Forward blue scatter, red fluorescence and background green fluorescence of each sample was measured and recorded prior to FDA staining. Less than 0.1 ml of the sample was consumed during these measurements. The intensity of the forward blue scatter signal is proportional to the cross-sectional area of a cell (Trask et al., 1982; Benson et al., 1984). Forward blue scatter measurements were converted to equivalent spherical cell diameters (ESD) following calibration of scattering response with standardized 7.5 μm diameter beads. The proportionality constant (a) was calculated for each flow cytometric analysis (Equation 3),

$$a = \text{FBS}/(\pi r^2) \quad [4]$$

where: FBS = mean forward blue scatter of 7.5 μm diameter beads and r = radius (3.75). The mean forward blue scatter for each sample was converted to mean ESD (Equation 4) using the analysis-specific proportional constant (a).

$$\text{ESD (in } \mu\text{m)} = \sqrt{\text{FBS}/a\pi} \quad [5]$$

where: FBS = mean forward blue scatter of sample.

Generally, ESD for S. capricornutum was between 6.5 - 7.5 μm . The three replicate mean forward blue scatter values were combined to obtain a mean cell size for each treatment after 4 and 28 h exposure.

The inherent fluorescence properties of unstained algal cells were also measured by flow cytometric analysis. Chlorophyll fluorescence per cell was measured for each sample by monitoring red fluorescence ($> 620 \text{ nm}$). Red fluorescence, as measured by the flow cytometer, is linearly related to the chlorophyll concentration of plant cells (Galbraith et al., 1988). Because chlorophyll fluorescence per cell increased with increasing cell size, the effects of anthracene and UV-A radiation on cellular chlorophyll concentration were isolated by normalizing chlorophyll fluorescence for cell size. The mean red fluorescence of each sample was divided by that sample's mean forward blue scatter raised to $2/3$ power. The $2/3$ power rule was utilized because it best explained the variability and relationship between red fluorescence (chlorophyll) and forward blue scatter (cell size) in unstained control S. capricornutum samples. The three replicate mean normalized red fluorescence values were combined to obtain a mean cellular chlorophyll concentration for each treatment after 4 and 28 h exposure. Background green fluorescence (515-530 nm) was also recorded for each unstained sample. These measurements were utilized to correct FDA results for background green fluorescence.

Flow cytometric measures of cell viability were performed on the samples by staining them with 10 μ l of fluorescein diacetate (FDA, Sigma #F-7378, 1 mg/ml in acetone) for four minutes at 24°C. The FDA fluorescence assay is a standard technique (Rotman and Papermaster, 1966; Widholm, 1972) for determining the viability of a cell. FDA is a lipophilic, non-fluorescent molecule which is readily taken up by cells. Non-specific esterases within viable cells cleave the ester bonds, producing fluorescein, which when excited with 488 nm light from an argon laser in the flow cytometer will fluoresce green (Berglund and Eversman, 1988). Fluorescein which is hydrophilic does not easily leak back out through intact cell membranes. The intensity of the green fluorescence depends primarily on the esterase activity of the cell and, somewhat, on the integrity of the cell membrane (Berglund and Eversman, 1988), both of which are related to cell viability. Fluorescein (green) fluorescence was measured through a 515-530 nm bandpass filter. A bimodal distribution of green fluorescence was observed in samples stained with FDA (Figure 10). The group (region a in Figure 10) of cells which contained minimal green fluorescence, represents cells which did not convert the FDA to the green fluorescent compound, fluorescein. These cells contained no esterase activity and were considered non-viable cells. The small amount of green fluorescence observed in these non-viable cells was from background autofluorescence of the photosynthetic pigments.

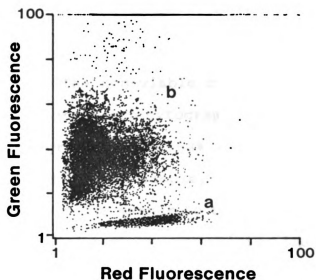


Figure 10. Flow cytometric analysis cytogram of fluorescein (green) fluorescence and chlorophyll (red) fluorescence of Selenastrum capricornutum cells stained with FDA. The two regions correspond to (a) non-viable (unstained) cells and (b) viable (stained) cells.

The second group (region b in Figure 10) contained cells of varying esterase activity and were considered viable cells.

Two measures of cell viability were calculated from the flow cytometry data. For each sample, the percentage of FDA-stained cells in the non-viable region (% non-viable cells) was calculated. The non-viable region was delimited in the green vs. red fluorescence cytogram (Figure 10) by a rectangle which included greater than 98% of cells in the unstained samples. Also, for each sample, a cell viability index was calculated in a similar manner to the stress index of Berglund and Eversman (1988). The cell viability index was considered to be a measure of the physiological "health" of the algal cells. The viable region started at the upper border of the non-viable region and included the main portion of stained cells. The only cells excluded were cells off-scale and cells demonstrating abnormally intense green fluorescence (possibly due to doublet cells being recorded). Generally, 90% of the stained cells were included in the viable region. The cell viability index (CVI) equals the mean FDA (green) fluorescence in the viable region multiplied by the number of stained cells in that region. The cell viability index for each sample was corrected for background green fluorescence (unstained CVI) measured prior to staining. For both cell viability measures, the three replicate values were combined to obtain a mean response for each treatment after 4 and 28 h exposure.

The utilization of the green vs. red fluorescence cytogram to delimit non-viable and viable regions is an improvement of the previous method (Gala and Giesy, 1989), which utilized the green fluorescence histogram. By utilizing the green vs. red cytogram the regions could be set to exclude particles without red fluorescence, which are obviously non-algal particles. Also, occasionally, especially for greatly inhibited samples, there was no clear demarcation between unstained and stained cells when utilizing the green fluorescence histogram. This occurred following FDA staining when small cells did not increase their green fluorescence sufficiently to surpass the background green fluorescence of larger cells. This phenomena did not pose a problem when utilizing the green vs. red cytogram to delimit the non-viable and viable regions.

Controls

Appropriate controls were performed to ensure that any toxic effects observed were due to the photo-induced toxicity of anthracene. Direct toxicity of anthracene was determined by exposing algal cells in the absence of UV-A radiation to the greatest anthracene exposure concentration tested. Direct UV-A radiation toxicity was investigated by exposing cells to the maximum UV-A intensity, in the absence of anthracene.

The direct and photo-induced toxicity of anthraquinone (Fluka, >99% purity), the major stable photoproduct of anthracene (Giesy et al., 1978), was also investigated.

Anthraquinone (in acetonitrile) was added to flasks at a concentration assuming all anthracene added to the High treatment was converted to anthraquinone. Nominal concentrations were utilized because anthraquinone concentrations were below the detection limit (1 mg/L) of the HPLC reverse phase-fluorescence detector method (Oris and Giesy, 1985) utilized to determine anthracene concentrations in the test medium. Direct toxicity of anthraquinone was determined by performing the experiment in the absence of UV-A radiation. Potential photo-induced toxicity of anthraquinone was investigated by exposing anthraquinone-treated algal cells to maximum UV-A radiation.

The toxicity of acetonitrile and any effects of acetonitrile on the photo-induced toxicity of anthracene were determined. The no observable effect concentration (NOEC) of acetonitrile, in the presence of UV-A radiation, was determined for all of the toxicity endpoints utilized in the photo-induced toxicity of anthracene experiments. Also, any possible effects of acetonitrile on altering the photo-induced toxicity (anthracene/UV-A interaction) of anthracene to algae were investigated by performing an experiment in which the effects of anthracene and UV-A radiation to algae were compared across two different exposure systems: anthracene introduced via acetonitrile carrier solvent and anthracene introduced without a carrier solvent via a shell coating technique (Allred and Giesy, 1985).

The experimental design and test conditions of all control experiments were similar to the photo-induced toxicity of anthracene experiments described previously. Most of the toxicity endpoints were measured during the control experiments, although, a computer malfunction caused the loss of the 28 h flow cytometric measures for the anthracene (no UV-A) and anthraquinone controls. Results from the control experiments were utilized to ensure that the effects of anthracene and UV-A radiation were compared to the appropriate control, which was determined to be an acetonitrile solvent control exposed to UV-A radiation.

Statistical analysis

An analysis of variance (ANOVA) was performed for each toxicity endpoint for each UV-A intensity to determine if a significant response was observed. Multiple range tests were performed to determine if the mean response of the different anthracene treatments were significantly different from the control treatment (Dunnett's test) or from each other (Tukey's test). The EC_{50} , the anthracene exposure concentration required to reduce the response to 50% of the control treatment at a specific UV-A intensity, was calculated using probit analysis (Finney, 1971). The flow cytometric endpoint, percent non-viable cells, was not converted to the percentage of the control treatment response but, rather, the EC_{50} concentration represented the anthracene concentration

required to cause 50% of the cells to be non-viable. All statistical analyses were performed utilizing SAS (SAS Institute, 1987), except the confidence intervals for the EC₅₀ were calculated using equations given by Neter et al. (1985).

RESULTS

Controls

UV-A radiation, in the absence of a photosensitizer, was generally not toxic to S. capricornutum at the UV-A intensities studied here. UV-A radiation had no effect on S. capricornutum specific growth rate or most flow cytometric endpoints at an UV-A intensity of 1080 $\mu\text{W}/\text{cm}^2$. A significant decrease in cellular chlorophyll concentration after 48 h UV-A exposure was the only observed effect at 1080 $\mu\text{W}/\text{cm}^2$ UV-A. At an UV-A intensity of 720 $\mu\text{W}/\text{cm}^2$, no effect was observed on algal growth rate or any flow cytometric endpoint. The direct effects of UV-A radiation on ^{14}C -bicarbonate incorporation were also measured at 720 $\mu\text{W}/\text{cm}^2$ UV-A. A significant decrease in ^{14}C incorporation was observed in UV-A exposed cells, relative to cells exposed to PAR only.

Acetonitrile was toxic to S. capricornutum but not at concentrations utilized during the photo-induced toxicity experiments. The 48 h EC₅₀ for specific growth rate and cell

viability index was 9528 mg/L and 15320 mg/L acetonitrile, respectively. The maximum acetonitrile concentration (approximately 1500 mg/L) in the photo-induced toxicity of anthracene experiments was six-fold less than the 48 h EC_{50} 's and was also three-fold less than the NOEC based on growth for acetonitrile. UV-A and acetonitrile exposed cells (at UV-A and acetonitrile exposure conditions identical to the photo-induced toxicity of anthracene experiments) had a greater growth rate (20% stimulation) than UV-A only exposed cells, but this increase was not significant (Tukey's test, $p > 0.05$). In all experiments, acetonitrile at identical exposure conditions to the photo-induced toxicity experiments had no effect on ^{14}C -bicarbonate incorporation or any flow cytometric endpoint.

Utilizing acetonitrile as a carrier solvent had little effect on the photo-induced toxicity of anthracene. Acetonitrile did minimally increase anthracene loss relative to anthracene exposures without carrier solvent. Acetonitrile decreased anthracene half-life by 10-30%. Although acetonitrile should have no photochemical effect on anthracene in this system, it is possible that the acetonitrile enhanced the solubility of some unknown triplet sensitizers released by the algae. This increased sensitizer concentration could have caused the greater photodegradation observed in treatments containing the acetonitrile carrier solvent. The difference in anthracene concentrations in the two anthracene

exposure treatments complicated analysis of the effects of acetonitrile on anthracene photo-induced toxicity. However, any differences in the responses of measured endpoints observed between the two introduction routes were fully explainable by the differences in the anthracene exposure concentrations. Therefore, as expected, acetonitrile did not have a significant effect on responses of algal cells to the photo-induced toxicity of anthracene.

Anthracene was directly toxic to algae in the absence of UV-A radiation at an anthracene concentration less than aqueous solubility (35 $\mu\text{g/L}$). Anthracene, in the absence of UV-A radiation and at a mean exposure concentration of 19.4 $\mu\text{g/L}$, did not have any effect on *S. capricornutum* growth rate. However, at this same concentration, flow cytometric endpoints were altered due to the direct toxicity of anthracene. After 28 h exposure, flow cytometric measures, except cell size and the percentage of non-viable cells, all detected sublethal toxicity. Cellular chlorophyll concentration increased 18% and the cell viability index was 17% smaller compared to cells not exposed to anthracene. After 52 h exposure to anthracene in the absence of UV-A radiation, all flow cytometric endpoints were not significantly different from control responses, except for cellular chlorophyll concentration. Although cellular chlorophyll concentration remained significantly greater in anthracene-exposed cells, the magnitude of the difference was reduced from 18% to 8% between

28 and 52 h exposure. Anthracene in the absence of UV-A radiation was not lethal, since no effect on algal growth rate or the percentage of non-viable cells was observed. However, anthracene in the absence of UV-A radiation did cause sublethal alterations in certain flow cytometric endpoints, such as the cell viability index and cellular chlorophyll concentration.

Anthraquinone, the major stable photoproduct of anthracene, was not toxic to S. capricornutum in the presence or absence of UV-A radiation (720 $\mu\text{W}/\text{cm}^2$). No effect on specific growth rate, ^{14}C incorporation or any flow cytometric endpoint was observed in anthraquinone-treated cells compared to the appropriate control. Because of instrument malfunction, anthraquinone effects on flow cytometric endpoints after 28 h UV-A exposure or 40 h exposure in the absence of UV-A radiation were not recorded. However, there is no evidence that a delayed toxicity of anthraquinone would occur or be expected. Therefore, anthracene photoproducts are not expected to cause either direct or photo-induced toxicity at the concentrations utilized in the photo-induced toxicity experiments.

Anthracene photo-induced toxicity

Specific growth rate -- Anthracene inhibited algal growth rate only in combination with UV-A exposure. Algal cells exposed to anthracene concentrations greater than 12 $\mu\text{g}/\text{L}$ had

reduced growth rate at all UV-A intensities (Table 9). Growth rate was also inhibited at concentrations of 5-6 $\mu\text{g/L}$ anthracene in combination with UV-A intensities greater than 400 $\mu\text{W/cm}^2$. No effect on growth rate was observed at concentrations of anthracene less than 3 $\mu\text{g/L}$ at any UV-A intensity tested. The inhibition of algal growth rate due to the photo-induced toxicity of anthracene increased with increasing anthracene concentration and UV-A intensity (Figure 11).

Inhibition of the specific growth rate due to anthracene and UV-A radiation demonstrated a toxicity threshold concentration for anthracene but no UV-A radiation threshold was apparent. The threshold concentration for anthracene was 3 $\mu\text{g/L}$. Concentrations below 3 $\mu\text{g/L}$ anthracene had no effect on algal growth rate. A small, but significant inhibition of algal growth rate was observed at concentrations of anthracene greater than 12 $\mu\text{g/L}$ even at the smallest UV-A intensity (125 $\mu\text{W/cm}^2$) tested.

The effect of anthracene and UV-A radiation on algal growth rate can also be characterized using probit analysis to estimate the EC_{50} and EC_{10} , the anthracene concentrations which cause a 50% and 10% decrease in the specific growth rate (0-22 h) at a specific UV-A intensity, respectively. The EC_{10} was considered the threshold for an ecologically significant reduction in the algal growth rate. The 22 h EC_{50} for specific growth rate was inversely related to UV-A radiation and ranged

Table 9. The effects of anthracene (ANTH) and UV-A radiation on the specific growth rate (0-22 h) of Selenastrum capricornutum. The values in parentheses are one standard deviation of the mean. Concentrations with asterisks are significantly different from the control mean (Control = 0 $\mu\text{g/L}$ anthracene; Dunnett's test, $p < 0.05$). Concentrations with the same letters are not significantly different from each other (Tukey's test, $p < 0.05$). Values represent mean of three replicates.

UV-A ($\mu\text{W}/\text{cm}^2$)	ANTH ($\mu\text{g/L}$)	Specific growth rate		
765	0	1.536	(0.186)	a
	1.42	1.413	(0.058)	a
	4.90	0.503	(0.373)	* b
	12.74	0.062	(0.127)	* b
410	0	1.473	(0.149)	a
	2.35	1.357	(0.075)	a
	5.97	0.709	(0.027)	* b
	14.24	0.264	(0.118)	* c
406	0	1.571	(0.070)	a
	5.03	1.001	(0.201)	* b
	6.39	0.461	(0.296)	* c
	16.02	0.062	(0.056)	* c
218	0	1.335	(0.165)	a
	2.63	1.360	(0.077)	a
	5.93	1.332 ¹	(0.003)	a
	14.60	0.331	(0.146)	* b
125	0	1.477	(0.052)	a
	2.86	1.448	(0.180)	a
	6.20	1.369	(0.043)	ab
	14.40	1.157	(0.110)	* b

¹ Mean of two replicates.

Specific Growth Rate (0-22 h)

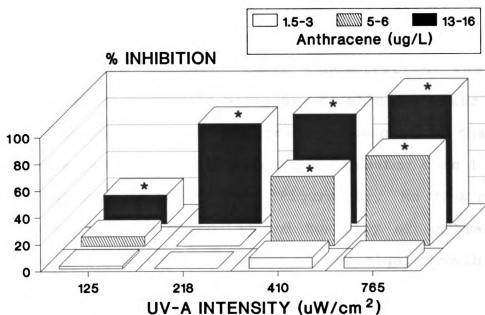


Figure 11. The effects of anthracene and UV-A radiation on the specific growth rate (0-22 h) of *Selenastrum capricornutum*. Anthracene/UV-A combinations with asterisks are significantly different from the control mean at same UV-A intensity (Dunnett's, $p < 0.05$).

from 37.4 to 3.9 $\mu\text{g/L}$ anthracene (Table 10). The 22 h EC_{10} ranged from 7.8 to 1.5 $\mu\text{g/L}$ anthracene. Therefore, a toxicity threshold of 1.5 $\mu\text{g/L}$ anthracene may be more ecologically relevant. The incipient toxic concentration, the minimum anthracene concentration necessary to elicit a toxic response at maximum UV-A intensity, appears to be greater than 3 $\mu\text{g/L}$ for a 50% decrease in growth rate and greater than 1 $\mu\text{g/L}$ for a 10% decrease in growth rate (Figure 12). No UV-A radiation threshold for the photo-induced toxicity of anthracene was evident for causing a decrease of the algal growth rate by 10%. However, an UV-A intensity greater than 100 $\mu\text{W}/\text{cm}^2$ was necessary to elicit a 50% decrease in algal growth rate.

^{14}C -bicarbonate incorporation -- No anthracene/UV-A combination tested produced inhibition of ^{14}C -bicarbonate incorporation after 4 h UV-A exposure (Table 11). Differences in the mean ^{14}C -bicarbonate incorporation of the control treatments at different UV-A intensities were caused by differences in the activity of ^{14}C -bicarbonate stocks. Only one anthracene/UV-A combination appeared to cause a significant decrease in ^{14}C incorporation (Table 11). However, the apparent difference in ^{14}C incorporation was removed by normalizing ^{14}C incorporation to cell numbers. Therefore, any effects of anthracene and UV-A radiation on ^{14}C incorporation after 4 h exposure appears to be chiefly due to the effects of the photo-induced toxicity of anthracene on cell numbers, not for any direct effects on photosynthesis.

Table 10. EC_{50} and EC_{10} for the specific growth rate (0-22 h) of Selenastrum capricornutum exposed to anthracene and UV-A radiation. EC_{xx} is the anthracene concentration required to decrease algal growth rate by XX%. Values in parentheses are 95% confidence intervals.

UV-A intensity ($\mu W/cm^2$)	EC_{50} ($\mu g/L$)	EC_{10} ($\mu g/L$)	Probit regression equation ¹		
			slope	y-intercept	r^2
765	3.9 (2.8-5.4)	1.5 (0.9-2.5)	-3.133	6.834	0.87
410	6.6 (5.5-7.8)	2.5 (2.0-3.3)	-3.103	7.534	0.94
406	5.3 (3.6-7.8)	2.3 (1.0-5.4)	-3.462	7.508	0.68
218	12.1 (10.2-14.3)	8.7 (7.5-10.1)	-8.981	14.723	0.94
125	37.4 (11.8-118.6)	7.8 (5.5-11.2)	-1.888	7.970	0.75

¹ Probit regression equation ($y = a + bx$) where:
 $y = \text{Probit}(\% \text{ Control})$ and $x = \log_{10}(\text{anthracene (in } \mu g/L))$.

Figure 12. Effects isopleths for the specific growth rate (0 - 22 h) of Selenastrum capricornutum exposed to anthracene and UV-A radiation.

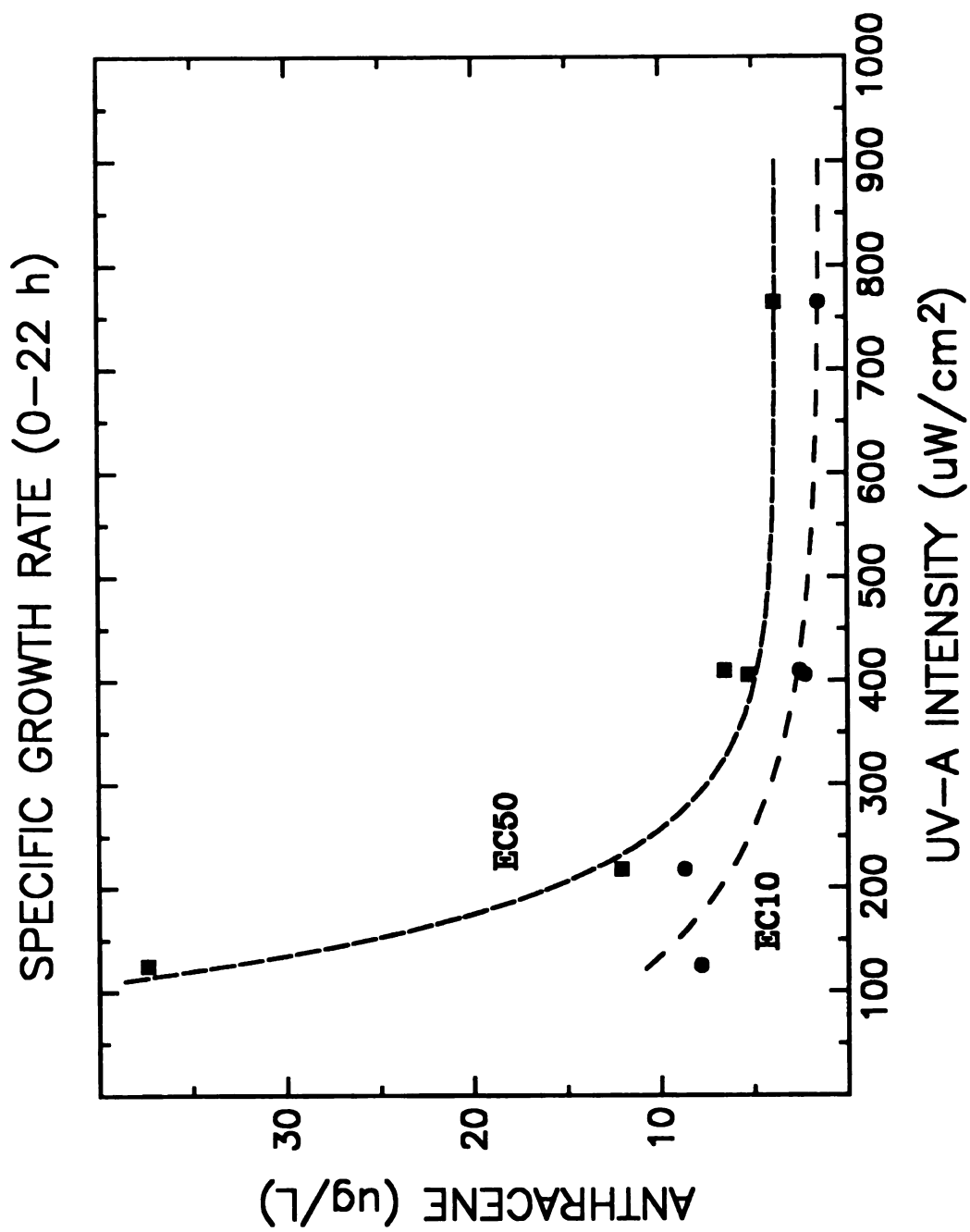


Figure 12.

Table 11. The effects of anthracene (ANTH) and UV-A radiation on the incorporation of ^{14}C -bicarbonate in Selenastrum capricornutum after 4 h exposure. The values in parentheses are one standard deviation of the mean. Concentrations with asterisks are significantly different from the control mean (Control = 0 $\mu\text{g/l}$ anthracene; Dunnett's test, $p < 0.05$). Concentrations with the same letters are not significantly different from each other (Tukey's test, $p < 0.05$). Values represent mean of three replicates.

UV-A ($\mu\text{W}/\text{cm}^2$)	ANTH ($\mu\text{g}/\text{L}$)	^{14}C incorporation (DPM/ml)		^{14}C incorporation ¹ (DPM/ 10^5 cells)	
765	0	2269.1 (196.7)	a	10.0 (0.7)	a
	2.13	2284.5 (252.5)	a	10.8 (1.6)	a
	6.86	2161.3 (256.0)	a	11.4 (2.5)	a
	16.08	2346.9 (427.2)	a	13.0 (1.7)	a
410	0	1595.4 (64.0)	a	8.1 (0.4)	a
	3.89	1517.1 (146.7)	a	7.7 (1.0)	a
	9.28	1531.1 (49.7)	a	8.6 (0.7)	a
	18.08	1365.7 (68.1)	* a	8.5 (0.7)	a
218	0	3911.2 (316.5)	a	20.6 (3.0)	a
	3.42	3901.1 (271.0)	a	20.6 (1.7)	a
	7.71	4035.8 (207.4)	a	21.5 (1.2)	a
	16.98	3887.4 (382.4)	a	25.8 (2.9)	a
125	0	3253.9 (147.9)	a	18.2 (0.6)	a
	3.74	3294.9 (64.4)	a	19.6 (1.1)	a
	8.06	3189.4 (42.6)	a	18.8 (0.9)	a
	17.83	3374.6 (223.1)	a	20.4 (0.9)	* a

¹ ^{14}C incorporation normalized for cell numbers by dividing DPM incorporated by the estimated number of cells in 5 ml sample after 4 h exposure.

The photo-induced toxicity of anthracene caused a decrease in the ^{14}C -bicarbonate incorporation by algal cells after 28 h UV-A exposure (Table 12). Incorporation of ^{14}C -bicarbonate on a volume basis (DPM/ml) is comparable to primary production measures and was reduced at concentrations of anthracene greater than 4 $\mu\text{g/L}$ for most UV-A intensities tested. Converting ^{14}C -bicarbonate incorporation to a per cell basis is comparable to cellular photosynthesis measures. Decreases in ^{14}C incorporation on a per cell basis were limited to anthracene/UV-A combinations containing concentrations of anthracene greater than 12 $\mu\text{g/L}$ and UV-A intensities greater than 400 $\mu\text{W/cm}^2$ (Table 12, Figure 13). Inhibition of ^{14}C incorporation on a per cell basis was complete (> 98%) in the greatest anthracene/UV-A combination.

The 24 h EC_{50} for primary production (^{14}C incorporation in units of DPM/ml) was less than the 24 h EC_{50} for ^{14}C incorporation on a per cell basis (Table 13). Primary production measures demonstrated two-fold greater sensitivity to photo-induced toxicity of anthracene than ^{14}C incorporation on a per cell basis. For primary production, the 24 h EC_{50} ranged from 24.0 to 3.3 $\mu\text{g/L}$ anthracene. This was similar to the 22 h EC_{50} range for specific growth rate. The 24 h EC_{50} for ^{14}C incorporation on a per cell basis ranged from not calculatable to 6.9 $\mu\text{g/L}$. The EC_{50} was not calculatable because either none or only one anthracene treatment had smaller ^{14}C incorporation on a per cell basis than the control

Table 12. The effects of anthracene (ANTH) and UV-A radiation on the incorporation of ^{14}C -bicarbonate in Selenastrum capricornutum after 24 h exposure. The values in parentheses are one standard deviation of the mean. Concentrations with asterisks are significantly different from the control mean (Control = 0 $\mu\text{g/l}$ anthracene; Dunnett's test, $p < 0.05$). Concentrations with the same letters are not significantly different from each other (Tukey's test, $p < 0.05$). Values represent mean of three replicates.

UV-A ($\mu\text{W}/\text{cm}^2$)	ANTH ($\mu\text{g}/\text{L}$)	^{14}C incorporation (DPM/ml)			^{14}C incorporation ¹ (DPM/ 10^5 cells)		
765	0	5274.2	(449.2)	a	6.9	(0.6)	ab
	1.36	5089.5	(168.6)	a	8.1	(0.1)	a
	4.72	1691.1	(747.9)	* b	5.9	(1.2)	b
	12.42	20.9	(12.6)	* c	0.11	(0.08)	* c
410	0	3330.0	(112.3)	a	5.7	(0.8)	ab
	2.26	3176.8	(105.7)	a	5.9	(0.2)	a
	5.79	1299.0	(317.3)	* b	4.4	(0.5)	b
	14.04	333.1	(67.5)	* c	1.8	(0.6)	* c
406	0	10510.6	(221.2)	a	21.8	(0.5)	a
	4.87	5195.8	(418.5)	* b	18.1	(1.5)	a
	6.23	3779.9	(189.1)	* c	24.5	(6.7)	a
	15.75	326.5	(169.1)	* d	2.9	(1.5)	* b
218	0	8484.5	(1374.8)	a	15.9	(3.7)	a
	2.51	7327.4	(740.3)	a	14.1	(1.8)	a
	5.75 ²	6462.3	(258.4)	a	12.5	(0.6)	a
	14.29	2014.9	(288.7)	* b	10.9	(2.1)	a
125	0	7783.8	(597.5)	a	14.0	(1.5)	a
	2.81	7154.9	(340.8)	ab	14.4	(1.5)	a
	6.03	6730.4	(296.1)	* b	15.0	(1.8)	a
	13.65	4960.3	(331.9)	* c	12.8	(1.0)	a

¹ ^{14}C incorporation normalized for cell numbers by dividing DPM incorporated by the estimated number of cells in 5 ml sample after 24 h exposure.

² Mean of two replicates.

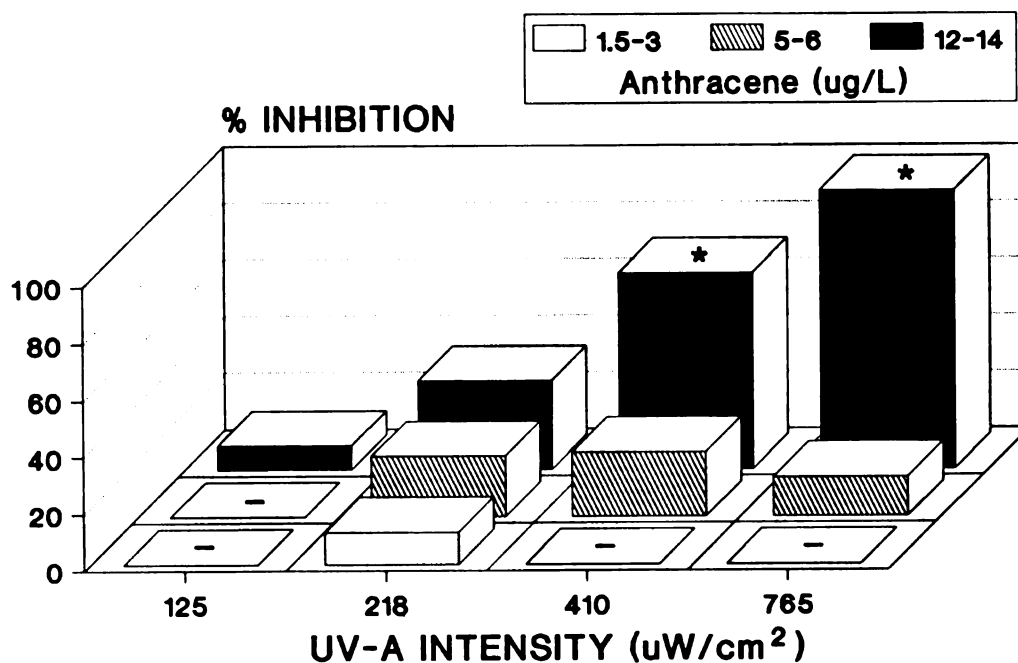
¹⁴C Incorporation per cell (24 h exposure)

Figure 13. The effects of anthracene and UV-A radiation on the ¹⁴C-bicarbonate incorporation on a per cell basis of *Selenastrum capricornutum* after 24 h UV-A exposure. Anthracene/UV-A combinations with asterisks are significantly different from the control mean at the same UV-A intensity (Dunnett's, $p < 0.05$). Dashes (-) are anthracene/UV-A combinations where stimulation occurred.

Table 13. EC_{50} and EC_{10} for ^{14}C -bicarbonate incorporation of Selenastrum capricornutum after 24 h UV-A exposure. EC_{xx} is the concentration of anthracene required to decrease ^{14}C incorporation measures by XX%. Values in parentheses are 95% confidence intervals.

UV-A intensity ($\mu W/cm^2$)	EC ₅₀ ($\mu g/L$)	EC ₁₀ ($\mu g/L$)	Probit regression equation ¹ slope y-intercept r ²		
(a) Primary production (DPM/ml)					
765	3.3 (2.8-3.9)	1.7 (1.4-2.2)	-4.507	7.345	0.97
410	5.9 (5.0-6.9)	2.7 (2.2-3.4)	-3.830	7.947	0.95
406	4.9 (4.4-5.4)	2.2 (1.8-2.7)	-3.744	7.584	0.97
218	8.1 (6.2-10.6)	2.5 (1.7-3.8)	-2.547	7.309	0.87
125	24.0 (13.0-44.3)	3.9 (2.8-5.3)	-1.614	7.227	0.83
(b) ¹⁴ C incorporation on a per cell basis (DPM/cell)					
765	6.9 (5.6-8.5)	4.9 (3.7-6.4)	-8.500	12.118	0.92
410	9.9 (8.1-12.1)	4.1 (3.2-5.3)	-3.386	8.366	0.94
406	11.2 (8.5-14.6)	7.7 (5.5-10.8)	-7.841	13.216	0.91
218	Not calculated ²				
125	Not calculated				

¹ Probit regression equation ($y = a + bx$) where:
 $y = \text{Probit}(\% \text{ control})$ and $x = \log_{10}(\text{anthracene (in } \mu g/L))$.

² Probit regression not calculated because slope was not significantly different from zero.

treatment at that UV-A intensity.

Anthracene concentration and UV-A intensity thresholds were apparent for the effects of the photo-induced toxicity of anthracene on both ^{14}C incorporation measures. Anthracene concentration thresholds for primary production (Figure 14) were similar to anthracene concentration thresholds for specific growth rate. The incipient concentrations for inhibition of primary production by the photo-induced toxicity of anthracene were greater than 3 $\mu\text{g/L}$ and 1 $\mu\text{g/L}$ anthracene for 50% and 10% inhibition, respectively. The UV-A radiation threshold was 50 $\mu\text{W/cm}^2$ for a 50% inhibition of primary production and appeared to be very small for a 10% inhibition of primary production. The thresholds for effects on the ^{14}C incorporation on a per cell basis due to the photo-induced toxicity of anthracene were greater than thresholds for effects on primary production and growth rate. The incipient concentrations were greater than 6 $\mu\text{g/L}$ and 4 $\mu\text{g/L}$ anthracene for a 50% and 10% decrease, relative to controls, in the ^{14}C incorporation on a per cell basis, respectively. The UV-A radiation thresholds were approximately 200 and 100 $\mu\text{W/cm}^2$ for a 50% and 10% inhibition of ^{14}C incorporation on a per cell basis. The incorporation of ^{14}C -bicarbonate on a per cell basis was more resistant to the photo-induced toxicity of anthracene than cell growth or primary production.

Cell size -- Anthracene and UV-A radiation affected cell size, as measured by the flow cytometer, after 4 h UV-A

Figure 14. Effects isopleths for the primary production (^{14}C -bicarbonate incorporation in DPM/ml) of Selenastrum capricornutum after 24 h UV-A exposure.

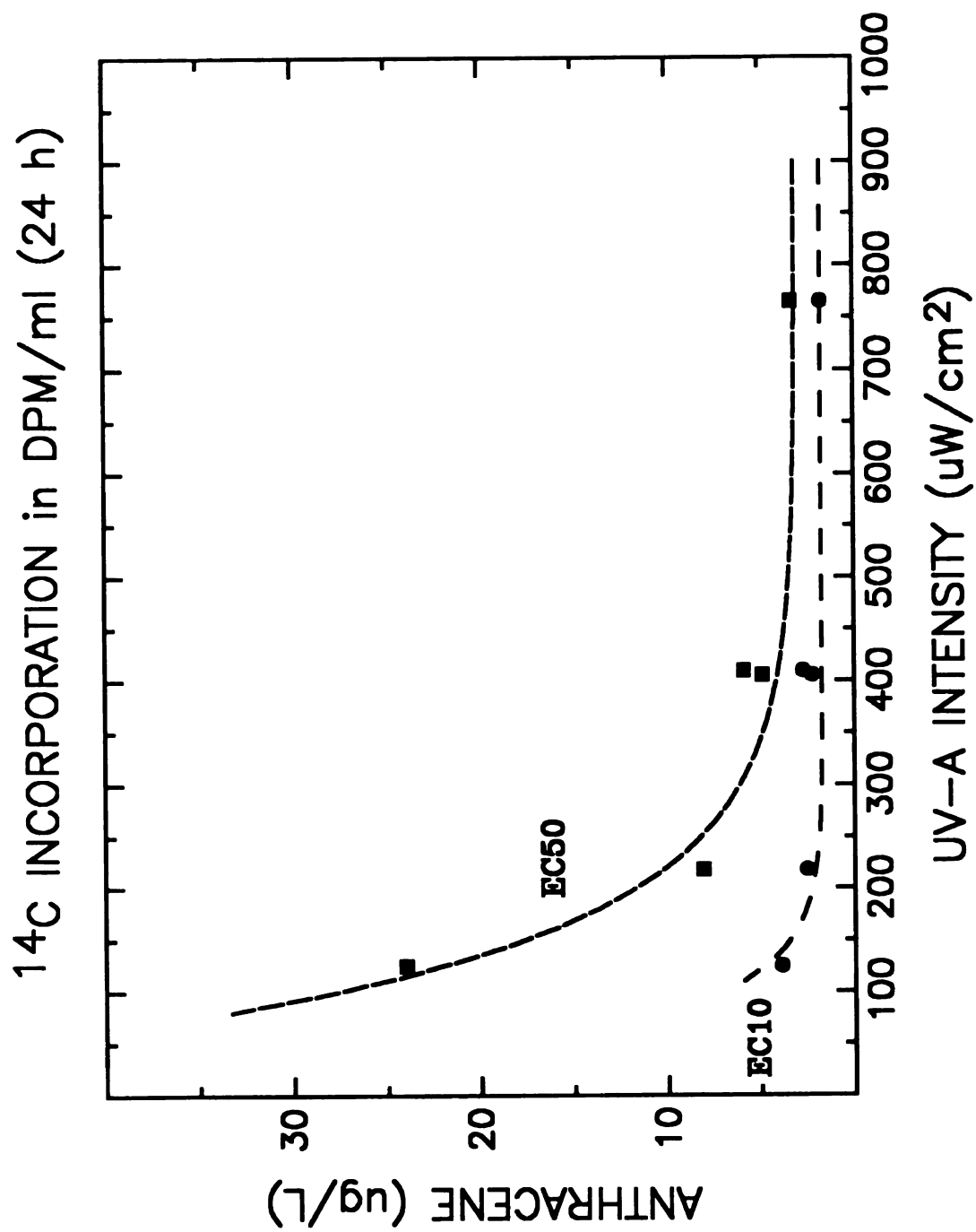


Figure 14.

exposure. Cell size, as measured by mean forward blue scatter, was significantly greater for cells exposed to the greatest concentration of anthracene and to UV-A radiation greater than $400 \mu\text{W}/\text{cm}^2$ (Table 14). Only at an UV-A intensity of $406 \mu\text{W}/\text{cm}^2$ was cell size significantly greater in cells exposed to concentrations of anthracene less than $12 \mu\text{g}/\text{L}$, relative to the control treatments. The equivalent spherical diameter (ESD) of S. capricornutum cells exposed to the control treatments was similar among photo-induced toxicity experiments. The mean cell size of S. capricornutum, as measured by the flow cytometer, was approximately $7.0 \mu\text{m}$ in diameter.

Algal cell size was greater, relative to the cell size in the control treatments, after 28 h UV-A exposure in all anthracene/UV-A combinations which inhibited algal growth rate, except for the smallest anthracene treatment at $406 \mu\text{W}/\text{cm}^2$ UV-A (Table 14). Generally, the ESD did not increase greatly between the 4 h and 28 h flow cytometry samples. The great ESD increase observed at $406 \mu\text{W}/\text{cm}^2$ UV-A in all anthracene treatments was most probably caused by improper analysis of the $7.5 \mu\text{m}$ calibration beads. No observable trend was observed in algal cell size with increasing anthracene concentration and UV-A intensity after either 4 or 28 h UV-A exposure (Figure 15). Dose-response analysis based on cell size, as measured by the flow cytometer, proved to be incompatible with standard probit

Table 14. The effects of anthracene (ANTH) and UV-A radiation on forward blue scatter (cell size) of *Selenastrum capricornutum*, as measured by flow cytometric techniques. Mean forward blue scatter was normalized to control mean (set equal to 100). The values in parentheses are one standard deviation of the mean. Concentrations with asterisks are significantly different from the control mean (Control = 0 $\mu\text{g/L}$ anthracene; Dunnett's test, $p < 0.05$). Concentrations with the same letters are not significantly different from each other (Tukey's test, $p < 0.05$). Values represent mean of three replicates. NOTE: ESD = mean equivalent spherical diameter.

UV-A ($\mu\text{W}/\text{cm}^2$)	4 h exposure				28 h exposure			
	ANTH ($\mu\text{g/L}$)	ESD (μm)	mean forward blue scatter	ANTH ($\mu\text{g/L}$)	ESD (μm)	mean forward blue scatter	ANTH ($\mu\text{g/L}$)	ESD (μm)
765	0	7.2	100.0 (4.8)	0	nc ¹	100.0 (0.2)	0	100.0 (0.2)
	2.13	7.2	98.8 (3.8)	1.42		103.1 (3.4)	1.42	103.1 (3.4)
	6.86	7.4	104.5 (3.3)	5.00		112.3 (2.8)	5.00	112.3 (2.8)
	16.08	7.6	109.6 (2.4)	13.15		107.7 (0.8)	13.15	107.7 (0.8)
410	0	nc	100.0 (2.0)					
	3.89		100.4 (2.2)					
	9.28		104.0 (0.3)					
	18.08		109.7 (2.4)					
406	0	7.2	100.0 (2.5)	0	8.2	100.0 (3.0)	0	100.0 (3.0)
	3.83	7.4	105.2 (2.0)	4.72	8.3	103.9 (1.1)	4.72	103.9 (1.1)
	8.69	7.5	107.9 (1.4)	6.45	8.7	120.2 (3.2)	6.45	120.2 (3.2)
	19.20	7.6	109.7 (1.0)	16.31	8.7	113.6 (3.8)	16.31	113.6 (3.8)
218	0	7.1	100.0 (5.8)	0	7.2	100.0 (7.1)	0	100.0 (7.1)
	3.42	7.2	102.8 (4.4)	2.50	7.3	101.4 (2.2)	2.50	101.4 (2.2)
	7.71	7.2	102.1 (2.9)	5.79	7.4	105.0 ² (2.2)	5.79	105.0 ² (2.2)
	16.98	7.4	107.0 (3.8)	14.71	7.7	112.0 (3.6)	14.71	112.0 (3.6)

Table 14. Cont.

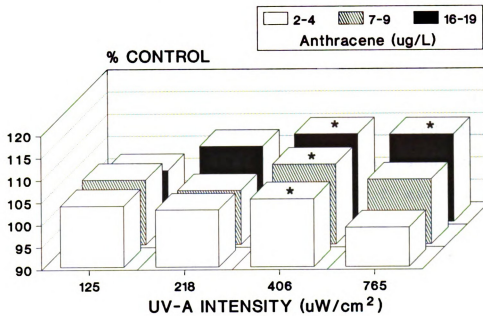
UV-A ($\mu\text{W}/\text{cm}^2$)	4 h exposure				28 h exposure			
	ANTH ($\mu\text{g}/\text{L}$)	ESD (μm)	mean forward blue scatter		ANTH ($\mu\text{g}/\text{L}$)	ESD (μm)	mean forward blue scatter	
125	0	6.5	100.0 (4.5)	a	0	6.4	100.0 (5.0)	a
	3.74	6.6	103.7 (1.2)	a	2.88	6.3	99.0 (2.7)	a
	8.06	6.6	104.5 (4.3)	a	6.09	6.6	107.2 (3.4)	a
	17.83	6.5	101.6 (2.1)	a	13.76	6.9	117.9 (3.1)	* b

¹ nc = not calculated because calibration beads were not analyzed.

² Mean of two replicates.

Figure 15. The effects of anthracene and UV-A radiation on cell size (forward blue scatter) of Selenastrum capricornutum after 4 and 28 h UV-A exposure. Anthracene/UV-A combinations with asterisks are significantly different from the control mean at the same UV-A intensity (Dunnett's, $p < 0.05$).

Cell Size (4 h exposure)



Cell Size (28 h exposure)

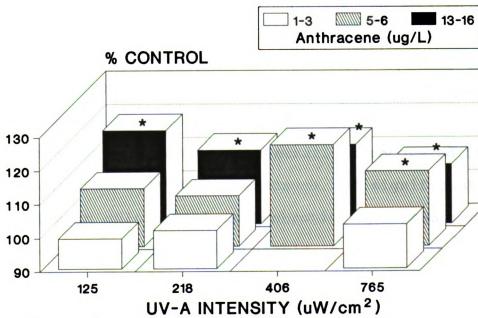


Figure 15.

analysis because of this weak dose-response relationship. Therefore, EC_{50} and EC_{10} values were not calculated.

Cellular chlorophyll concentration -- Cellular chlorophyll concentration, measured as red fluorescence by the flow cytometer, increased due to the effects of anthracene and UV-A radiation after 4 h UV-A exposure. Because red fluorescence increased with increasing cell size in the absence of toxicant exposure, the mean red fluorescence of each sample was corrected for the mean cell size of the sample. In this manner, the effects of the photo-induced toxicity of anthracene on cellular chlorophyll concentration could be isolated from the effects of anthracene and UV-A radiation on algal cell size. Generally, anthracene/UV-A combinations which inhibited algal growth rate caused a significant increase in cellular chlorophyll concentration (Table 15). No dose-response relationship was apparent for the effects of photo-induced toxicity of anthracene on cellular chlorophyll concentration after 4 h UV-A exposure (Figure 16). This was similar to the effects of anthracene and UV-A radiation on cell size.

Cellular chlorophyll concentrations recovered to control concentrations by 28 h UV-A exposure. No significant increase in cellular chlorophyll concentration was measured for any anthracene/UV-A combination (Table 15, Figure 16). Only two anthracene/UV-A combinations significantly altered cellular chlorophyll concentrations after 28 h UV-A exposure. The

Table 15. The effects of anthracene (ANTH) and UV-A radiation on red fluorescence (cellular chlorophyll concentration), normalized for cell size, of *Selenastrum capricornutum*, as measured by flow cytometric techniques. Mean red fluorescence was normalized to the control mean (set equal to 100). The values in parentheses are one standard deviation of the mean. Concentrations with asterisks are significantly different from the control mean (Control = 0 $\mu\text{g/L}$ anthracene; Dunnett's test, $p < 0.05$). Concentrations with the same letters are not significantly different from each other (Tukey's test, $p < 0.05$). Values represent mean of three replicates.

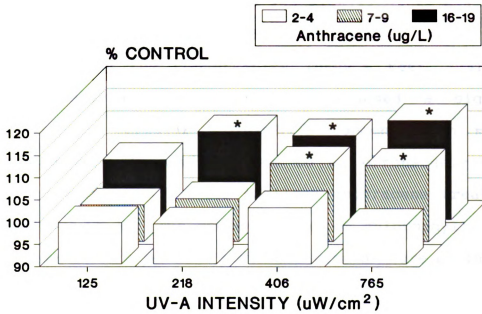
UV-A ($\mu\text{W}/\text{cm}^2$)	4 h exposure				28 h exposure			
	ANTH ($\mu\text{g/L}$)	mean red fluorescence			ANTH ($\mu\text{g/L}$)	mean red fluorescence		
765	0	100.0	(3.0)	a	0	100.0	(14.5)	ab
	2.13	98.7	(1.2)	a	1.42	108.6	(7.1)	ab
	6.86	107.2	(0.4)	* b	5.00	117.1	(11.1)	a
	16.08	112.2	(1.0)	* b	13.15	82.5	(14.8)	* b
410	0	100.0	(2.2)	a				
	3.89	106.2	(0.4)	a				
	9.28	108.0	(4.4)	ab				
	18.08	117.8	(6.6)	* b				
406	0	100.0	(3.3)	a	0	100.0	(2.0)	a
	3.83	102.7	(3.0)	ab	4.72	72.9	(2.6)	* b
	8.69	107.6	(3.0)	* ab	6.45	102.4	(14.5)	a
	19.20	108.8	(2.6)	* b	16.31	108.6	(5.2)	a
218	0	100.0	(3.9)	a	0	100.0	(5.6)	a
	3.42	99.0	(1.2)	a	2.50	97.1	(1.4)	a
	7.71	99.7	(3.4)	a	5.79	92.5 ¹	(1.7)	a
	16.98	109.7	(4.6)	* b	14.71	101.2	(7.8)	a
125	0	100.0	(2.0)	a	0	100.0	(0.9)	a
	3.74	99.3	(2.8)	a	2.88	98.3	(1.4)	a
	8.06	98.3	(5.0)	a	6.09	98.0	(2.0)	a
	17.83	103.5	(3.0)	a	13.76	100.8	(2.1)	a

¹ Mean of two replicates.

Figure 16. The effects of anthracene and UV-A radiation on cellular chlorophyll concentration (red fluorescence), normalized to cell size, of Selenastrum capricornutum after 4 and 28 h UV-A exposure. Anthracene/UV-A combinations with asterisks are significantly different from the control mean at the same UV-A intensity (Dunnett's $p < 0.05$).

120

Chlorophyll (4 h exposure)



Chlorophyll (28 h exposure)

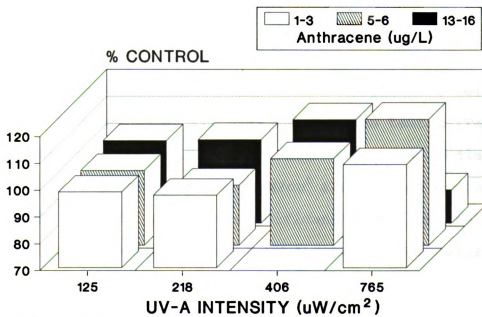


Figure 16.

cellular chlorophyll concentration of cells exposed to 13 $\mu\text{g/L}$ anthracene at 765 $\mu\text{W/cm}^2$ UV-A was significantly smaller than the control treatment. However, significance was not registered by the conservative Tukey's test. The other anthracene/UV-A combination which caused a significant decrease in cellular chlorophyll concentration may have resulted from an artifact due to an erroneously elevated anthracene renewal in the smallest anthracene treatment at 406 $\mu\text{W/cm}^2$ UV-A. The concentration of chlorophyll in algal cells appears to be the least sensitive measure of the photo-induced toxicity of anthracene to algae because recovery of cellular chlorophyll concentrations to control concentrations occurred in anthracene/UV-A combinations which caused detrimental alterations of other measures.

Cell viability index -- Inhibition of cell viability, as measured by the cell viability index (CVI), due to exposure to anthracene and UV-A radiation was readily apparent after 4 h UV-A exposure. Algal cells exposed to concentrations of anthracene greater than 16 $\mu\text{g/L}$ had a smaller CVI relative to control treatments at all UV-A intensities tested (Table 16). Exposure to 6-9 $\mu\text{g/L}$ anthracene and UV-A radiation at intensities greater than 200 $\mu\text{W/cm}^2$ also caused depression of the CVI. The CVI was also significantly smaller, relative to control treatments, after 4 h UV-A exposure for cells exposed to 3.8 $\mu\text{g/L}$ anthracene at UV-A intensities of 406 and 410 $\mu\text{W/cm}^2$. However, at 410 $\mu\text{W/cm}^2$ UV-A, the significant

Table 16. The effects of anthracene (ANTH) and UV-A radiation on the cell viability index (CVI) of Selenastrum capricornutum, as measured by flow cytometric techniques. Mean CVI was normalized to the control mean (set equal to 100). The values in parentheses are one standard deviation of the mean. Concentrations with asterisks are significantly different from the control mean (Control = 0 $\mu\text{g/L}$ anthracene; Dunnett's test, $p < 0.05$). Concentrations with the same letters are not significantly different from each other (Tukey's test, $p < 0.05$). Values represent mean of three replicates.

4 h exposure					28 h exposure				
UV-A ($\mu\text{W}/\text{cm}^2$)	ANTH ($\mu\text{g/L}$)	mean CVI			ANTH ($\mu\text{g/L}$)	mean CVI			
765	0	100.0	(5.6)	a	0	100.0	(2.0)	a	
	2.13	99.4	(5.7)	a	1.42	102.9	(9.7)	a	
	6.86	73.3	(3.8)	* b	5.00	33.6	(12.9)	* b	
	16.08	47.6	(3.4)	* c	13.15	1.6	(2.5)	* c	
410	0	100.0	(1.5)	a					
	3.89	93.4	(1.4)	* b					
	9.28	86.7	(3.6)	* c					
	18.08	71.6	(2.0)	* d					
406	0	100.0	(5.9)	a	0	100.0	(2.8)	a	
	3.83	71.5	(7.0)	* b	4.72	71.2	(3.4)	* b	
	8.69	81.3	(1.2)	* b	6.45	46.5	(3.2)	* c	
	19.20	56.0	(2.0)	* c	16.31	7.0	(1.7)	* d	
218	0	100.0	(8.2)	a	0	100.0	(1.9)	a	
	3.42	90.7	(6.5)	a	2.50	105.7	(7.3)	a	
	7.71	81.0	(8.9)	* ab	5.79	105.6 ¹	(1.7)	a	
	16.98	64.1	(6.6)	* b	14.71	39.9	(6.4)	* b	
125	0	100.0	(4.8)	a	0	100.0	(4.5)	a	
	3.74	99.0	(4.2)	a	2.88	103.0	(4.2)	a	
	8.06	95.9	(1.9)	a	6.09	102.2	(4.5)	a	
	17.83	73.6	(5.0)	* b	13.76	61.8	(4.0)	* b	

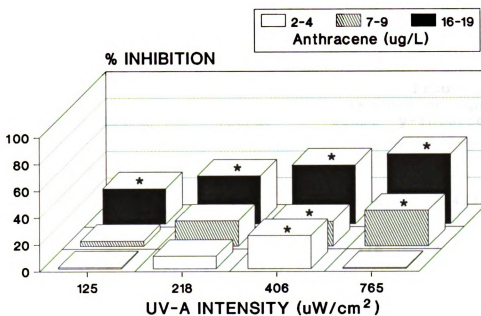
¹ Mean of two replicates.

decrease in cell viability observed at a concentration of 3.8 $\mu\text{g/L}$ anthracene was more attributable to the small variability of the CVI measurement than the magnitude of the decrease, which was only 7%. A dose-response relationship between cell viability, as measured by the CVI, and anthracene/UV-A exposure was discernable after 4 h UV-A exposure, especially at concentrations of anthracene greater than 16 $\mu\text{g/L}$ (Figure 17). A significant reduction of the CVI after 4 h UV-A exposure (Figure 17) was a good predictor of anthracene/UV-A combinations which also inhibited the specific growth rate (0-22 h) (Figure 11). The great sensitivity and predictability of the CVI demonstrates the utility of the flow cytometric FDA cell viability assay in algal toxicity testing.

Effect thresholds for anthracene and UV-A radiation were estimated for the CVI after 4 h UV-A exposure by probit analysis (Table 17, Figure 18). Algal cells were resistant to great reductions in the CVI if as much as 50% (EC_{50}) after 4 h UV-A exposure. The threshold for a 50% reduction in the CVI was approximately 10 $\mu\text{g/L}$ anthracene and 100 $\mu\text{W/cm}^2$ UV-A. The apparent resistance of this cell viability measure, the CVI, to the photo-induced toxicity of anthracene most probably resulted from the brief UV-A exposure of only 4 h. The threshold for a 10% reduction in the CVI was greater than 3 $\mu\text{g/L}$ anthracene and less than 50 $\mu\text{W/cm}^2$ UV-A. The EC_{10} isopleth for the CVI after 4 h UV-A exposure (Figure 18) was identical to the 22 h EC_{50} isopleth for specific growth rate

Figure 17. The effects of anthracene and UV-A radiation on the cell viability index (CVI) of Selenastrum capricornutum after 4 and 28 h UV-A exposure. Anthracene/UV-A combinations with asterisks are significantly different from the control mean at the same UV-A intensity (Dunnett's, $p < 0.05$). Dashes (-) are anthracene/UV-A combinations where stimulation occurred.

FDA Cell viability index (4 h exposure)



FDA Cell viability index (28 h exposure)

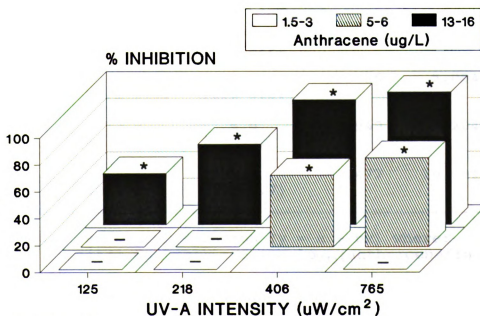


Figure 17.

Table 17. EC_{50} and EC_{10} for the cell viability index (CVI) of Selenastrum capricornutum after 4 and 28 h UV-A exposure. EC_{xx} is the anthracene concentration required to decrease the CVI by XX%. Values in parentheses are 95% confidence intervals.

UV-A intensity (μ W/cm ²)	EC ₅₀ (μ g/L)	EC ₁₀ (μ g/L)	Probit regression equation ¹ slope y-intercept r ²		
(a) 4 h UV-A exposure					
765	14.5 (12.6-16.9)	3.5 (3.0-4.1)	-2.079	7.417	0.98
410	51.7 (29.3-91.1)	6.1 (4.9-7.5)	-1.376	7.357	0.90
406	22.6 (20.5-25.0)	5.7 (5.0-6.5)	-2.143	7.902	0.99
218	30.1 (12.6-72.0)	4.2 (2.5-7.0)	-1.504	7.224	0.71
125	27.8 (19.3-40.1)	11.4 (9.7-13.3)	-3.292	9.754	0.93
(b) 28 h UV-A exposure					
765	3.6 (2.8-4.7)	1.6 (1.0-2.5)	-3.577	7.008	0.96
406	6.4 (6.1-6.8)	2.9 (2.6-3.3)	-3.716	8.004	0.99
218	12.2 (10.1-14.7)	4.5 (3.5-5.7)	-2.949	8.204	0.98
125	16.1 (13.6-19.0)	8.3 (7.1-9.7)	-4.477	10.401	0.99

¹ Probit regression equation ($y = a + bx$) where:
 $y = \text{Probit}(\% \text{ Control})$ and $x = \log_{10}(\text{anthracene (in } \mu g/L))$.

Figure 18. Effects isopleths for the cell viability index (CVI) of Selenastrum capricornutum after 4 and 28 h UV-A exposure. Note: Results from 410 $\mu\text{W}/\text{cm}^2$ UV-A exposure (4 h) were not included.

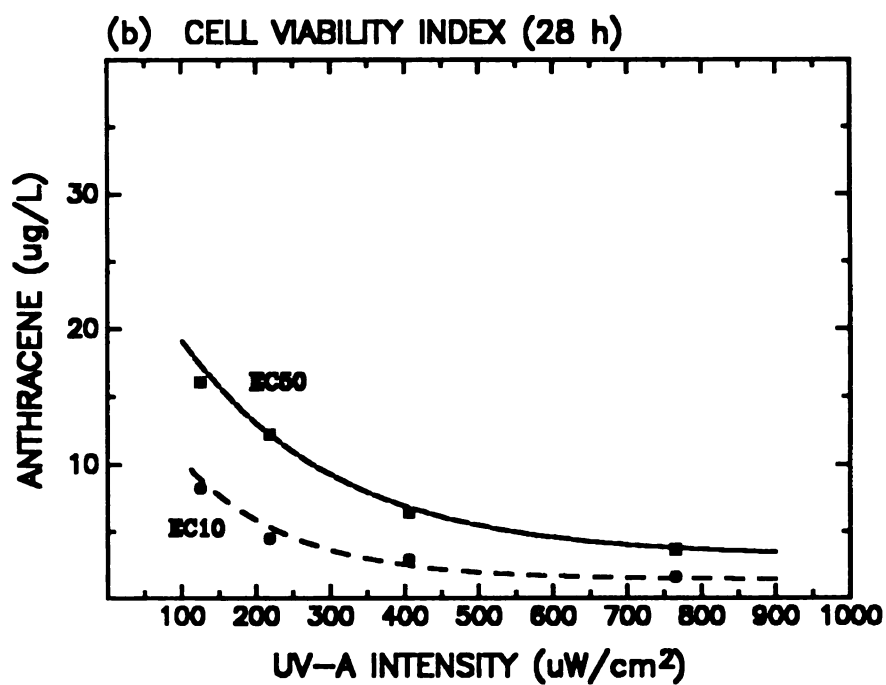
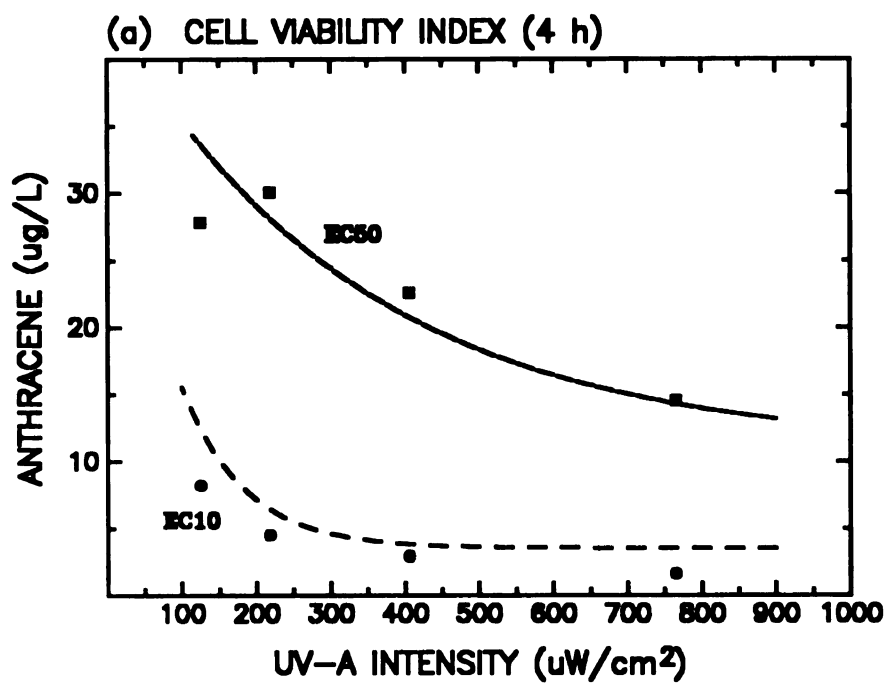


Figure 18.

at UV-A intensities greater than $400 \mu\text{W}/\text{cm}^2$ and to the 22 h EC_{10} isopleth for specific growth rate at smaller UV-A intensities (Figure 12).

Further reductions in the CVI occurred with continued exposure to UV-A radiation and anthracene. A significant reduction of the CVI after 28 h UV-A exposure (Table 16) only occurred in anthracene/UV-A combinations which also caused significant inhibition of algal growth rate. The only anthracene/UV-A combination which recovered to the control CVI between 4 and 28 h UV-A exposure was not significantly smaller than the control CVI after 4 h exposure, according to analysis by Tukey's test.

A definite threshold was evident for the effects of the photo-induced toxicity of anthracene to the CVI after 28 h UV-A exposure. Anthracene/UV-A combinations either caused a great reduction in the CVI (greater than 30% reduction relative to control CVI) or a small enhancement (less than 6%) after 28 h exposure (Figure 17). The 28 h EC_{50} for the CVI ranged from 3.6 to 16.1 $\mu\text{g}/\text{L}$ anthracene, depending on the UV-A intensity (Table 17). The 28 h EC_{10} for the CVI ranged from 1.6 to 8.3 $\mu\text{g}/\text{L}$ anthracene. The CVI and growth rate endpoints appeared to be equally sensitive to the photo-induced toxicity of anthracene because their EC_{50} and EC_{10} were of similar magnitude at the UV-A intensities tested. The EC_{10} isopleth for the 28 h CVI (Figure 18) was identical to the EC_{10} isopleth for the 22 h specific growth rate (Figure 12). Direct

toxicity of anthracene may be occurring at the smallest UV-A intensity because there did not appear to be a threshold of UV-A radiation for inhibition of cell viability, as measured by the CVI. The thresholds of anthracene concentration for reducing the CVI after 28 h UV-A exposure by 50% and 10% were greater than 3 $\mu\text{g/L}$ and 1 $\mu\text{g/L}$, respectively.

% Non-viable cells -- Exposure to anthracene and UV-A radiation resulted in significant alterations in the proportions of non-viable *S. capricornutum* cells after 4 h UV-A exposure. The percentage of non-viable cells increased due to the photo-induced toxicity of anthracene for anthracene treatments containing 16-18 $\mu\text{g/L}$ anthracene at 765 and 410 $\mu\text{W/cm}^2$ UV-A (Table 18). The percentage of non-viable cells significantly decreased in the greatest anthracene treatment at 406 $\mu\text{W/cm}^2$ UV-A. Therefore, it appears that the increase in the percentage of non-viable cells at 410 $\mu\text{W/cm}^2$ UV-A may not be real and was not reproducible. A significant decrease in the percentage of non-viable cells was observed in concentrations of anthracene greater than 7 $\mu\text{g/L}$ at 406 and 218 $\mu\text{W/cm}^2$ UV-A. Although, the decrease was statistically significant, it probably was not biologically significant because the percentage of non-viable cells measured was within the range of the percentage of non-viable cells observed for the control treatments. Therefore, except for the greatest anthracene/UV-A combination, the photo-induced toxicity of anthracene had minimal effects on percentage of non-viable

Table 18. The effects of anthracene (ANTH) and UV-A radiation on cell viability (% non-viable cells) of Selenastrum capricornutum, as measured by flow cytometric techniques. The values in parentheses are one standard deviation of the mean. Concentrations with asterisks are significantly different from the control mean (Control = 0 $\mu\text{g/L}$ anthracene; Dunnett's test, $p < 0.05$). Concentrations with the same letters are not significantly different from each other (Tukey's test, $p < 0.05$). Values represent mean of three replicates.

4 h exposure				28 h exposure			
UV-A ($\mu\text{W}/\text{cm}^2$)	ANTH ($\mu\text{g/L}$)	mean % non-viable cells		ANTH ($\mu\text{g/L}$)	mean % non-viable cells		
765	0	6.7	(1.6) a	0	7.0	(0.5)	a
	2.13	5.1	(1.5) a	1.42	6.5	(0.9)	a
	6.86	6.7	(2.3) a	5.00	53.5	(11.9)	* b
	16.08	17.0	(3.1) * b	13.15	92.9	(0.9)	* c
410	0	7.6	(1.1) ab				
	3.89	8.6	(0.5) a				
	9.28	6.7	(0.7) b				
	18.08	12.7	(0.5) * c				
406	0	14.6	(2.1) a	0	5.8	(0.7)	a
	3.83	12.9	(2.0) ac	4.72	11.4	(3.0)	a
	8.69	7.0	(0.7) * b	6.45	32.0	(2.8)	* b
	19.20	9.0	(2.5) * bc	16.31	72.9	(3.2)	* c
218	0	11.1	(1.9) a	0	11.8	(1.8)	a
	3.42	10.7	(1.1) a	2.50	11.5	(1.6)	a
	7.71	7.0	(0.3) * b	5.79	7.9 ¹	(0.5)	a
	16.98	7.6	(0.4) * b	14.71	46.3	(4.8)	* b
125	0	9.4	(2.4) a	0	7.6	(0.4)	a
	3.74	7.9	(0.7) a	2.88	7.1	(0.6)	a
	8.06	7.4	(2.4) a	6.09	9.4	(0.8)	* b
	17.83	9.0	(3.1) a	13.76	5.1	(0.4)	* c

¹ Mean of two replicates.

cells after 4 h UV-A exposure.

The photo-induced toxicity of anthracene increased the percentage of non-viable cells after 28 h UV-A exposure. All anthracene/UV-A combinations which inhibited algal growth rate demonstrated significant increases in the percentage of non-viable cells after 28 h exposure, except for the greatest anthracene treatment at $125 \mu\text{W}/\text{cm}^2$ UV-A and the smallest anthracene treatment at $406 \mu\text{W}/\text{cm}^2$ UV-A (Table 18). In fact, a significant decrease in the percentage of non-viable cells was measured in the greatest anthracene treatment at $125 \mu\text{W}/\text{cm}^2$ UV-A. For the same reasons discussed previously, the biological importance of such a decrease is suspect. The biological importance of the significant increase in the percentage of non-viable cells in $6 \mu\text{g}/\text{L}$ anthracene at $125 \mu\text{W}/\text{cm}^2$ UV-A, an anthracene/UV-A combination which did not inhibit growth, was also questionable because the percentage of non-viable cells measured was within the range typically observed for the control treatments.

A threshold was evident for the effects of the photo-induced toxicity of anthracene on the percentage of non-viable cells after 28 h UV-A exposure (Figure 19). Effects thresholds were apparent for both UV-A radiation and anthracene (Figure 20). The threshold for 50% non-viable cells was $7 \mu\text{g}/\text{L}$ anthracene and $200 \mu\text{W}/\text{cm}^2$ UV-A and for 10% non-viable cells was $5 \mu\text{g}/\text{L}$ anthracene and $100 \mu\text{W}/\text{cm}^2$ UV-A. The 28 h EC_{50} and EC_{10} for percent non-viable cells ranged from

% Non-viable cells (28 h exposure)

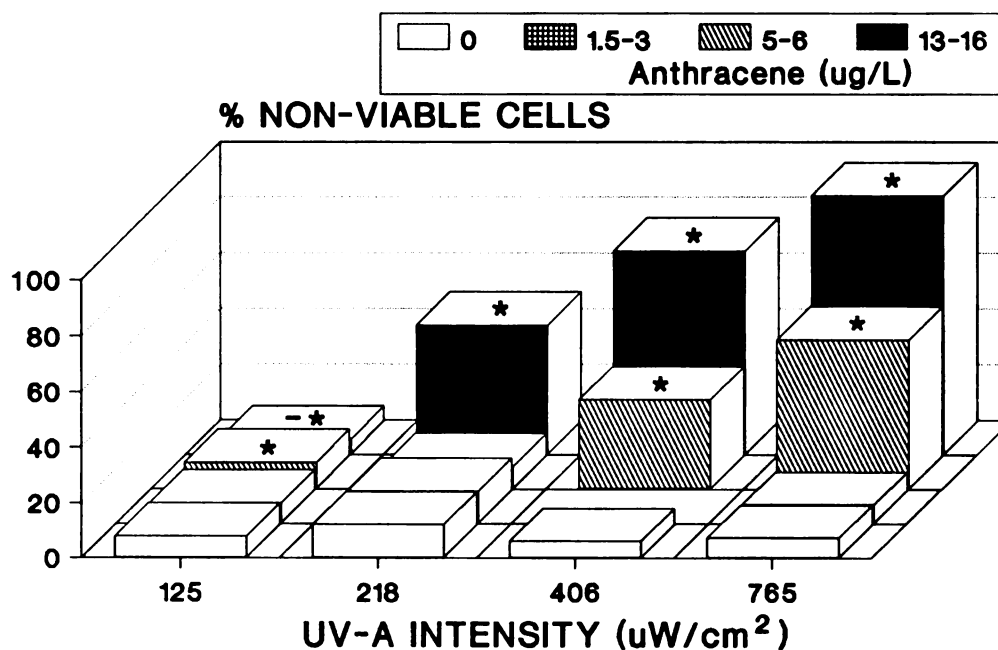


Figure 19. The effects of anthracene and UV-A radiation on the percentage of non-viable Selenastrum capricornutum cells after 28 h UV-A exposure. Anthracene/UV-A combinations with asterisks are significantly different from the control mean at the same UV-A intensity (Dunnett's, $p < 0.05$). Dashes (-) are anthracene/UV-A combinations where stimulation occurred.

Figure 20. Effects isopleths for the percentage of non-viable Selenastrum capricornutum cells after 28 h UV-A exposure.

ntage :
er is:

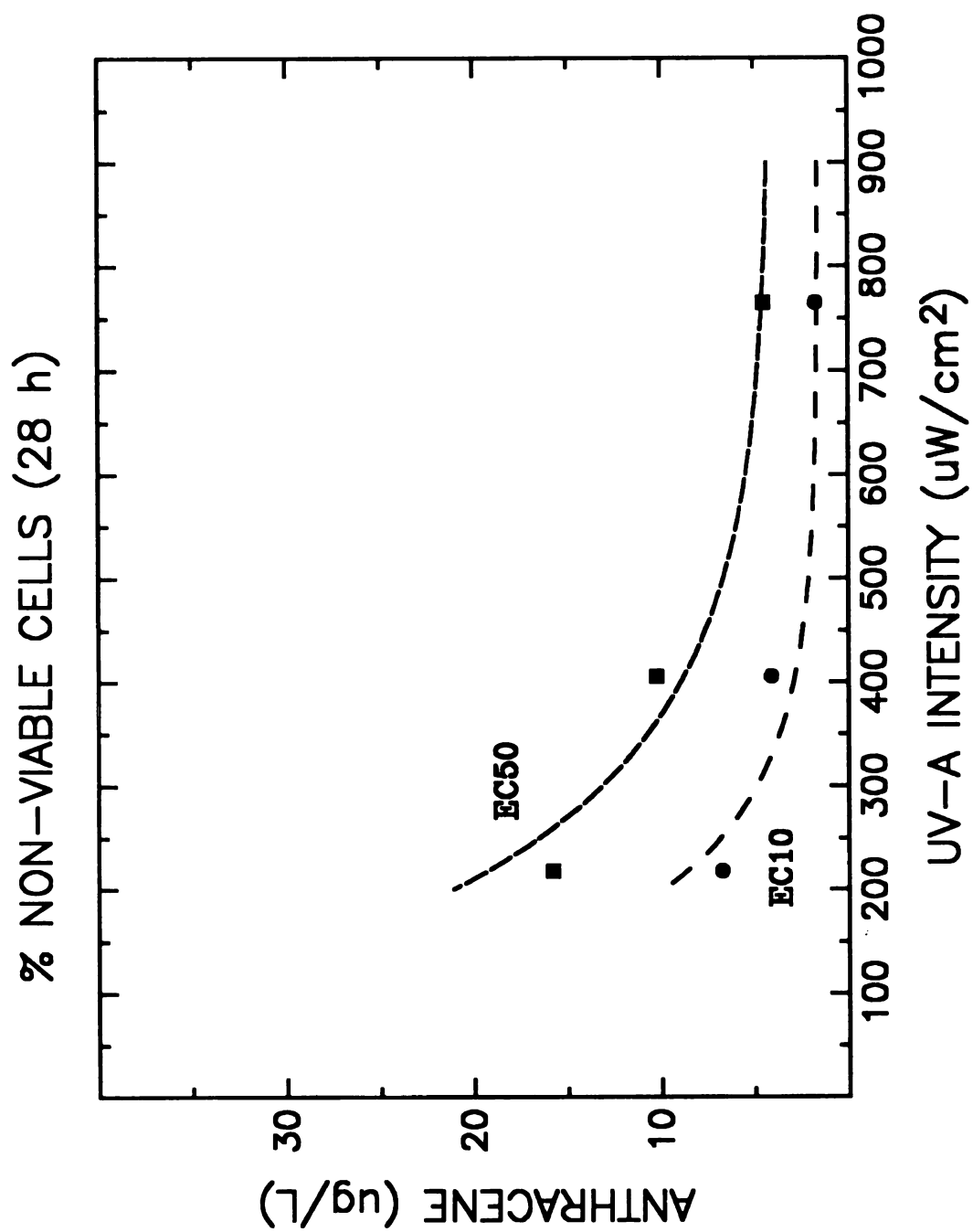


Figure 20.

4.5 to 15.8 $\mu\text{g/L}$ and 1.7 to 6.8 $\mu\text{g/L}$ anthracene, respectively (Table 19). The proportion of non-viable algal cells in the exposed populations was a less sensitive measure of photo-induced toxicity of anthracene than the specific growth rate and the flow cytometric cell viability index.

DISCUSSION

These results demonstrate that algae are sensitive to photo-induced toxicity caused by anthracene and UV-A radiation at anthracene concentrations less than the aqueous solubility of anthracene (35 $\mu\text{g/L}$). Concentrations of anthracene greater than 3 $\mu\text{g/L}$ produced significant inhibition of measured endpoints during the 28 h UV-A exposure. Probit analysis placed the threshold of inhibition (EC_{10}) as small as 1.5 $\mu\text{g/L}$ anthracene. These results suggest that algae may be slightly more resistant to the photo-induced toxicity of anthracene than fishes (Oris and Giesy, 1985; 1986; 1987), and invertebrates (Newsted and Giesy, 1987; Holst, 1987).

The inability of earlier studies (Oris et al., 1984; Cody et al., 1984) to detect the photo-induced toxicity of anthracene to algae at anthracene concentrations less than aqueous solubility most probably resulted from their inadequate experimental designs and insensitive endpoints. The absence of inhibition of ^{14}C incorporation in Chlorella pyrenoidosa exposed to anthracene and UV-A radiation (Oris et

Table 19. EC_{50} and EC_{10} for the cell viability (% non-viable cells) of Selenastrum capricornutum after 28 h UV-A exposure. EC_{xx} is the anthracene concentration that results in XX% non-viable cells. Values in parentheses are 95% confidence intervals.

UV-A intensity ($\mu W/cm^2$)	EC_{50} ($\mu g/L$)	EC_{10} ($\mu g/L$)	Probit regression equation ¹		
			slope	y-intercept	r^2
765	4.5 (4.0-5.0)	1.7 (1.5-2.0)	3.075	2.994	0.98
406	10.2 (9.1-11.5)	4.1 (3.5-4.8)	3.230	1.740	0.96
218	15.8 (13.1-19.1)	6.8 (5.8-7.9)	3.474	0.837	0.96
125	Not calculated ²				

¹ Probit regression equation ($y = a + bx$) where:
 $y = \text{Probit}(\% \text{ non-viable})$ and $x = \log_{10}(\text{anthracene (in } \mu g/L))$.

² Probit regression not calculated because the slope was not significantly different from zero.

al., 1984) is partially explained by the resistance of ^{14}C incorporation as a measure of the photo-induced toxicity of anthracene. Statistically significant inhibition of ^{14}C incorporation endpoints was not observed in S. capricornutum (this study) at exposure durations comparable to Oris and co-workers (1984). However, C. pyrenoidosa was exposed to greater UV-A intensity (solar radiation maximum UV-A intensity = $6800 \mu\text{W}/\text{cm}^2$) and anthracene concentration ($35 \mu\text{g}/\text{L}$) than S. capricornutum in this study. The utilization of an improper control, in which photo-induced toxicity also occurred, greatly contributed to their inability to observe the photo-induced toxicity of anthracene at these greater exposure conditions.

The greater concentration of anthracene ($178 \mu\text{g}/\text{L}$) required to detect photo-induced toxicity to growth of S. capricornutum by Cody and co-workers (1984) resulted from: (1) The reporting of nominal PAH concentrations rather than the undoubtedly lower actual concentrations and (2) the use of unfiltered cool-white illumination for the UV-A source. In the current studies it was observed that the anthracene half-life in the absence of UV-A radiation was approximately 12 h. This suggests that the actual anthracene concentration could have been reduced to 0.4% of the nominal concentration reported by Cody and co-workers (1984) during their 4 day exposure duration. Cool-white bulbs produce 1% of the UV-A radiation of blacklight bulbs and, therefore, are a poor

source of anthracene excitation-wavelengths. These two experimental design flaws contributed to their underestimation of the photo-induced toxicity of anthracene to algae. If more sensitive endpoints or better experimental designs were utilized, the previous studies (Oris et al., 1984; Cody et al., 1984) may have corroborated the photo-induced toxicity of anthracene observed in this study.

This study also detected the direct toxicity of anthracene to algae at anthracene concentrations less than aqueous solubility and in the absence of UV-A radiation for the first time. Anthracene, at aqueous solubility, had been reported to have no effect on ^{14}C -bicarbonate incorporation in S. capricornutum (Giddings, 1979). The EC_{50} for ^{14}C incorporation by Chlamydomonas angulosa and Chlorella vulgaris has been reported to be 245 $\mu\text{g/L}$ and 550 $\mu\text{g/L}$ anthracene, respectively (Hutchinson et al., 1980). These EC_{50} are 5-10 fold greater than the aqueous solubility of anthracene. The detection of the direct toxicity of anthracene in this study at a concentration of 19 $\mu\text{g/L}$ anthracene most probably resulted from the utilization of extremely sensitive flow cytometric measures. Sublethal toxicity was also detected in flow cytometric measures in SDS-exposed algal cells (W. Gala, unpublished data). An increase in cellular chlorophyll concentration, as measured by the flow cytometer, occurred at SDS concentrations which did not inhibit algal growth rate. Direct anthracene toxicity only caused a reversible 18%

reduction in the CVI and a small increase in cellular chlorophyll concentration. Therefore, it appears that direct anthracene toxicity will not be important in assessing the environment hazard posed to algae by anthracene and PAH contamination. However, the detection of direct anthracene toxicity to algae by flow cytometric measures does demonstrate the great sensitivity of flow cytometric techniques.

Algal toxicity endpoints demonstrated differential sensitivity to the effects of the photo-induced toxicity of anthracene. Growth rate and flow cytometric measures of cell viability were the most sensitive endpoints to the photo-induced toxicity of anthracene. Photosynthetic endpoints, such as cellular chlorophyll concentration and ^{14}C incorporation on a per cell basis, were the least sensitive endpoints. Primary production (^{14}C incorporation in DPM/ml), which includes both growth and photosynthesis components, demonstrated sensitivity similar to growth rate endpoints. The 28 h EC_{50} for the cell viability index was identical to the 22 h EC_{50} for specific growth rate at all UV-A intensities greater than $200 \mu\text{W}/\text{cm}^2$. At $125 \mu\text{W}/\text{cm}^2$ UV-A, the cell viability index was more sensitive than growth rate. Similar sensitivity and EC_{50} were also observed between the cell viability index and growth rate in SDS-exposed algal cells (Gala and Giesy, 1989).

Responses in certain toxicity endpoints to the photo-induced toxicity of anthracene appeared to be related.

Similarity of the responses of the CVI and algal growth rate has been previously discussed. The CVI was able to detect sublethal toxicity in anthracene/UV-A combinations which did not inhibit growth rate. Cell viability endpoints, such as the CVI and the percentage of non-viable cells, were directly related to the growth rate endpoint. This suggests that general esterase activity, as measured by the FDA flow cytometric assay, is an excellent measure of cell viability and physiological "health" of algal cells. Algal cell size, measured as forward blue scatter by the flow cytometer, was inversely related to algal growth rate. This inverse relationship between cell size and growth rate was also evident in SDS-exposed algal cells (W. Gala, unpublished data). Surprisingly, there was no correlation between cellular chlorophyll concentration, as measured by red fluorescence, and ^{14}C incorporation on a per cell basis to the photo-induced toxicity of anthracene. Alterations in cellular chlorophyll concentrations occurred without significant changes in ^{14}C incorporation on a per cell basis, as did the converse.

The suite of responses of different toxicity endpoints can be considered a characteristic of a toxicant (Mount, 1989). Analysis of responses of different endpoints can also elucidate possible mechanisms of toxic action of a toxicant. The photo-induced toxicity of anthracene to algae is characterized by acute algicidal action with inhibition of

enzyme systems and cell division occurring prior to inhibition of photosynthesis. Algicidal toxicants characteristically cause increases in the percentage of non-viable cells in conjunction with inhibition of growth rate (Gala and Giesy, 1989). This was the response observed for the photo-induced toxicity of anthracene to S. capricornutum.

These results suggest carotenoids or another antioxidant may be protecting the chloroplasts because of the observed resistance of photosynthesis measures to the photo-induced toxicity of anthracene. Beta-carotene is an efficient singlet oxygen quencher and is the major photoprotection pigment in algae as well as higher plants (Krinsky, 1979; Braumann et al., 1984). The photo-induced toxicity of PAH is expected to proceed via a type II (singlet oxygen) mechanism (Foote, 1976; Sinha and Chignell, 1983; Landrum et al., 1986), and, therefore, beta-carotene should provide protection against photo-induced damage by PAH. Singlet oxygen reacts rapidly with adjacent biomolecules, thus, beta-carotene must be in close proximity to the PAH-generated singlet oxygen to provide effective protection. In green algae, beta-carotene is localized in the chloroplasts thylakoid membranes (Grumbach, 1984) and would protect the chloroplasts and photosynthetic apparatus to the greatest extent against singlet oxygen toxic action. Therefore, the greater resistance of photosynthesis measures suggests that: (1) Beta-carotene protects chloroplasts of S. capricornutum against the photo-induced

toxicity of anthracene and (2) the photo-induced toxicity of anthracene proceeds via a type II (singlet oxygen) mechanism, in vivo. These hypotheses were further tested by investigating the effects of the carotenoid biosynthesis inhibiting herbicide, fluridone, on the photo-induced toxicity of anthracene (Chapter 3).

Photoprotection by carotenoids does convey to algae greater resistance to the photo-induced toxicity of anthracene relative to other aquatic organisms. The 28 h EC_{50} and EC_{10} for the cell viability index, the most sensitive algal endpoint, for S. capricornutum were 16.1 $\mu\text{g/L}$ and 8.3 $\mu\text{g/L}$ anthracene, respectively, at 125 $\mu\text{W/cm}^2$ UV-A. Fishes have been found to be slightly more sensitive to anthracene photo-induced lethality. The acute 96 h LC_{50} and chronic NOEC for juvenile bluegill sunfish exposed continuously to 100 $\mu\text{W/cm}^2$ of UV-A radiation has been reported to be 4.5 $\mu\text{g/L}$ and 1.2 $\mu\text{g/L}$ anthracene, respectively (Oris and Giesy, 1986). The 21 day chronic EC_{50} and EC_{10} for Daphnia magna reproduction at 117 $\mu\text{W/cm}^2$ UV-A (16 L:8 D photoperiod) were approximately 4.2 $\mu\text{g/L}$ and 1.0 $\mu\text{g/L}$ anthracene, respectively (Holst, 1987). The relative sensitivity of aquatic organisms to photo-induced toxicity of anthracene is: Fish, zooplankton > phytoplankton. The greater sensitivity of aquatic animals to photo-induced toxic effects is additional evidence that carotenoids, present

in greater concentrations in algae, are providing protection from the photo-induced toxicity of anthracene.

Ecological consequences

The dose-response relationship characterized for the photo-induced toxicity of anthracene to S. capricornutum can be utilized to estimate the hazard to natural phytoplankton communities posed by PAH contamination of aquatic ecosystems. Two basic assumptions of the hazard assessment are: (1) S. capricornutum is representative of algal sensitivity to the photo-induced toxicity of PAH and (2) anthracene is representative of the potential photo-induced toxicity of the mixture of PAHs found in the environment. Green algae demonstrated intermediate sensitivity to direct UV-B toxicity relative to diatoms (sensitive) and blue-greens (resistant) (Jokiel and York, 1984), thus, the intermediate sensitivity of green algae to indirect UV toxicity (photo-induced toxicity of PAH) is plausible. Anthracene had an intermediate photo-induced toxicity potential to fishes and zooplankton, relative to other PAHs (Oris and Giesy, 1987; Newsted and Giesy, 1987). The two assumptions appear valid, and therefore, the photo-induced toxicity of anthracene to S. capricornutum characterized in this study should be an adequate predictor of the effects of the photo-induced toxicity of PAH to natural phytoplankton populations.

Several components were included in the relationship which was utilized to assess the potential hazard of the photo-induced toxicity of PAH to phytoplankton. These were a measure of the intensity of solar radiation to which phytoplankton in natural waters would be exposed and the concentrations of PAH in natural waters. No UV-A radiation threshold was evident for the photo-induced toxicity of anthracene to S. capricornutum based on many of the endpoints investigated here. The greatest UV-A intensity tested ($765 \mu\text{W}/\text{cm}^2$ UV-A) was only 11% of the maximum summer UV-A intensity at the surface of Lake Michigan and corresponded to the UV-A intensity at a depth of approximately 6 m in offshore Lake Michigan in August (Chapter 1). This suggests that for the photo-induced toxicity of PAH to algae in the environment, solar radiation will not be limiting. It should be noted that the relative intensities of the wavelengths of UV-A radiation from the lighting apparatus utilized in the laboratory are not similar to the UV-A portion of solar radiation. Therefore, it would be inappropriate to utilize laboratory-derived dose-response relationships to quantitatively predict the potential photo-induced toxicity of PAH in natural environments. However, laboratory-derived dose-response relationships could be used for qualitative assessments of the environmental hazard due to the photo-induced toxicity of PAH. It should also be stressed that not all surface waters are as transparent as offshore Lake Michigan and phytoplankton are

not exposed to constant UV radiation due to vertical movement within the water column. These factors would mitigate the hazard of the photo-induced toxicity of PAH to algae by decreasing the UV radiation component of the hazard assessment.

The concentration of PAH to which algal cells will be exposed will be the limiting factor for photo-induced toxicity of PAH for most natural waters. The threshold concentration of PAH to cause photo-induced toxicity, which is approximately 3 $\mu\text{g/L}$, is seldom reached in surface waters (Neff, 1979). The greatest concentrations of PAH measured in the Rhine River, Germany, and the Trent River, England, just approach the PAH concentration threshold (Neff, 1979). Most waters contain concentrations of PAH which are 10 to 100 times less than the threshold concentration for photo-induced toxic effects (Neff, 1979; Eadie et al., 1983; Eisler, 1987). Because of the difficulty in measuring small concentrations of PAH in water, most monitoring of PAH contamination in aquatic systems focuses on PAH in sediments. Typically, concentrations of PAH in the overlying water are 1000 to 10,000 times less than concentrations of PAH in the sediments (Griest, 1980; Andelman and Suess, 1970). Therefore, the concentrations of PAH in sediments corresponding to the threshold for photo-induced toxicity is approximately 3-30 mg/kg total PAH. If this threshold concentration is utilized, then PAH photo-induced toxicity could be inhibiting

phytoplankton in heavily contaminated sites, such as the Black, Fox, and Cuyahoga Rivers in the Great Lakes watershed (Fabacher et al., 1988), Puget Sound (Barrick and Prah1, 1987), and the Charles River and New Bedford Harbor, Massachusetts (Eisler, 1987). As with the solar radiation component, environmental factors will mitigate the concentration of PAH to which phytoplankton are exposed in natural systems. For example, dissolved organic matter reduces the bioavailability of PAH to aquatic organism (Leversee et al., 1983; Landrum et al., 1985). Any reduction in the bioavailability of PAH in natural waters will decrease the PAH component of the photo-induced toxicity hazard assessment.

Conclusions

The photo-induced toxicity of anthracene to algae was demonstrated for the first time at concentrations of anthracene less than aqueous solubility. The threshold for photo-induced toxicity of anthracene was 1.5-3 $\mu\text{g/L}$ anthracene, however, no UV-A radiation threshold was evident for many of the measures of toxicity studied. Measures of the growth rate and viability of algal cells were more sensitive than measures of photosynthesis. This suggests that carotenoids may be protecting algal cells from the photo-induced toxicity of anthracene. Many aquatic systems are sufficiently contaminated by PAH that a hazard to natural

algal communities due to the photo-induced toxicity of PAH may be present. However, the photo-induced toxicity of PAH to animals, such as fish and zooplankton, would be a greater hazard to these ecosystems than effects on algal populations. Field assessments to determine PAH contamination in natural waters and in situ exposures of natural phytoplankton communities to environmentally relevant PAH concentrations under solar radiation are the important gaps of knowledge which should be addressed first. Additional laboratory studies investigating the photo-induced toxicity of other PAH to algae and their mechanism of action are also warranted.

CHAPTER 3

THE EFFECT OF THE CAROTENOID BIOSYNTHESIS INHIBITING HERBICIDE, FLURIDONE, ON THE PHOTO-INDUCED TOXICITY OF ANTHRACENE TO Selenastrum capricornutum.

INTRODUCTION

Polycyclic aromatic hydrocarbons (PAH) probably are the most important photosensitizing contaminants in the environment. The photo-induced toxicity of anthracene was observed in algae (Chapter 2), invertebrates (Allred and Giesy, 1985), fishes (Bowling et al., 1983; Oris and Giesy, 1985), amphibians (Kagan et al., 1984), and mammals (Kaidbey and Nonaka, 1984), at concentrations significantly less than previously thought to be toxic (Giddings, 1979; Eisler, 1987; Neff, 1979). Possibly due to their great concentrations of carotenoid pigments, algae have greater resistance to the photo-induced toxicity of anthracene relative to aquatic animals (Chapter 2; Cody et al., 1984; Oris et al., 1984; Landrum et al., 1986). Protection by carotenoid pigments against the effects of visible light and the photo-induced toxicity of alpha-terthienyl has been observed in aquatic invertebrates (Hairston, 1976; Bennett et al., 1986).

Organisms must be able to protect themselves against photo-induced oxidations by endogenous photosensitizers. Carotenoid pigments protect plants by having the capacity to quench triplet chlorophyll and singlet oxygen (Krinsky, 1979). One carotenoid pigment, beta-carotene, is closely associated with chlorophyll in the thylakoid membranes of chloroplasts (Grumbach, 1984) and is the major photoprotection pigment in algae and higher plants (Braumann et al., 1984). The capacity of carotenoid pigments to quench singlet oxygen is related to the number of conjugated carbon-carbon double bonds in the carotenoid molecule (Foote et al., 1970; Mathis and Kleo, 1973; Mathews-Roth et al., 1974). Carotenoid pigments with at least nine conjugated carbon-carbon double bonds, such as beta-carotene and other colored carotenoid pigments, can quench singlet oxygen because their triplet energies are less than singlet oxygen (Krinsky, 1979).

Manufacturers of herbicides have taken advantage of the importance of the photoprotection capacity of carotenoid pigments by developing herbicides which inhibit carotenoid biosynthesis (Britton, 1979). The carotenoid biosynthesis inhibiting herbicide, fluridone, inhibits the synthesis of beta-carotene and other colored carotenoid pigments in algae as well as higher plants (Bartels and Watson, 1978; Sandmann et al., 1984). Concentrations of colored carotenoid pigments, including beta-carotene, in Scenedesmus acutus were only 17% of control concentrations after 48 h exposure to fluridone

(Sandmann et al., 1984). Chlorophyll synthesis was also reduced, however, this was a secondary response to the deficiency of colored carotenoid pigments in the algal cells (Sandmann et al., 1984).

The objective of this study was to investigate the effects of beta-carotene and other colored carotenoid pigments on the photo-induced toxicity of anthracene to algae. Fluridone was used to decrease the concentrations of colored carotenoid pigments in algal cells exposed to anthracene in the presence of UV-A radiation. This study also determined if the photo-induced toxicity of anthracene proceeds via a type I (free radical) or type II (singlet oxygen) mechanism, in vivo.

MATERIALS AND METHODS

The green alga, Selenastrum capricornutum, was grown in 250 ml flasks under sterile conditions. Media and culture conditions have been given previously (Chapter 2). Fluridone (99% purity, Eli Lilly Co.) in acetonitrile was added to algal cultures in log growth phase. Acetonitrile, if necessary, was added to each flask, including the control (no fluridone added), to bring the total volume of acetonitrile added to 100 μ l. Each treatment consisted of duplicate flasks and the concentrations were control, 1.65, 3.3, 16.5, 33, and 165 μ g/L fluridone. The control and 1.65 μ g/L fluridone treatments were repeated.

Nominal concentrations of fluridone were utilized because the purpose of the fluridone treatments were to generate algal cells with different concentrations of colored carotenoid pigments for subsequent exposure to anthracene and UV-A radiation. Also, concentrations of fluridone in a range-finding study decreased by less than 30% after 96 h exposure, thus, it was deemed unnecessary to determine actual fluridone exposure concentrations for this study. After 48 h exposure, the duplicate flasks were combined and a portion served as the algal inoculum for the exposure to anthracene and UV-A radiation. The remainder was utilized for determination of the concentration of total colored carotenoid pigments in the algal cells.

The concentrations of total colored carotenoid pigments were determined for each fluridone treatment by a standard spectrophotometric method (Parsons et al., 1984). Cell density was enumerated using a hemocytometer and a known volume (60-90 ml) of fluridone-exposed (or control) algal cultures were filtered through a 0.45 μm membrane filter (47 mm), under less than 0.5 atmospheric vacuum. Each filter was placed in a 15 ml centrifuge tube and 10 ml of 90% acetone was added. The tubes were sealed under nitrogen, vortexed, and the pigments were extracted overnight in the dark at 4°C. The tubes were brought to room temperature and centrifuged for 10 minutes at 2000 rpm to remove cellular and filter debris. The supernatant was decanted into a 1 cm path length cuvette and

the absorbance at 750, 510 and 480 nm, relative to a 90% acetone reference blank, was measured by a Gilford 2600 UV/VIS spectrophotometer. The absorbance readings at 510 and 480 nm were corrected for turbidity (750 nm) and the concentration of total colored carotenoid pigments (TCC) was calculated using equation 5 (Parsons et al., 1984),

$$\text{TCC (as } \mu\text{g/ml)} = 7.6 (A_{480} - 1.49 A_{510}) \quad [5]$$

The concentration of total colored carotenoid pigments were reported on a per cell basis (ng colored carotenoid/ 10^6 cells).

The experimental design for the exposure to anthracene and UV-A radiation was eight concentrations of colored carotenoid pigments x two anthracene treatments, with six replicate (16 x 125 mm, borosilicate) test tubes per treatment combination. The two anthracene treatments were no anthracene added (acetonitrile solvent control) and anthracene added (target conc. = 35 $\mu\text{g/L}$ anthracene). All treatment combinations were exposed to 375 $\mu\text{W/cm}^2$ UV-A radiation and 50 $\mu\text{M/m}^2\text{-sec}$ PAR for 8 h. Nominal concentrations of anthracene were utilized because anthracene loss kinetics were predictable from previous studies (Chapter 2) and the 5 ml test volume was insufficient to allow subsampling for anthracene determination. Each tube received 4.5 ml of algal medium to which anthracene (in acetonitrile) or only acetonitrile was

added. Then, an algal inoculum of 0.5 ml from the eight different concentrations of colored carotenoid pigments was added to form the 16 (8 x 2) treatment combinations. Initial cell density ranged from $1.8-3.9 \times 10^5$ cells/ml. The final acetonitrile concentration in the test tubes was 25% of the concentration utilized in the experiments on the photo-induced toxicity of anthracene (Chapter 2).

The effects of the concentration of colored carotenoid pigments in algal cells on the photo-induced toxicity of anthracene were determined by measuring ^{14}C -bicarbonate incorporation on a per cell basis. This simple indicator of toxicity was chosen because it was the most resistant to the photo-induced toxicity of anthracene and it is the cellular function that would be expected to be affected the most by the protective effects of carotenoid pigments (Chapter 2). After 4 and 8 h exposure to anthracene and UV-A radiation, three tubes from each treatment combination were removed for determination of ^{14}C -bicarbonate incorporation. Cell density was enumerated for each tube using a hemocytometer. The ^{14}C incorporation method described in Chapter 2 was utilized. All ^{14}C incorporation values were reported on a per cell basis.

The mean percent inhibition of ^{14}C incorporation due to the photo-induced toxicity of anthracene was determined for the eight concentrations of colored carotenoid pigments after 4 and 8 h exposure to anthracene and UV-A radiation. The percent inhibition of ^{14}C incorporation for each concentration

of colored carotenoid pigments was calculated by dividing the ^{14}C incorporation (DPM/ 10^6 cells) in the anthracene treatment by ^{14}C incorporation in the no anthracene treatment. The statistical significance of the difference in the mean incorporation of ^{14}C -bicarbonate for the two anthracene treatments at each concentration of colored carotenoid pigments was determined by using the t-test (SAS Institute, 1987). The relationship between the concentration of colored carotenoid pigments in the algal cells and the percent inhibition of ^{14}C incorporation due to the photo-induced toxicity of anthracene was determined by correlation and regression analysis (SAS Institute, 1987).

RESULTS AND DISCUSSION

Concentrations of colored carotenoid pigments in S. capricornutum cells, reported as ng carotenoids/ 10^6 cells, were reduced after 48 h exposure to concentrations of fluridone greater than $3.3\ \mu\text{g/L}$, relative to the control treatments (Table 20). A slight increase in the concentration of colored carotenoid pigments was observed in algal cells exposed to the smallest concentration of fluridone. The mean coefficient of variation for three replicate measurements of the concentration of colored carotenoid pigments were determined in a pilot study to be less than 8%. Therefore,

Table 20. The effect of the concentration of colored carotenoid pigments in *S. capricornutum* cells on the percent inhibition of ^{14}C -bicarbonate incorporation due to the photo-induced toxicity of 35 $\mu\text{g/L}$ anthracene in the presence of 375 $\mu\text{W/cm}^2$ UV-A radiation.

Colored carotenoid (ng/ 10^6 cells)	Fluridone ($\mu\text{g/L}$)	% inhibition of ^{14}C incorporation	
		4 h exposure	8 h exposure
117.4	1.65	4.0	-2.9 ¹
115.7	0	13.6	16.8
106.6	1.65	14.1 *	7.3
100.6	0	-3.7	23.0 *
89.1	3.3	3.5	30.0 *
76.9	16.5	18.3	17.4 *
37.4	165.0	-15.6	62.6 *
27.8	33.0	47.1 *	59.1 **

¹ Negative % inhibition means stimulation of ^{14}C incorporation was observed in the treatment with anthracene relative to ^{14}C incorporation in the absence of exposure to anthracene.

Note: * = $p < 0.05$, ** = $p < 0.01$ (t-test)

differences in concentrations of colored carotenoid pigments in the algal cells of less than 20% are probably not significant.

Inhibition of ^{14}C incorporation due to the photo-induced toxicity of anthracene was greater in algal cells with smaller concentrations of colored carotenoid pigments. Statistically significant inhibition of ^{14}C incorporation after 4 h exposure to anthracene and UV-A radiation was observed in only two of the eight concentrations of colored carotenoid pigments (Table 20). Inhibition of ^{14}C incorporation due to the photo-induced toxicity of anthracene was not significant in the two control (no fluridone) treatments after 4 h exposure to anthracene and UV-A radiation. This is similar to the results observed in the photo-induced toxicity of anthracene experiments discussed in Chapter 2, where no anthracene/UV-A combination produced significant inhibition of ^{14}C incorporation (on a per cell basis) after 4 h exposure to anthracene and UV-A radiation. Inhibition of ^{14}C incorporation due to the photo-induced toxicity of anthracene increased after 8 h exposure to anthracene and UV-A radiation and five of eight concentrations of colored carotenoid pigments demonstrated significant inhibition of ^{14}C incorporation (Table 20).

The inhibition of ^{14}C incorporation due to the photo-induced toxicity of anthracene after 8 h exposure to anthracene and UV-A radiation was inversely correlated to the

concentration of colored carotenoid pigments in the algal cells ($r = -0.928$, $p = 0.0009$). Inhibition of ^{14}C incorporation after 4 h exposure to anthracene and UV-A radiation was also inversely correlated to the concentration of colored carotenoid pigments. However, the relationship was not significant after 4 h exposure ($r = -0.270$, $p = 0.52$). The concentration of colored carotenoid pigments in the control treatments was $108 \text{ ng}/10^6$ cells. A reduction in the concentration of colored carotenoid pigments in S. capricornutum cells to $54 \text{ ng}/10^6$ cells, which is one-half of control concentrations, would be expected to increase the percent inhibition of ^{14}C incorporation due to the photo-induced toxicity of anthracene by 2.3 times relative to the control (Figure 21).

Carotenoid pigments are important antioxidants in algae and higher plants (Krinsky, 1979) and, thus, should protect algal and plant cells from the toxic action of anthracene and UV-A radiation. The photo-induced toxicity of PAH has been found to proceed via a type II (singlet oxygen) mechanism, in vitro (Foote, 1976; Sinha and Chignell, 1983). Colored carotenoid pigments, which have nine or more conjugated carbon-carbon double bonds, are efficient quenchers of singlet oxygen (Foote et al., 1970; Mathis and Kleo, 1973; Mathews-Roth et al., 1974). The capacity of an algal cell to quench singlet oxygen and protect itself from the photo-induced toxicity of anthracene should be directly related to

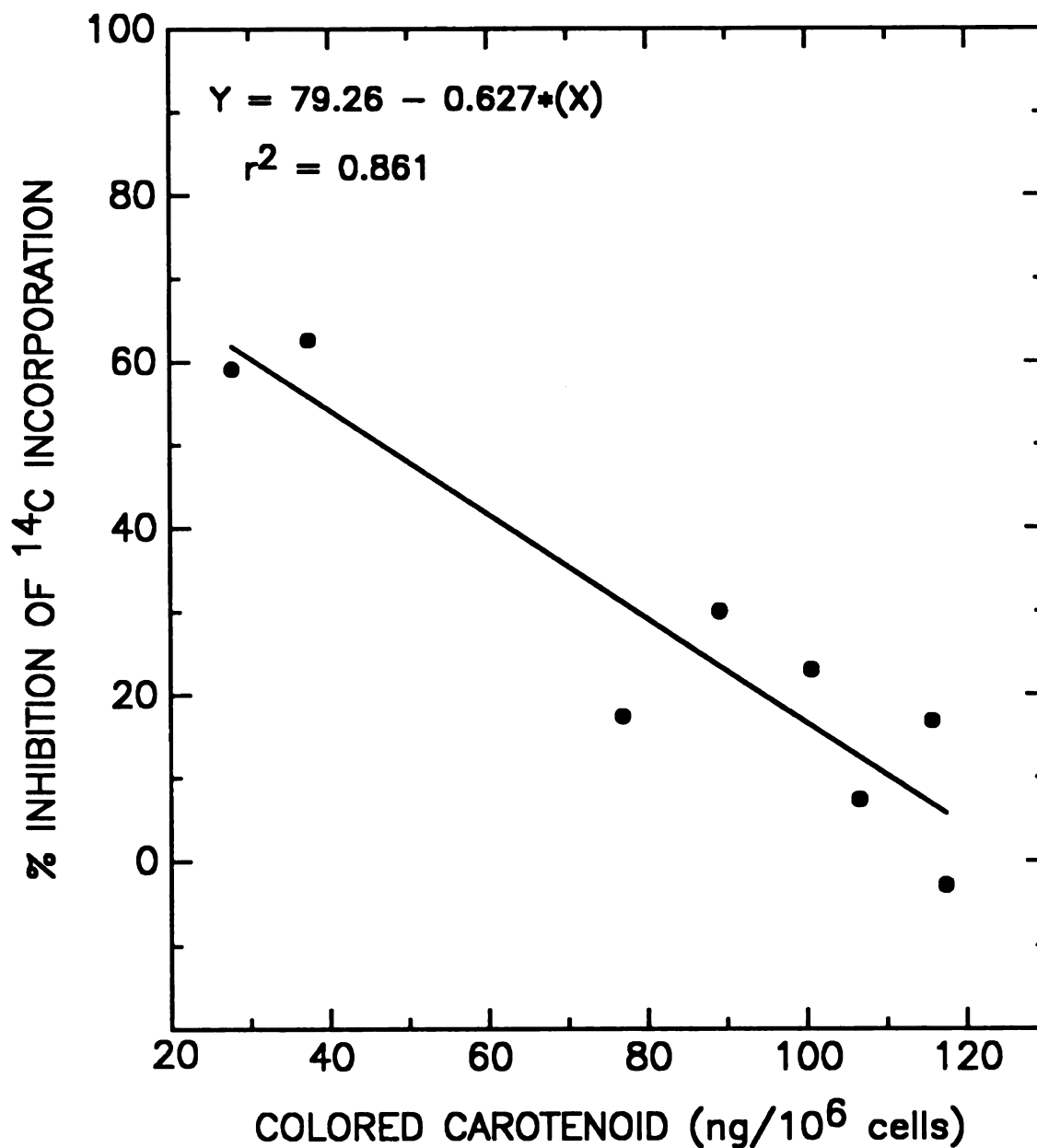


Figure 21. The effect of the concentration of colored carotenoid pigments (ng carotenoids/ 10^6 cells) on the percent inhibition of ^{14}C -bicarbonate incorporation ($\text{DPM}/10^4$ cells) after an 8 h exposure to $35 \mu\text{g}/\text{L}$ anthracene and $375 \mu\text{W}/\text{cm}^2$ UV-A radiation.

the concentration of colored carotenoid pigments contained within the algal cells. The significant inverse relationship for the concentration of colored carotenoid pigments in S. capricornutum cells and the inhibition of ^{14}C incorporation due to the photo-induced toxicity of anthracene clearly indicates a type II (singlet oxygen) mechanism for the photo-induced toxicity of anthracene to algae, in vivo.

In addition to direct evidence for a type II mechanism of action, the effects of fluridone on carotenoid pigment biosynthesis argue against a type I (free radical) mechanism for the photo-induced toxicity of anthracene to algae. Inhibition of carotenoid pigment biosynthesis by fluridone has been observed to cause the accumulation of colorless carotenoid pigments, phytoene and phytofluene, in algal cells (Sandmann et al., 1984). The concentration of the total carotenoid pigments was observed to have been slightly greater in algal cells exposed to fluridone, relative to the control treatment, because the increase in the concentration of colorless carotenoid pigments was greater than the decrease in the concentration of colored carotenoid pigments (Sandmann et al., 1984). Phytoene, which has three conjugated carbon-carbon double bonds, and phytofluene, which has five conjugated carbon-carbon double bonds, have triplet energies equal to 200 kJ/mol and 140 kJ/mol, respectively (Krinsky, 1979). The triplet energies of phytoene and phytofluene are much greater than the energy difference between singlet and

triplet oxygen (94 kJ/mol) (Krinsky, 1979) and, therefore, the colorless carotenoid pigments are unable to quench singlet oxygen. However, the triplet energies of colorless carotenoid pigments are sufficiently small to quench photo-excited triplet anthracene (178 kJ/mol) (Morgan et al., 1977). Phytoene has demonstrated the capacity to quench free radicals (Mathews-Roth et al. 1974). Therefore, the accumulation of colorless carotenoid pigments in algal cells exposed to fluridone should have minimal effect on the capacity of carotenoid pigments to protect algal cells from a toxicant with a type I (free radical) mechanism of action. The results of this study suggest that the photo-induced toxicity of anthracene does not proceed via a type I mechanism, because exposure of algal cells to concentrations of fluridone which caused inhibition of carotenoid biosynthesis had a great effect on the capacity of algal cells to protect themselves from the toxic action of anthracene and UV-A radiation.

CONCLUSIONS

The concentration of colored carotenoid pigments in S. capricornutum cells was inversely correlated to the percent inhibition of ^{14}C incorporation due to the photo-induced toxicity of anthracene. The increased sensitivity of algal cells exposed to anthracene and UV-A radiation caused by smaller concentrations of colored carotenoid pigments in the

algal cells suggests that the photo-induced toxicity of anthracene proceeds via a type II (singlet oxygen) mechanism, in vivo. Additional experiments are suggested from these results. The relationship between concentrations of colored carotenoid pigments in other organisms and their resistance to the photo-induced toxicity of PAH should be investigated. Also, it should be determined if smaller concentrations of colored carotenoid pigments within algal cells causes increased sensitivity to the photo-induced toxicity of PAH, as determined by growth rate and cell viability endpoints.

SUMMARY

The studies presented in this dissertation suggest that solar UV radiation (SUVR) can have considerable impact on natural algal communities directly through the effects of UV radiation and indirectly from the photo-induced toxicity of PAH. Current intensities of SUVR are clearly inhibiting primary production in the upper surface waters of offshore Lake Michigan. The effect of SUVR on the annual primary production of Lake Michigan and other aquatic systems appears to be small. However, when sensitive phytoplankton dominate the assemblages and primary production is concentrated near the surface, SUVR can cause great decreases in the potential primary production. During these situations, SUVR can be an important environmental parameter for determining the structure and successional patterns of phytoplankton communities.

It is interesting that all studies utilizing in situ incubations of natural phytoplankton assemblages have observed that inhibition of primary production by SUVR is limited to the top third of the euphotic zone. The strong convergence of widely different phytoplankton communities, from hyper-oligotrophic oceanic communities to marine coastal communities

to oligotrophic freshwater communities, to an identical sensitivity to SUVR implicates the effects of solar UV radiation as an important environmental parameter influencing phytoplankton evolutionary history. Investigations into phytoplankton adaptive strategies, such as increasing their concentration of carotenoid pigments, to limit the direct effects of UV radiation are strongly suggested by these results.

Although primary production is clearly inhibited by current intensities of SUVR, little concern is warranted for the possible effects of increased intensities of SUVR due to stratospheric ozone depletion. Even assuming a worst-case scenario of cloudless skies, no vertical phytoplankton movement, and an action spectra (DNA) which maximizes the amplification factor, little additional inhibition of primary production would be expected to occur, due to projected increased intensities of SUVR from a reasonable estimate of ozone depletion. Ozone depletion is also of little concern for the photo-induced toxicity of PAH to algae, because few phototoxic PAH absorb the short UV wavelengths (less than 300 nm) that will increase appreciably due to ozone depletion.

The photo-induced toxicity of anthracene experiments demonstrated that algae were sensitive to photo-induced toxicity of PAH at environmentally relevant concentrations and intensities of UV radiation. Sufficient UV radiation appears to be present in most aquatic systems to cause

significant photo-induced toxicity of PAH to aquatic organisms. The magnitude of PAH contamination appears to be the limiting component for determining if photo-induced toxicity of PAH is currently impacting algal communities in the environment. Procurement of more accurate and comprehensive measurements of concentrations of PAH in surface waters are required to permit a more definite assessment of the hazard posed by contamination of aquatic systems by PAH to algal communities.

Algae appear to be more resistant to photo-induced toxicity of anthracene, relative to fishes and zooplankton. Therefore, water and sediment quality criteria promulgated to protect aquatic animals from the photo-induced toxicity of PAH should also be sufficient to protect algal communities. The greater resistance of algae appears to be related to the great concentration of colored carotenoid pigments, such as beta-carotene, present in algal cells. Colored carotenoid pigments can protect algal cells by quenching singlet oxygen generated from photo-excited PAH. The significant inverse relationship between concentrations of colored carotenoid pigments and the sensitivity of algal cells to the photo-induced toxicity of anthracene, as determined in the carotenoid biosynthesis inhibiting herbicide experiment, indicates the photo-induced toxicity of anthracene proceeds via a type II (singlet oxygen) mechanism, in vivo. Additional investigations to assess the utility of using algal cells

whose carotenoid biosynthesis has been inhibited, as a bioassay system to determine the mechanism of toxicity of other PAH and photosensitizers are clearly warranted. The importance of the protection provided by carotenoid pigments within algal cells against other toxicants, such as SUVR, could be assessed utilizing this proposed bioassay system.

These studies were not designed to answer the question of whether the photo-induced toxicity of PAH is merely an enhancement of the direct effects of UV radiation. The site of action of UV radiation appears to be inhibition of photosynthesis via inactivation of photosystem II reaction centers. The great resistance of algal photosynthesis function and structure endpoints to the photo-induced toxicity of PAH suggests that the site of action of photo-induced toxicity of PAH is outside the chloroplast and different from the site of action of UV radiation. Singlet oxygen has been demonstrated to be the causal agent for the photo-induced toxicity of PAH, while rarely has singlet oxygen been implicated to explain the direct effects of UV radiation on organisms. Therefore, all evidence suggests that the site(s) of toxic action, and probably also the mode(s) of toxicity, are distinct for direct and PAH-mediated UV toxicity.

The construction of valid and proper experimental designs to investigate the photo-induced toxicity of PAH requires comprehensive understanding of the basic principles of physics, chemistry, and biology. Too often invalid

experiments have been performed because a basic tenet of one of these three disciplines had been neglected. It is hoped that the challenges involved in constructing and performing valid experiments to investigate the photo-induced toxicity of PAHs and other environmental photosensitizers will not discourage other researchers from studying this interesting toxicological phenomenon. To quote Robert Frost:

Two roads diverged in a wood, and I
I took the one less travelled by,
and that has made all the difference.

REFERENCES

- Allred, P.M., and J.P. Giesy. 1985. Solar radiation-induced toxicity of anthracene to Daphnia pulex. Environ. Toxicol. Chem. 4: 219-226.
- Andelman, J.B., and M.J. Suess. 1970. Polynuclear aromatic hydrocarbons in the water environment. Bull. Wld. Hlth. Org. 43: 479-508.
- Andren, A.W., and J.W. Strand. 1981. Atmospheric deposition of particulate organic carbon and polyaromatic hydrocarbons to Lake Michigan. In: Atmospheric Pollutants in Natural Waters, S.J. Eisenreich (ed.). Ann Arbor Science, Ann Arbor, MI, pp. 459-479.
- Anon. 1981. OECD guidelines for testing of chemicals: 201. Alga growth inhibition test. Organization for Economic Cooperation and Development, Paris, France.
- Arnason, T., J.R. Stein, E. Graham, C.-K. Wat, G.H.N. Towers, and J. Lam. 1981. Phototoxicity to selected marine and freshwater algae of polyacetylenes from species in the Asteraceae. Can. J. Bot. 59: 54-58.
- Baker, K.S., R.C. Smith, and A.E.S. Green. 1980. Middle ultraviolet radiation reaching the ocean surface. Photochem. Photobiol. 32: 367-374.
- Barrick, R.C., and F.G. Prahl. 1987. Hydrocarbon geochemistry of the Puget Sound region - III. Polycyclic aromatic hydrocarbons in sediments. Estuar. Coastal Shelf Sci. 25: 175-191.
- Bartels, P.G., and C.W. Watson. 1978. Inhibition of carotenoid synthesis by fluridone and norflurazon. Weed Sci. 26: 198-203.
- Bates, T.S., P.P. Murphy, H.C. Curl, and R.A. Feely. 1987. Hydrocarbon distributions and transport in an urban estuary. Environ. Sci. Technol. 21: 193-198.

- Baumann, P.C., W.D. Smith, and W.K. Parland. 1987. Tumor frequencies and contaminant concentrations in brown bullheads from an industrialized river and a recreational lake. *Trans. Am. Fish. Soc.* 116: 79-86.
- Bennett, W.E., J.L. Maas, S.A. Sweeney, and J. Kagan. 1986. Phototoxicity in aquatic organisms: The protecting effect of beta-carotene. *Chemosphere* 15: 781-786.
- Benson, M.C., D.C. McDougal, and D.S. Coffey. 1984. The application of perpendicular and forward light scatter to assess nuclear and cellular morphology. *Cytometry* 5: 515-522.
- Berglund, D.L., and S. Eversman. 1988. Flow cytometric measurement of pollutant stresses on algal cells. *Cytometry* 9: 150-155.
- Bowling, J.W., G.J. Leversee, P.F. Landrum, and J.P. Giesy. 1983. Acute mortality of anthracene-contaminated fish exposed to sunlight. *Aquat. Toxicol.* 3: 79-90.
- Brandle, J.R., W.F. Campbell, W.B. Sisson, and M.M. Caldwell. 1977. Net photosynthesis, electron transport capacity, and ultrastructure of Pisum sativum L. exposed to ultraviolet-B radiation. *Plant Physiol.* 60: 165-169.
- Braumann, T.H., T.H. Gropper, I. Damn, and L.H. Grimme. 1984. Function of chlorophylls and carotenoids in thylakoid membranes. Pigment bleaching in relation to PS-I and PS-II activity of subchloroplast particles prepared with digitonin. In: Advances in Photosynthesis Research, Volume II, C. Sybesma (ed.). Kluwer Academic Publishers Group, Boston, pp. 137-140.
- Britton, G. 1979. Carotenoid biosynthesis - a target for herbicide activity. *Z. Naturforsch.* 34c: 979-985.
- Calkins, J. (ed.). 1982a. The Role of Solar Ultraviolet Radiation in Marine Ecosystems. Plenum Press, New York.
- Calkins, J. 1982b. A method for the estimation of the penetration of biologically injurious solar ultraviolet radiation into natural waters. In: The Role of Solar Ultraviolet Radiation in Marine Ecosystems, J. Calkins (ed.). Plenum Press, New York, pp. 247-261.
- Calkins, J., and T. Thordardottir. 1980. The ecological significance of solar UV radiation on aquatic organisms. *Nature* 283: 563-566.

- Cicerone, R.J. 1987. Changes in stratospheric ozone. *Science* 237: 35-42.
- Cody, T.E., M.J. Radike, and D. Warshawsky. 1984. The phototoxicity of benzo[a]pyrene in the green alga Selenastrum capricornutum. *Environ. Res.* 35: 122-132.
- Cox, R.A., and G.D. Hayman. 1988. The stability and photochemistry of dimers of ClO radical and implications for Antarctic ozone depletion. *Nature* 332: 796-800.
- Dohler, G. 1985. Effect of UV-B radiation (290-320 nm) on the nitrogen metabolism of several marine diatoms. *J. Plant Physiol.* 118: 391-400.
- Dohler, G., I. Biermann, and J. Zink. 1986. Impact of UV-B radiation on photosynthetic assimilation of ¹⁴C-bicarbonate and inorganic ¹⁵N-compounds by cyanobacteria. *Z. Naturforsch.* 41c: 426-432.
- Dwyer, D.J. 1988. Personal communication. Nalge Company, Rochester, New York.
- Eadie, B.J., W.R. Faust, P.F. Landrum, N.R. Morehead, W.S. Gardner, and T. Napela. 1983. Bioconcentration of PAH by some benthic organisms. In: Polynuclear Aromatic Hydrocarbons: Formation, Metabolism and Measurement, 7th International Symposium, M. Cooke and J. Dennis (eds.). Battelle Press, Columbus, OH, pp. 437-449.
- Eisenreich, S.J., B.B. Looney, and J.D. Thornton. 1981. Airborne organic contaminants in the Great Lakes ecosystem. *Environ. Sci. Technol.* 15: 30-38.
- Eisler, R. 1987. Polycyclic aromatic hydrocarbon hazards to fish, wildlife, and invertebrates: a synoptic review. U.S. Fish Wildl. Serv. Biol. Rep. 85 (1.11), U.S. Fish and Wildlife Service, Laurel, MD.
- Epstein, S.S., M. Burroughs, and M. Small. 1963. The photodynamic effect of the carcinogen, 3,4-benzpyrene, on Paramecium caudatum. *Cancer Res.* 23: 35-44.
- Fabacher, D.L., C.J. Schmitt, J.M. Besser, and M.J. Mac. 1988. Chemical characterization and mutagenic properties of polycyclic aromatic compounds in sediment from tributaries of the Great Lakes. *Environ. Toxicol. Chem.* 7: 529-543.
- Fahnenstiel, G.L., and D. Scavia. 1987. Dynamics of Lake Michigan phytoplankton: Primary production and growth. *Can. J. Fish. Aquat. Sci.* 44: 499-508.

- Finney, D.J. 1971. Probit Analysis, Third edition. Cambridge University Press, London.
- Foote, C.S. 1968. Mechanisms of photosensitized oxidation. *Science* 162: 963-970.
- Foote, C.S. 1976. Photosensitized oxidation and singlet oxygen: Consequences in biological systems. *Free Radicals in Biology* 2: 86-133.
- Foote, C.S., Y.C. Chang, and R.W. Denny. 1970. Chemistry of singlet oxygen. X. Carotenoid quenching parallels biological protection. *J. Amer. Chem. Soc.* 92: 5216-5218.
- Freeman, B.A., and J.D. Crapo. 1982. Biology of disease: Free radicals and tissue injury. *Laboratory Investigations* 47: 412-426.
- Futoma, D.J., S.R. Smity, T.E. Smith, and J. Tanaka. 1981. Polycyclic Aromatic Hydrocarbons in Water Systems. CRC Press, Boca Raton, FL, pp. 25-27.
- Gala, W.R., and J.P. Giesy. 1989. Flow cytometric techniques to assess toxicity to algae. In: Aquatic Toxicology and Hazard Assessment: Thirteenth Symposium, submitted.
- Galbraith, D.W., K.R. Harkins, and R.A. Jefferson. 1988. Flow cytometric characterization of the chlorophyll contents and size distributions of plant protoplasts. *Cytometry* 9: 75-83.
- Giddings, J.M. 1979. Acute toxicity to Selenastrum capricornutum of aromatic compounds from coal conversion. *Bull. Environ. Contam. Toxicol.* 23: 360-364.
- Giese, A.C. 1964. Studies on ultraviolet radiation action upon animal cells. In: Photophysiology, A.C. Giese (ed.). Academic Press, New York, pp. 203-245.
- Giesy, J.P., S.M. Bartell, P.F. Landrum, G.J. Leversee, J.W. Bowling, M.G. Bruno, T.E. Fannin, S. Gerould, J.D. Haddock, K. LaGory, J.T. Oris, and A. Spacie. 1978. Fates and biological effects of polycyclic aromatic hydrocarbons in aquatic systems. EPA-78-D-X0290, U.S. Environmental Protection Agency, Athens, GA.
- Green, B.F. 1977. A practical interactive program for randomization tests of location. *Amer. Statistician* 31: 37-39.

- Griest, W.H. 1980. Multicomponent polycyclic aromatic hydrocarbon analysis of inland water and sediment. In: Hydrocarbons and Halogenated Hydrocarbons in the Aquatic Environment, B.K. Afgan and D. Mackay (eds.). Plenum Press, New York, pp. 173-183.
- Grossweiner, L.I., and E.F. Zwicker. 1961. Transient measurements of photochemical processes in dyes. I. The photosensitized oxidation of phenol by eosin and related dyes. *J. Chem. Physics* 34: 1141-1147.
- Grumbach, K.H. 1984. Does the chloroplast envelope contain carotenoids and quinones in vivo? *Physiol. Plant.* 60: 180-186.
- Gschwend, P.M., and R.A. Hites. 1981. Fluxes of polycyclic aromatic hydrocarbons to marine and lacustrine sediments in the northeastern United States. *Geochim. Cosmochim. Acta* 45: 2359-2367.
- Hairston, N.G., 1976. Photoprotection by carotenoid pigments in the copepod Diaptomus nevadensis. *Proc. Natl. Acad. Sci. U.S.A.* 73: 971-974.
- Hammitt, J.K., F. Camm, P.S. Connell, W.E. Mooz, K.A. Wolf, D.J. Wuebbles, and A. Bemezai. 1987. Future emission scenarios for chemicals that may deplete stratospheric ozone. *Nature* 330: 711-716.
- Hites, R.A., R.E. Laflamme, and J.G. Windsor. 1980. Polycyclic aromatic hydrocarbons in the marine environment: Gulf of Maine sediments and Nova Scotia soils. In: Hydrocarbons and Halogenated Hydrocarbons in the Aquatic Environment, B.K. Afgan and D. Mackay (eds.). Plenum Press, New York, pp. 397-403.
- Hobson, L.A., and F.A. Hartley. 1983. Ultraviolet irradiance and primary production in a Vancouver Island fjord, British Columbia, Canada. *J. Plankton Res.* 5: 325-331.
- Hoffman, E.J., G.L. Mills, J.S. Latimer, and J.G. Quinn. 1984. Urban runoff as a source of polycyclic aromatic hydrocarbons to coastal waters. *Environ. Sci. Technol.* 18:580-587.
- Holst, L.L. 1987. The chronic effects of the photo-enhanced toxicity of anthracene on Daphnia magna reproduction. Department of Fisheries and Wildlife, Michigan State University. M.S. Thesis.

- Hutchinson, T.C., J.A. Hellebust, D. Tam, D. Mackay, R.A. Mascarenhas, and W.Y. Shiu. 1980. The correlation of the toxicity to algae of hydrocarbons and halogenated hydrocarbons with their physical-chemical properties. In: Hydrocarbons and Halogenated Hydrocarbons in the Aquatic Environment, B.K. Afgan and D. Mackay (eds.). Plenum Press, New York, pp. 577-586.
- Jahnke, L.S., and A. Frenkel. 1978. Photooxidation of epinephrine sensitized by methylene blue - evidence for the involvement of singlet oxygen and superoxide. *Photochem. Photobiol.* 28: 517-523.
- Jerlov, N.G. 1950. Ultra-violet radiation in the sea. *Nature* 116: 111-112.
- Jitts, H.R., A. Morel, and Y. Saijo. 1976. The relation of oceanic primary production to available photosynthetic irradiance. *Aust. J. Mar. Freshwater Res.* 27: 441-454.
- Jokiel, P.L., and R.H. York. 1984. Importance of ultraviolet radiation in photoinhibition of microalgal growth. *Limnol. Oceanogr.* 29: 192-199.
- Jones, L.W., and B. Kok. 1966. Photoinhibition of chloroplast reactions. I. Kinetics and action spectra. *Plant Physiol.* 41: 1037-1043.
- Joshi, P.C., and M.A. Pathak. 1983. Production of singlet oxygen and superoxide radicals by psoralens and their biological significance. *Biochem. Biophys. Res. Commun.* 112: 638-646.
- Kagan, J., P.A. Kagan, and H.E. Bushe. 1984. Light-dependent toxicity of α -terthienyl and anthracene toward late embryonic stages of Rana pipiens. *J. Chem. Ecol.* 10: 1115-1122.
- Kagan, J., E.D. Kagan, I.A. Kagan, P.A. Kagan, and S. Quigley. 1985. The phototoxicity of non-carcinogenic polycyclic aromatic hydrocarbons in aquatic organisms. *Chemosphere* 14: 1829-1834.
- Kaidbey, K.H., and S. Nonaka. 1984. Action spectrum for anthracene-induced photosensitization of human skin. *Photochem. Photobiol.* 39: 375-378.
- Krinsky, N.I. 1979. Carotenoid protection against oxidation. *Pure Appl. Chem.* 51: 649-660.

- Landrum, P.F., J.P. Giesy, J.T. Oris, and P.M. Allred. 1986. The photoinduced toxicity of polycyclic aromatic hydrocarbons to aquatic organisms. In: Oil and Freshwater: Chemistry, Biology, Technology, J.H. Vandermeulen and S. Hrudey (eds.). Pergamon Press, NY, pp. 304-318.
- Landrum, P.F., M.D. Reinhold, S.R. Nihart, and B.J. Eadie. 1985. Predicting the bioavailability of organic xenobiotics to Pontoporeia hoyi in the presence of humic and fulvic materials and natural dissolved organic matter. *Environ. Toxicol. Chem.* 4: 459-467.
- Leversee, G.J., P.F. Landrum, J.P. Giesy, and T. Fannin. 1983. Humic acids reduce bioaccumulation of some polycyclic aromatic hydrocarbons. *Can. J. Fish. Aquat. Sci.* 40 (Suppl): 63-69.
- Lorenzen, C.J. 1979. Ultraviolet radiation and phytoplankton photosynthesis. *Limnol. Oceanogr.* 24: 1117-1120.
- Mailhot, H. 1987. Prediction of algal bioaccumulation and uptake rate of nine organic compounds by ten physiochemical properties. *Environ. Sci. Technol.* 27: 1009-1013.
- Mathis, P., and J. Kleo. 1973. The triplet state of β -carotene and of analog polyenes of different length. *Photochem. Photobiol.* 18: 343-346.
- Matthews-Roth, M.M., T. Wilson, E. Fujimori, and N.I. Krinsky. 1974. Carotenoid chromophore length and protection against photosensitization. *Photochem. Photobiol.* 19: 217-222.
- McCain, B.B., D.W. Brown, M.M. Krahm, M.S. Myers, R.C. Clark, S-L. Chan, and D.C. Malins. 1988. Marine pollution problems, North American West Coast. *Aquat. Toxicol.* 11: 143-162.
- Means, J.C., S.G. Wood, J.J. Hassett, and W.L. Banwart. 1980. Sorption of polynuclear aromatic hydrocarbons by sediments and soils. *Environ. Sci. Technol.* 14: 1524-1528.
- Mill, T., W.R. Mabey, D.C. Bomberger, T.- W. Chou, D.G. Hendry, and J.H. Smith. 1982. Laboratory protocols for evaluating the fate of organic chemicals in air and water. EPA 600/3-82-022, U.S. Environmental Protection Agency, Athens, GA.

- Miller, W.E., J.C. Greene and T. Shiroyama. 1978. The Selenastrum capricornutum Printz algal assay bottle test. EPA 600/9-78-018, U.S. Environmental Protection Agency, Corvallis, OR.
- Morgan, D.D., and D. Warshawsky. 1977. The photodynamic immobilization of Artemia salina nauplii by polycyclic aromatic hydrocarbons and its relationship to carcinogenic activity. Photochem. Photobiol. 25: 39-46.
- Morgan, D.D., D. Warshawsky, and T. Atkinson. 1977. The relationship between carcinogenic activities of polycyclic aromatic hydrocarbons and their singlet, triplet, and singlet-triplet splitting energies and phosphorescence lifetimes. Photochem. Photobiol. 25: 31-38.
- Morimura, U., P. Kotin, and H.L. Falk. 1964. Photodynamic toxicity of polycyclic aromatic hydrocarbons in tissue culture. Cancer Res. 24: 1249-1255.
- Mottram, J.C., M.B. Lond, I. Doniach, and M.D. Lond. 1938. The photodynamic action of carcinogenic agents. Lancet 234: 1156-1159.
- Mount, D.I. 1989. Methods for aquatic toxicity identification evaluations. Phase III toxicity confirmation procedures. EPA/600/3-88/036. U.S. Environmental Protection Agency, Duluth, MN
- National Research Council. 1979. Protection Against Depletion of Stratospheric Ozone by Chlorofluorocarbons. National Academy of Sciences, Washington, D.C.
- National Research Council. 1982. Causes and Effects of Stratospheric Ozone Reduction: An Update. National Academy of Sciences, Washington, D.C.
- Neff, J.M. 1979. Polycyclic Aromatic Hydrocarbons in the Aquatic Environment. Applied Science Publ. Ltd., London.
- Neter, J., W. Wasserman, and M.H. Kutner. 1985. Applied Linear Statistical Models, Second edition. Richard D. Irwin, Inc., Homewood, IL, pp. 171-174.
- Newsted, J.L., and J.P. Giesy. 1987. Predictive model for photoinduced acute toxicity of polycyclic aromatic hydrocarbons to Daphnia magna, Strauss (Cladocera, Crustacea). Environ. Toxicol. Chem. 6: 445-461.

- Noorudeen, A.M., and G. Kulandaivelu. 1982. On the possible site of inhibition of photosynthetic electron transport by ultraviolet-B (UV-B) radiation. *Physiol. Plant.* 55: 161-166.
- Oris, J.T., and J.P. Giesy. 1985. The photoenhanced toxicity of anthracene to juvenile sunfish (Lepomis spp.) *Aquat. Toxicol.* 6: 133-146.
- Oris, J.T., and J.P. Giesy. 1986. Photoinduced toxicity of anthracene to juvenile bluegill sunfish (Leopmis macrochirus Rafinesque): Photoperiod effects and predictive hazard evaluation. *Environ. Toxicol. Chem.* 5: 761-768.
- Oris, J.T., and J.P. Giesy. 1987. The photo-induced toxicity of selected polycyclic aromatic hydrocarbons to larvae of the fathead minnow (Pimephales promelas): comparative toxicities and structure-activity relationship. *Chemosphere* 16: 1395-1404.
- Oris, J.T., J.P. Giesy, P.M. Allred, D.F. Grant, and P.F. Landrum. 1984. Photoinduced toxicity of anthracene in aquatic organisms: An environmental perspective. In: The Biosphere: Problems and Solutions, T.N. Veziroglu (ed.). Elsevier Science Publ. B.V., Amsterdam, pp. 639-658.
- Paerl, H.W., P.T. Bland, N.D. Bowles, and M.E. Haibach. 1985. Adaptation to high-intensity, low-wavelength light among surface blooms of the cyanobacterium Microcystis aeruginosa. *Appl. Environ. Microbiol.* 49: 1046-1052.
- Paerl, H.W., J. Tucker, and P.T. Bland. 1983. Carotenoid enhancement and its role in maintaining blue-green algal (Microcystis aeruginosa) surface blooms. *Limnol. Oceanogr.* 28: 847-857.
- Parsons, T.R., Y. Maita, and C.M. Lalli. 1984. A Manual of Chemical and Biological Methods for Seawater Analysis. Plenum Press, New York, pp. 101-104.
- Peak, J.G., C.S. Foote, and M.J. Peak. 1981. Protection by DABCO against inactivation of transforming DNA by near-ultraviolet light: Action spectra and implications for involvement of singlet oxygen. *Photochem. Photobiol.* 34: 45-49.

- Peak, M.J., and J.G. Peak. 1982. Lethal effects on biological systems caused by solar ultraviolet light: Molecular considerations. In: The Role of Solar Ultraviolet Radiation in Marine Ecosystems, J. Calkins (ed.). Plenum Press, New York, pp. 325-336.
- Peterson, B.J. 1980. Aquatic primary productivity and ^{14}C - CO_2 method: A history of the productivity problem. *Ann. Rev. Ecol. Syst.* 11: 359-385.
- Pooler, J.P., and D.P. Valenzano. 1979. The role of singlet oxygen in photooxidation of excitable cell membranes. *Photochem. Photobiol.* 30: 581-584.
- Readman, J.W., R.F.C. Mantoura, and M.M. Rhead. 1987. A record of polycyclic aromatic hydrocarbon (PAH) pollution obtained from accreting sediments of the Tamar Estuary, U.K.: Evidence for non-equilibrium behaviour of PAH. *Sci. Total Environ.* 66: 73-94.
- Romesburg, H.C. 1985. Exploring, confirming, and randomization tests. *Computers Geosci.* 11: 19-37.
- Rotman, B.R., and R.O. Papermaster. 1966. Membrane properties of living cells as studied by enzymatic hydrolysis of fluorogenic esters. *Proc. Natl. Acad. Sci. U.S.A.* 55: 134-141.
- Sandmann, G., I.E. Clarke, P.M. Bramley, and P. Boger. 1984. Inhibition of phytoene desaturase - the mode of action of certain bleaching herbicides. *Z. Naturforsch.* 39c: 443-449.
- SAS Institute. 1985. SAS User's Guide: Statistics, Version 5 Edition. SAS Institute Inc., Cary, N.C.
- SAS Institute. 1987. SAS/STAT Guide for Personal Computers, Version 6 Edition. SAS Institute Inc., Cary, N.C.
- Scavia, D., G.L. Fahnensteil, M.S. Evans, D.J. Jude, and J.T. Lehman. 1986. Influence of salmonine predation and weather on long-term water quality in Lake Michigan. *Can. J. Fish. Aquat. Sci.* 43: 435-443.
- Schindler, D.W., R.V. Schmidt, and R.A. Reid. 1972. Acidification and bubbling as an alternative to filtration in determining phytoplankton production by the ^{14}C method. *J. Fish. Res. Bd. Canada* 29: 1627-1631.
- Setlow, R.B. 1974. The wavelengths in sunlight effective in producing skin cancer: A theoretical analysis. *Proc. Natl. Acad. Sci. U.S.A.* 71: 3363-3366.

- Sinha, B., and C.F. Chignell. 1983. Binding of anthracene to cellular macromolecules in the presence of light. *Photochem. Photobiol.* 37: 33-37.
- Smith, R.C., and K.S. Baker. 1981. Optical properties of the clearest natural waters (200-800 nm). *Appl. Optics* 20: 177-184.
- Smith, R.C., and K.S. Baker. 1982. Assessment of the influence of enhanced UV-B on marine primary productivity. In: The Role of Solar Ultraviolet Radiation in Marine Ecosystems, J. Calkins (ed.). Plenum Press, New York, pp.509-537.
- Smith, R.C., K.S. Baker, O. Holm-Hansen, and R. Olson. 1980. Photoinhibition of photosynthesis in natural waters. *Photochem. Photobiol.* 31: 585-592.
- Smith, R.C., and J. Calkins. 1976. The use of the Robertson meter to measure the penetration of solar middle-ultraviolet radiation (UV-B) into natural waters. *Limnol. Oceanogr.* 21: 746-749.
- Steemann Nielsen, E. 1964. On a complication in marine productivity work due to the influence of ultraviolet light. *J. Cons. Perm. Int. Explor. Mer* 29: 130-135.
- Trask, B.J., G.J. van den Engh, and J.H.B.W. Elgershuizen. 1982. Analysis of phytoplankton by flow cytometry. *Cytometry* 2: 258-264.
- Vollenweider, R.A. 1969. A Manual on Methods for Measuring Primary Production in Aquatic Environments. IBP Handbook, No. 12, F.A. Davis Company, Philadelphia, PA.
- Widholm, J.M. 1972. The use of fluorescein diacetate and phenosafranine for determining viability of cultured plant cells. *Stain Technol.* 47: 189-194.
- Worrest, R.C. 1983. Impact of solar ultraviolet-B radiation (290-320 nm) upon marine microalgae. *Physiol. Plant.* 58: 428-434.
- Worrest, R.C., D.L. Brooker, and H. Van Dyke. 1980. Results of a primary productivity study as affected by the type of glass in the culture bottles. *Limnol. Oceanogr.* 25: 360- 364.
- Worrest, R.C., B.E. Thomson, and H. Van Dyke. 1981. Impact of UV-B radiation upon estuarine microcosms. *Photochem. Photobiol.* 33: 861-867.